AD-A072 637 NORTH DAKOTA STATE UNIV FARGO DEPT OF ELECTRICAL AND--ETC F/G 20/6
USE OF PREDISTORTION TO REDUCE INTERMODULATION DISTORTION IN OP--ETC(U)
MAY 79 G L LARSON, D A SMITH AFOSR-78-3554

UNCLASSIFIED AFOSR-TR-79-0904 NL

1 OF 1
AD
A072637

END
DATE
FILMED
9-79
DDC

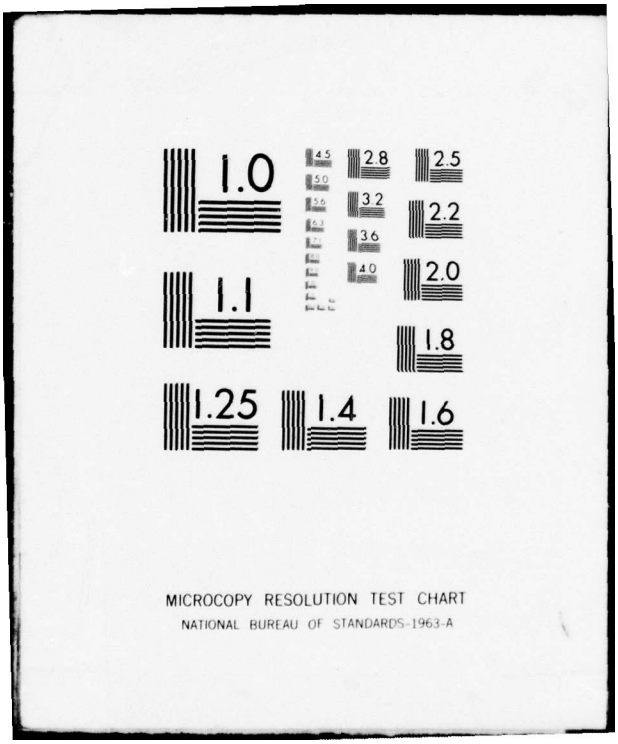
1.0
1.1
1.25
1.4
1.6
1.8
2.0
2.2
2.5
2.8
3.2
3.6
4.0
4.5
5.0
5.6
6.3
7.1
MICROCOPY RESOLUTION TEST CHART
NATIONAL BUREAU OF STANDARDS-1963-A

LEVEL II

12

AD A072637

USE OF PREDISTORTION TO REDUCE INTERMODULATION DISTORTION IN OPTICAL FIBER COMMUNICATION SOURCES

Gary L. Larson

Donald A. Smith

North Dakota State University
Fargo, North Dakota 58105

May 1979

Prepared for

Air Force Office of Scientific Research
Air Force Systems Command, USAF
Grant No. AFOSR-78-3554

SECURITY CLASSIFICATION OF THIS PAGE (When Data Entered) Unclassified

REPORT DOCUMENTATION PAGE

READ INSTRUCTIONS BEFORE COMPLETING FORM

1. REPORT NUMBER: AFOSR-TR- 79-0904	2. GOVT ACCESSION NO.
3. RECIPIENT'S CATALOG NUMBER	
4. TITLE (and Subtitle): Use of Predistortion to Reduce Intermodulation Distortion in Optical Fiber Communication Sources,	5. TYPE OF REPORT & PERIOD COVERED: Final Report March 1978 — May 1979
	6. PERFORMING ORG. REPORT NUMBER
7. AUTHOR(s): Gary L. Larson & Donald A. Smith	8. CONTRACT OR GRANT NUMBER(s): AFOSR-78-3554
9. PERFORMING ORGANIZATION NAME AND ADDRESS: Electrical and Electronics Engineering Department, North Dakota State University, Fargo, ND 58105	10. PROGRAM ELEMENT, PROJECT, TASK AREA & WORK UNIT NUMBERS: 61102F 2305/D9
11. CONTROLLING OFFICE NAME AND ADDRESS: AFOSR/NE, Bolling AFB, DC 20332	12. REPORT DATE: May 1979
	13. NUMBER OF PAGES: 83
14. MONITORING AGENCY NAME & ADDRESS (if different from Controlling Office)	15. SECURITY CLASS. (of this report): Unclassified
	15a. DECLASSIFICATION/DOWNGRADING SCHEDULE

16. DISTRIBUTION STATEMENT (of this Report)

Approved for public release;
distribution unlimited.

17. DISTRIBUTION STATEMENT (of the abstract entered in Block 20, if different from Report)

18. SUPPLEMENTARY NOTES

19. KEY WORDS (Continue on reverse side if necessary and identify by block number)

Fiber Optics
Intermodulation Distortion
Light-Emitting Diodes
Optical Communication
Optical Sources

20. ABSTRACT (Continue on reverse side if necessary and identify by block number)

Optical fiber communication is a new technology which has the potential of surpassing conventional communication techniques in many applications. As with any new technology, problem areas arise which limit the realization of its full potential. One such problem area is the introduction of distortion produced by nonlinearities in the system. When light-emitting diodes are used as sources in optical communication systems, they are the main contributors of the nonlinearities. → next page

- continued -

DD FORM 1 JAN 73 1473

Unclassified 41329

SECURITY CLASSIFICATION OF THIS PAGE

Item #20 (Continued)

A procedure for compensating for the nonlinearity of an LED is developed. An optical receiver and LED transmitter were constructed to measure the light intensity vs LED current characteristic of various LEDS. The static and dynamic characteristics of each of the LEDS were measured. A polynomial describing the dynamic characteristic is used to predict the intermodulation distortion vs percent modulation. Measurements of the intermodulation components of the received signal at different depths of modulation show a close correlation to the calculated values. A predistortion approach to compensating for the nonlinearity of the LED is pursued. Using the LED characteristic, a means of determining the parameters of the compensating network is sought. These parameters are used and measurement of the overall linearity of the system is again checked and compared to that of the uncompensated system. Using a simple compensating network a 6 db-15 db reduction of intermodulation is realized for most LEDS.

USE OF PREDISTORTION TO REDUCE INTERMODULATION DISTORTION IN OPTICAL FIBER COMMUNICATION SOURCES

Gary L. Larson

Donald A. Smith

North Dakota State University
Fargo, North Dakota 58105

May 1979

Prepared for

Air Force Office of Scientific Research
Air Force Systems Command, USAF
Grant No. AFOSR-78-3554

FORWARD

The research was sponsored by the Air Force Office of Scientific Research, Air Force Systems Command, USAF, under Grant No. AFOSR-78-3554 and was conducted in the Electrical and Electronics Engineering Department at North Dakota State University. This document is a thesis submitted to the graduate faculty of North Dakota State University by Gary L. Larson in partial fulfillment of the requirements for the Degree of Master of Science under the supervision of his advisor, Dr. Donald A. Smith, the principal investigator for the project.

ABSTRACT

Optical fiber communication is a new technology which has the potential of surpassing conventional communication techniques in many applications. As with any new technology, problem areas arise which limit the realization of its full potential. One such problem area is the introduction of distortion produced by nonlinearities in the system. When light-emitting diodes are used as sources in optical communication systems, they are the main contributors of the nonlinearities.

A procedure for compensating for the nonlinearity of an LED is developed. An optical receiver and LED transmitter were constructed to measure the light intensity vs LED current characteristic of various LEDS. The static and dynamic characteristics of each of the LEDS were measured. A polynomial describing the dynamic characteristic is used to predict the intermodulation distortion vs percent modulation. Measurements of the intermodulation components of the received signal at different depths of modulation show a close correlation to the calculated values. A predistortion approach to compensating for the nonlinearity of the LED is pursued. Using the LED characteristic, a means of determining the parameters of the compensating network is sought. These parameters are used and measurement of the overall linearity of the system is again checked and compared to that of the uncompensated system. Using a simple compensating network a 6 db-15 db reduction of intermodulation is realized for most LEDS.

ACKNOWLEDGMENTS

The authors wish to express their appreciation to the Air Force Office of Scientific Research, Air Force Systems Command, for the sponsorship of this project. Appreciation is also expressed to the faculty of the Electrical and Electronics Engineering Department at North Dakota State University for suggestions and encouragement throughout the investigation. Gratitude is also expressed to Wilma Jean McDonald for the typing of this manuscript during an especially busy part of the academic year.

TABLE OF CONTENTS

LIST OF TABLES

LIST OF ILLUSTRATIONS

LIST OF ILLUSTRATIONS (Continued)

LIST OF ILLUSTRATIONS (Continued)

CHAPTER I

INTRODUCTION

Since the development of low loss optical fibers, considerable interest has arisen in the use of optical fibers for communication applications. Optical fibers offer a number of appealing features such as: low loss, small size, light weight, high capacity, and small bending radius. In addition, since they contain no metal, they neither radiate nor pick up electromagnetic interference as do wire or cable systems. Also, there are no grounding probems or short circuits associated with optical fibers.

An area of great concern has been that of the source of the modulated optical signal. Internally modulated light-emitting diodes have received a great deal of attention because of the ease of modulation, small size, long lifetimes, and low cost. They do, however, suffer some disadvantages. One being the relatively low radiance emission compared to lasers. Another is the limited frequency response capabilities. [1,2] Still another is the nonlinear relationship between the diode current and the optical power emitted. This is especially troublesome when transmitting multichannel information at high modulation depths in that intermodulation distortion results. This distortion limits the number of channels that can be simultaneously transmitted and also the signal-to-noise ratio that can be achieved on each channel.

Since the output power of a light-emitting diode is at a low level, it is desirable to modulate at high modulation depths. The modulation

depth is limited, however, by the intermodulation distortion produced by its nonlinear characteristic. In light of the potential of analog optical communication systems, there is increasing concern in reducing the severity of the nonlinear effects. Standard methods in correcting for nonlinearities have recently been suggested for LEDS as well as goals which outline the effectiveness of each of the suggested techniques. [3,4,5] An effective compensating network resulting from the investigation of each LED characteristic is considered. A network which exhibits the flexibility of being adaptable to a wide variety of LEDS is sought.

CHAPTER 2

LINEARITY OF THE SYSTEM

A system for measuring the linearity of the light-emitting diodes is proposed in Figure 2-1.

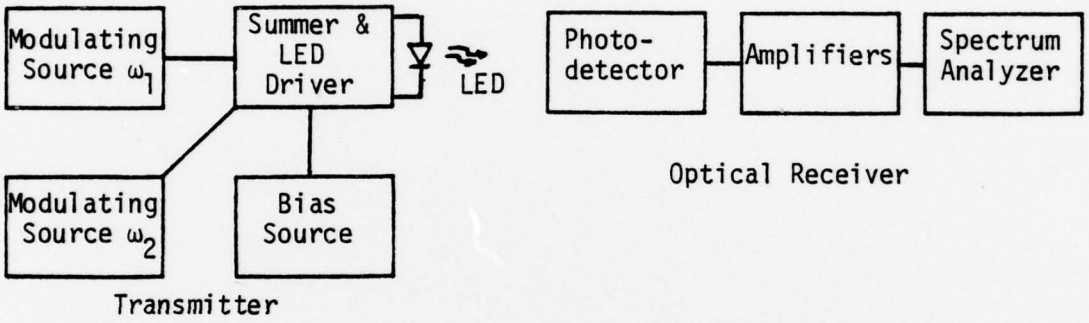

Figure 2-1. Block Diagram for Measuring LED Linearity.

In order to adequately measure the distortion introduced by the LED, the amount of distortion which is produced as a result of the rest of the system must be in excess of 10 db below the distortion amplitudes of concern. A level of intermodulation distortion of -45 db would be acceptable at a modulation depth of 50% for good quality multichannel transmission. To recognize this degree of distortion as being the result of the introduction of the component under test, the remainder of the system must introduce no more than -55 db of intermodulation distortion at the same modulation depth.

THE RECEIVER

In preparing to build the detector-receiver, one must be assured that the active components which are used in the amplification of the received signal are in fact linear.

The Photodetector

The SGD-040L silicon diffused PIN Photodiode is used as the photodetector. This device offers a combination of wide spectral range, high sensitivity, fast speed of response, and low noise. More importantly, however, a linearity of response of 5% over a seven decade range of incident power levels is typical for this photodetector. Considering the optical power swing of an LED, this detector is then highly linear, and therefore, suitable for this application.(6)

The Amplifiers

Operational Amplifiers were used as the active elements for amplification in the receiver. They were selected because of their monolithic design to insure close matching of components resulting in high linearity. Heavy feedback is used to control gain and to increase overall linearity. No guarantee of operational amplifier performance was published concerning linearity, so several devices were checked using the circuit diagrams shown in Figure 2-2. Where applicable, frequency compensating networks supplemented these diagrams (as indicated from the specifications of the device under test).

The CA3015A was used as the gain stage in the receiver because of its linearity as well as high bandwidth and low noise characteristic. In the test circuits of Figure 2-2, it had intermodulation levels of -59 db with an output swing of 6 volts p-p. The NE5534 and CA3100A had comparable linearity. Their bandwidths were less than the CA3015A and for this reason were not chosen.

The final receiver is as shown in Figure 2-3. Decoupling of the power supplies is used due to the high gain and large bandwidth of this amplifier. Emitter follower stages are used on the output when driving low impedance loads.

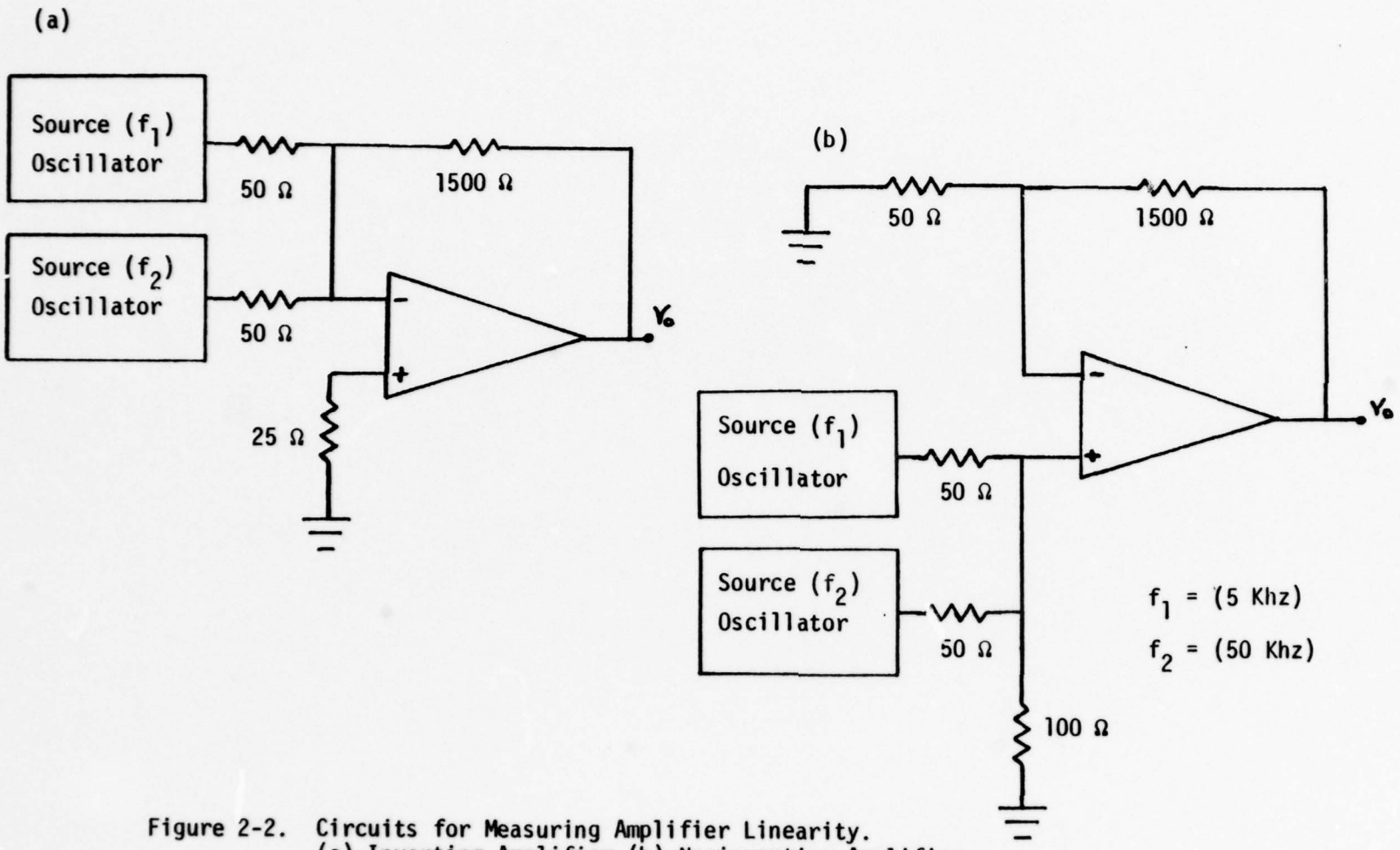

Figure 2-2. Circuits for Measuring Amplifier Linearity.
(a) Inverting Amplifier (b) Noninverting Amplifier

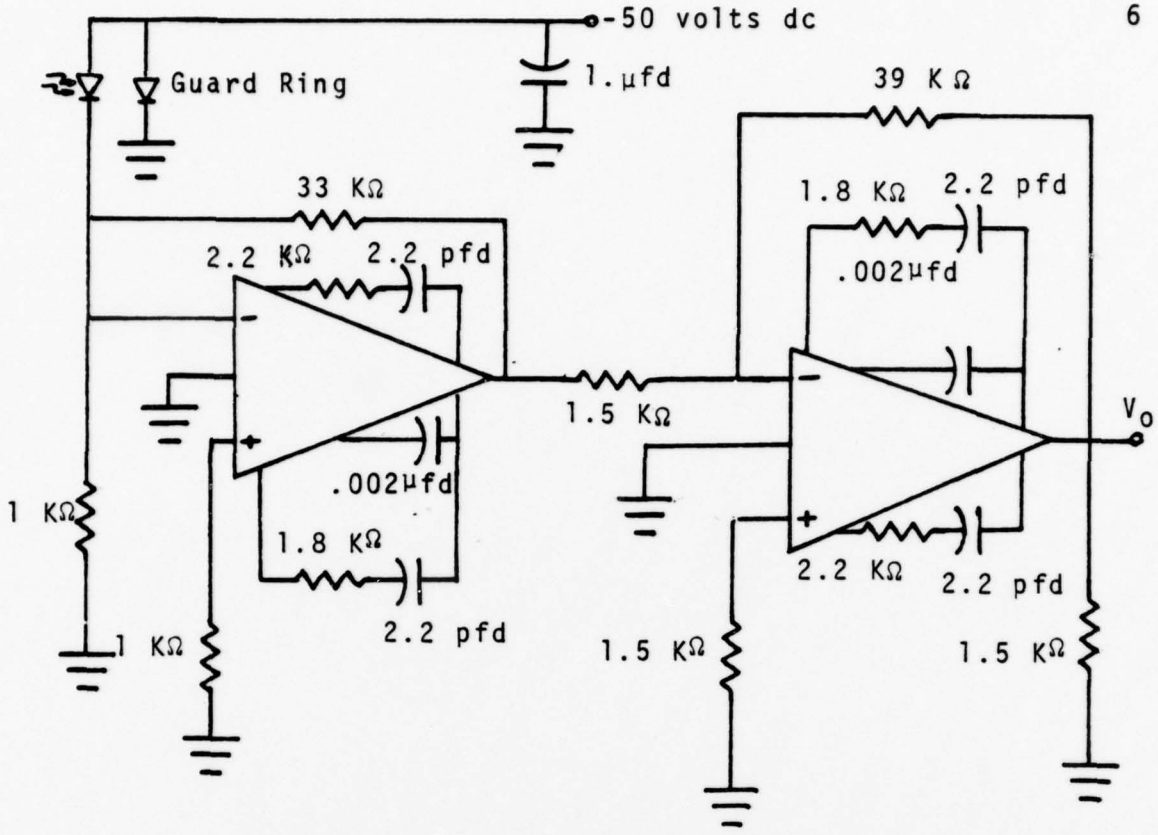

Figure 2-3. Circuit Diagram of the Optical Receiver

The overall linearity of the receiver was checked using the circuit shown in Figure 2-4.

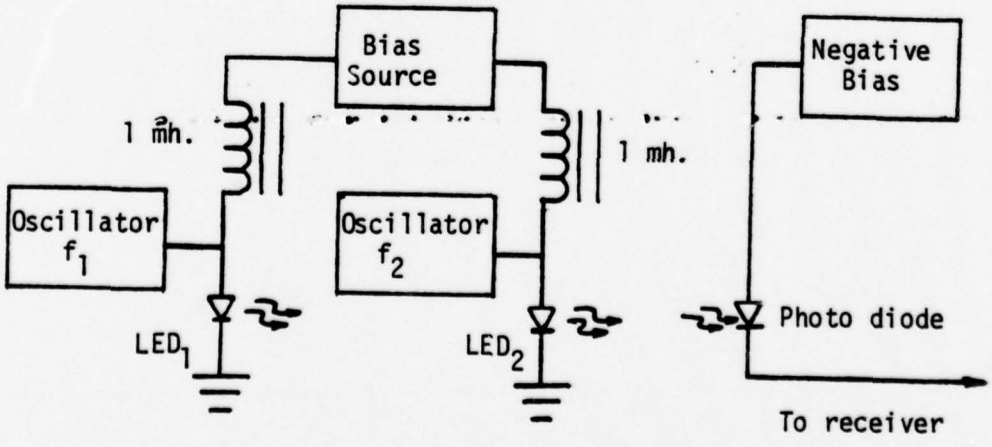

Figure 2-4. Circuit for Measuring Receiver Linearity.

With this circuit, any IM components in the received output are introduced by the receiver. The output swing was 4 volts p-p with intermodulation components at 62 db below the fundamentals. The distortion components were 52 db below the carriers when the output was swinging 8 volts p-p.

THE TRANSMITTER

The transmitter serves two functions. It is a voltage to current converter as well as the LED driver. Due to its insensitivity to the load in the collector circuit a common emitter amplifier serves well in driving a nonlinear load. An emitter resistance should be included to increase linearity and monitor the diode current levels. It was found that the amplifier still lacked sufficient linearity. Another common emitter stage was then used in the emitter feedback path to increase the negative feedback and therefore, the linearity. The circuit of Figure 2-5 then held intermodulation levels to -58 db at 150 mA current swings.

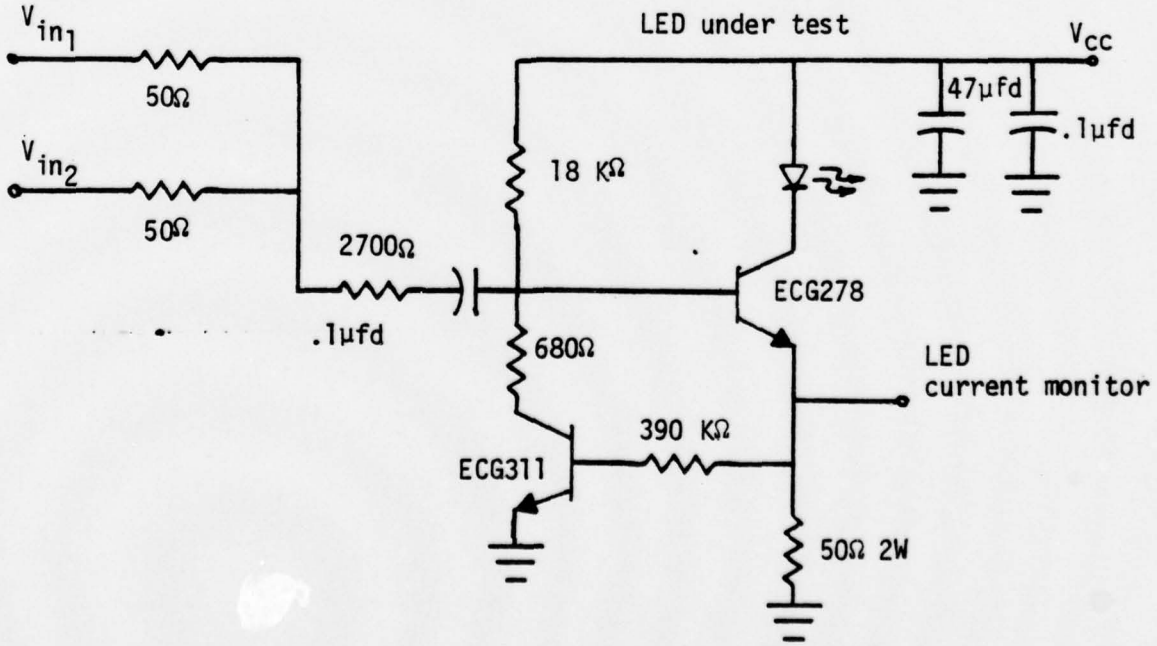

Figure 2-5. Circuit Diagram of the Optical Transmitter.

CHAPTER 3

LED CHARACTERISTIC

The emitted optical power of an LED is a function of either the voltage across, or current through the device. As with any diode, there is a relatively small variation in voltage corresponding to a large variation in current. It is for this reason that it is preferred to control the magnitude of the emitted light by varying the current rather than the voltage of the diodes. There is, however, a nonlinear relationship between the light intensity emitted from, and the current through, an LED. This is the LED characteristic with which attention is concentrated. This curve represents the transfer function between the input modulating signal and the output light. The nonlinear shape of this transfer function results in the introduction of distortion components to the original modulating signal. By mathematically describing the LED characteristic, the output can be computed for a known input.

A number of LEDS from several manufacturers were studied. The diodes used are listed in Table 3-1.

TABLE 3-1

MANUFACTURERS OF THE LEDS USED

LED Type Number	$Imax_{DC}$	Manufacturer
(4) FLV104	100 mA	Fairchild
(4) FPE104	100 mA	Fairchild
(4) FPE500	150 mA	Fairchild
(4) ME7024	100 mA	Monsanto
(4) ME7124	100 mA	Monsanto
(2) TIL31	100 mA	Texas Instruments
(4) HEMT3300	60 mA	Hewlett Packard

The static characteristic of these 26 light-emitting diodes were obtained from the network of Figure 3-1.

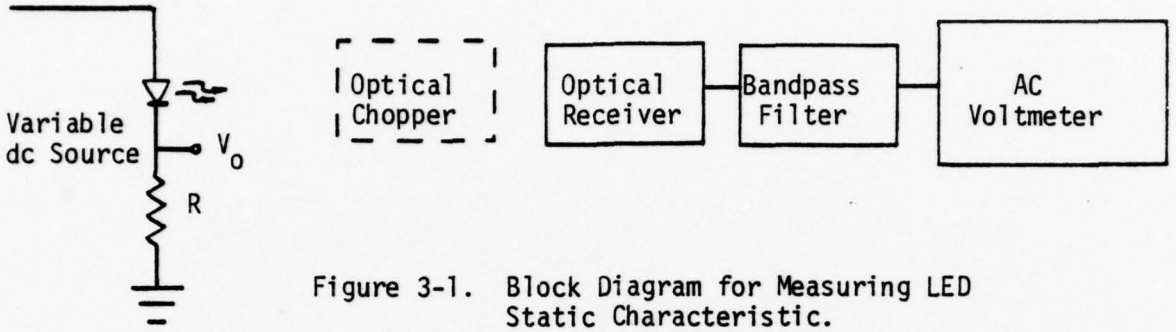

Figure 3-1. Block Diagram for Measuring LED Static Characteristic.

The magnitude of diode current is monitored at V_0. The diode current can be written as:

$$I_{LED} = V_0/R \qquad (1)$$

The receiver as can be seen from Figure 3-1, is direct coupled, which while making the frequency response flat to dc, is susceptible to dc drift. For this reason, an optical chopper was imposed on the network. This transforms the constant light intensity to an "optical square wave" having an amplitude which is equal to the magnitude of the emitted light. The receiver detects, then amplifies the pulsed waveform and couples the signal into a bandpass filter. The filter is tuned to the fundamental frequency of the chopper. Due to the narrow bandwidth of the filter, much of the noise in the detected signal, as well as the harmonics of the chopped signal, are greatly reduced leaving a sinusoidal signal. The amplitude of the sinusoid is then directly related to the intensity of the transmitted light. The magnitude of the output is determined with an AC voltmeter. The magnitude of the light intensity is monitored for differing values of dc current through the LEDS. The static characteristic of each of the devices is then obtained.

Regression analysis, which minimizes mean square error, is used to mathematically describe the characteristics obtained. It can be seen from Figure 3-2 that the best fit curve corresponds well with the actual data points. The curves representing the static characteristic for the 26 LEDS are plotted in Figures 3-3 through 3-9. LEDS of the same type are plotted together to better display the similarities of their characteristics.

While for many LEDS, manufacturers publish the static characteristics, rarely do they include in their specifications a graph of the dynamic characteristic, and for this reason a means for determining this plot is illustrated in Figure 3-10. By pulsing the input with a waveform of sufficiently short duty cycle, the temperature of the device is kept relatively constant. The temperature is approximately the temperature of the device at its bias current level. Changes of light intensity resulting from changes in temperature are thus minimized. The LEDS are pulsed at varying amplitudes to each side of the bias current. The magnitude of the current pulses, together with the corresponding light intensity is measured by the oscilloscope, yielding the dynamic characteristic of the device under test. As in the case of the static characteristic, these curves were best fit to an n^{th} order polynomial in order to mathematically describe the function. Figure 3-11 shows the correspondence between the actual data points and the mathematical function which was determined using the regression analysis. The coefficients for the dynamic characteristics of the LEDS are listed in Tables 3-2 and 3-3. Figures 3-12 through 3-18 illustrate the dynamic characteristics of the 26 LEDS being tested. Again, LEDS of the same type are plotted on the same graph to emphasize their similarities.

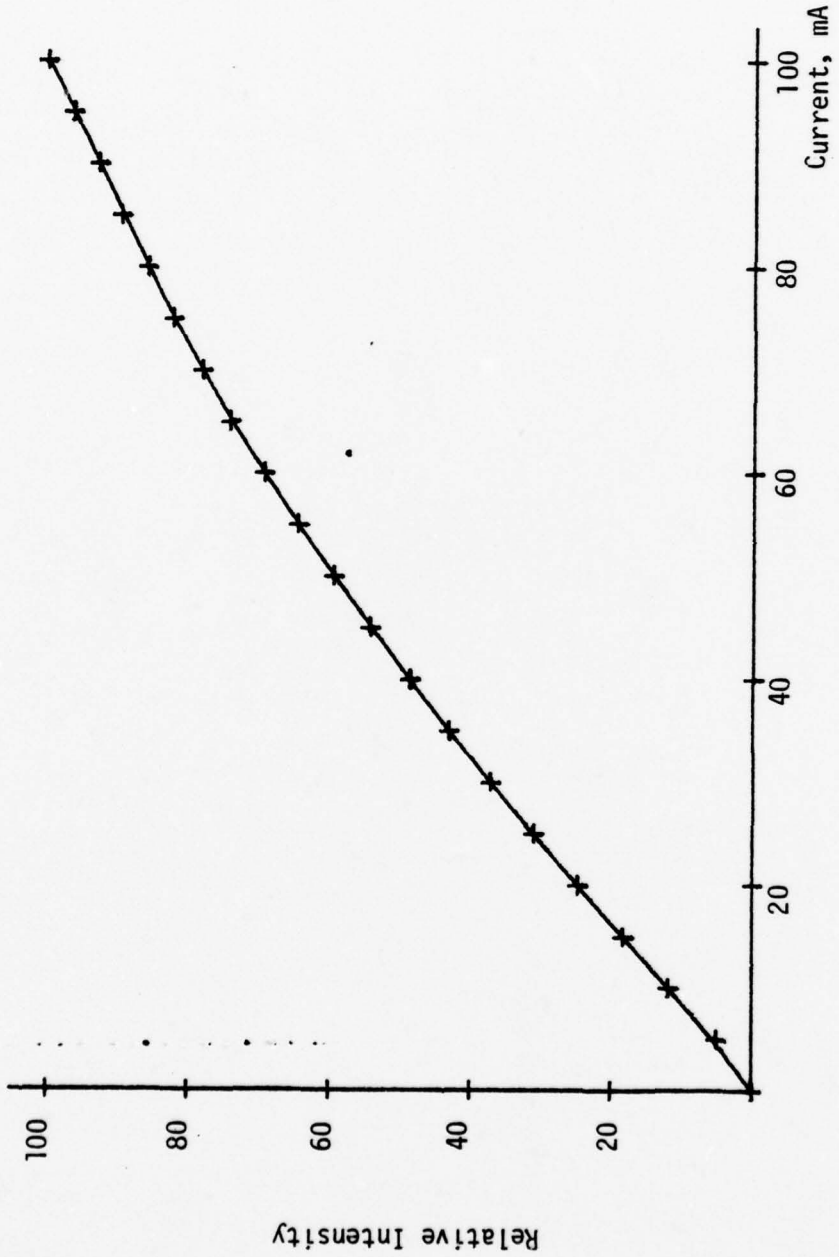

Figure 3-2. Best Fit Curve and Measured Data Points for the Static Characteristic of one FLV104 LED.

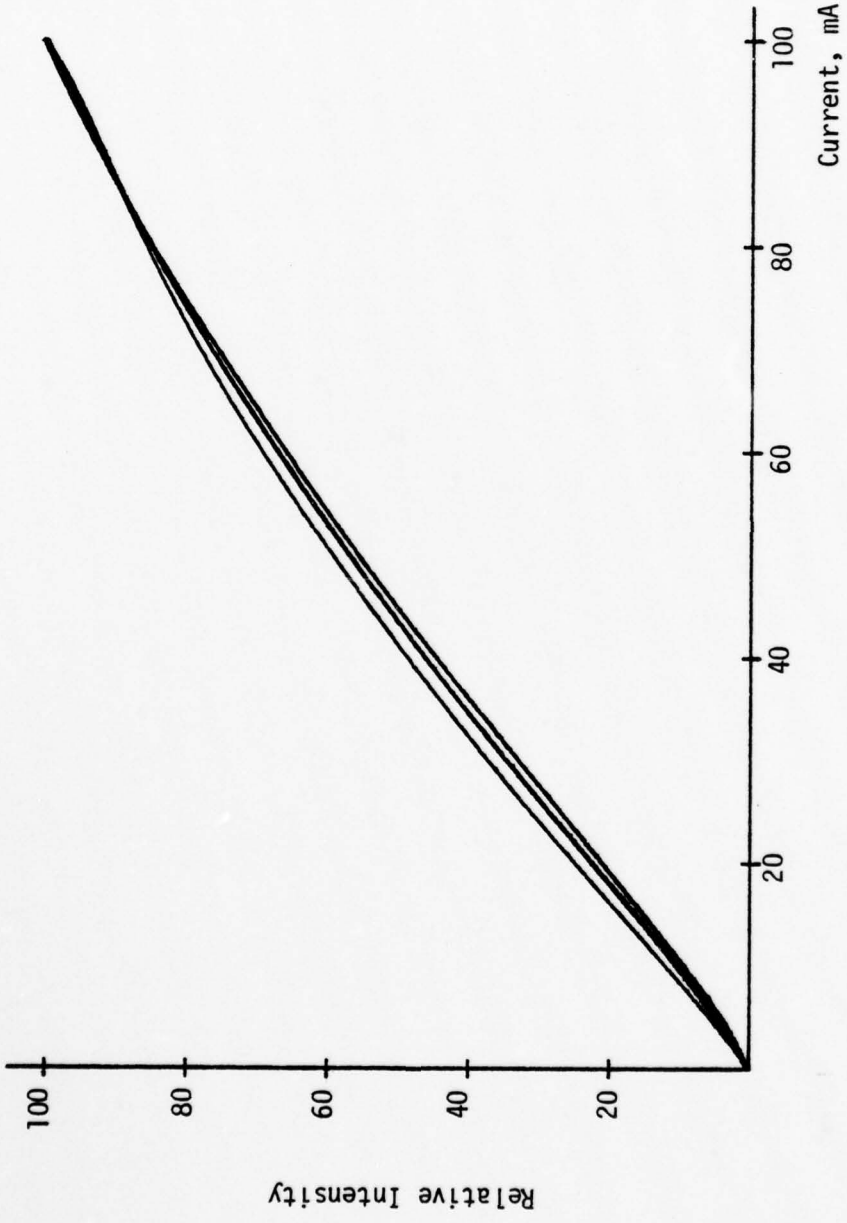

Figure 3-3. Static Characteristics of Four FLV104 LEDS.

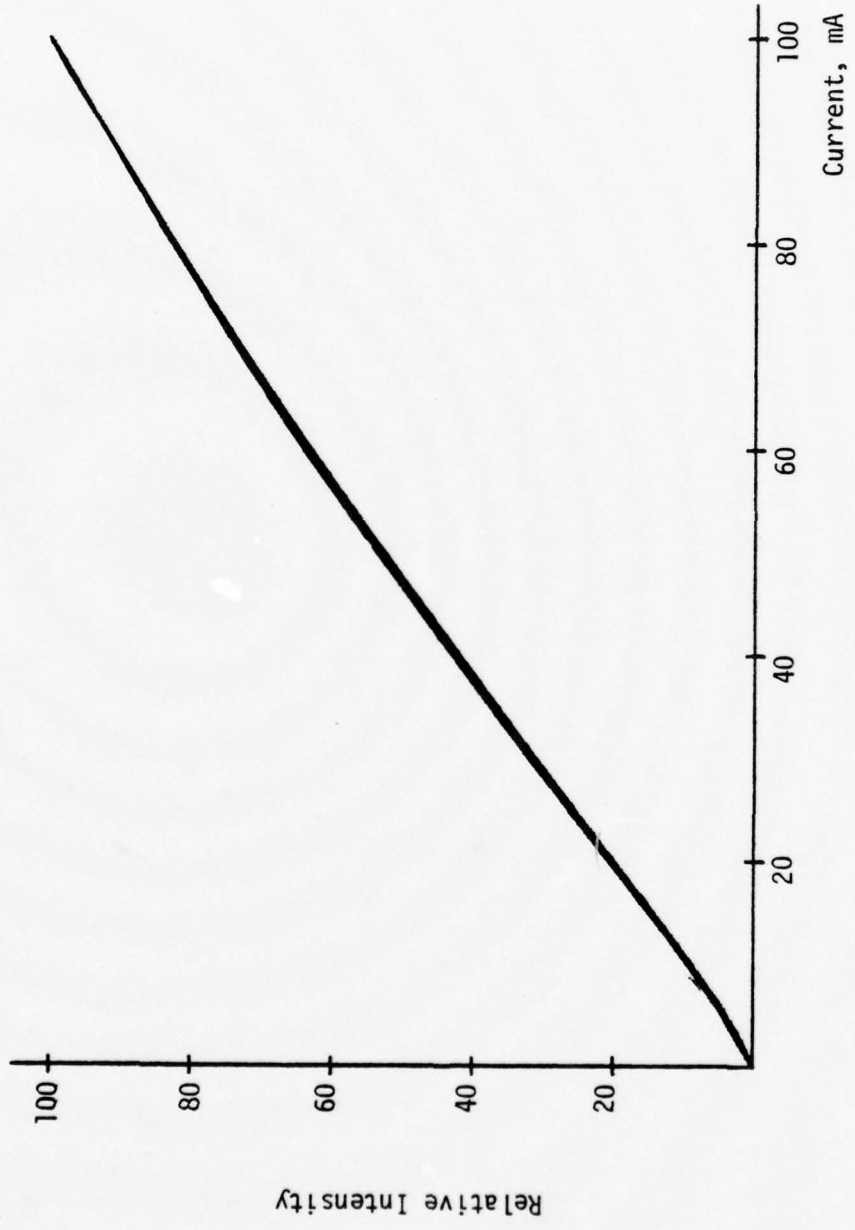

Figure 3-4. Static Characteristics of Four FPE104 LEDS.

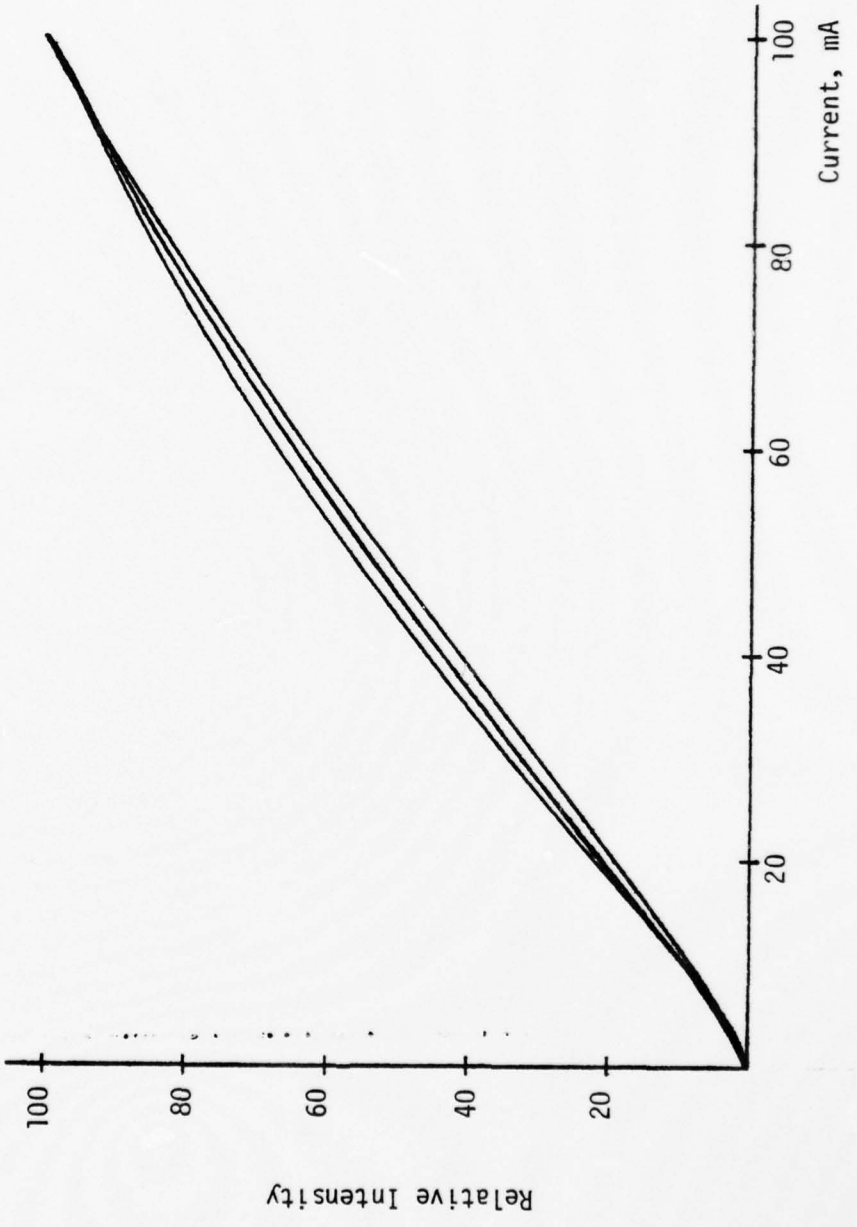

Figure 3-5. Static Characteristics of Four ME7024 LEDS.

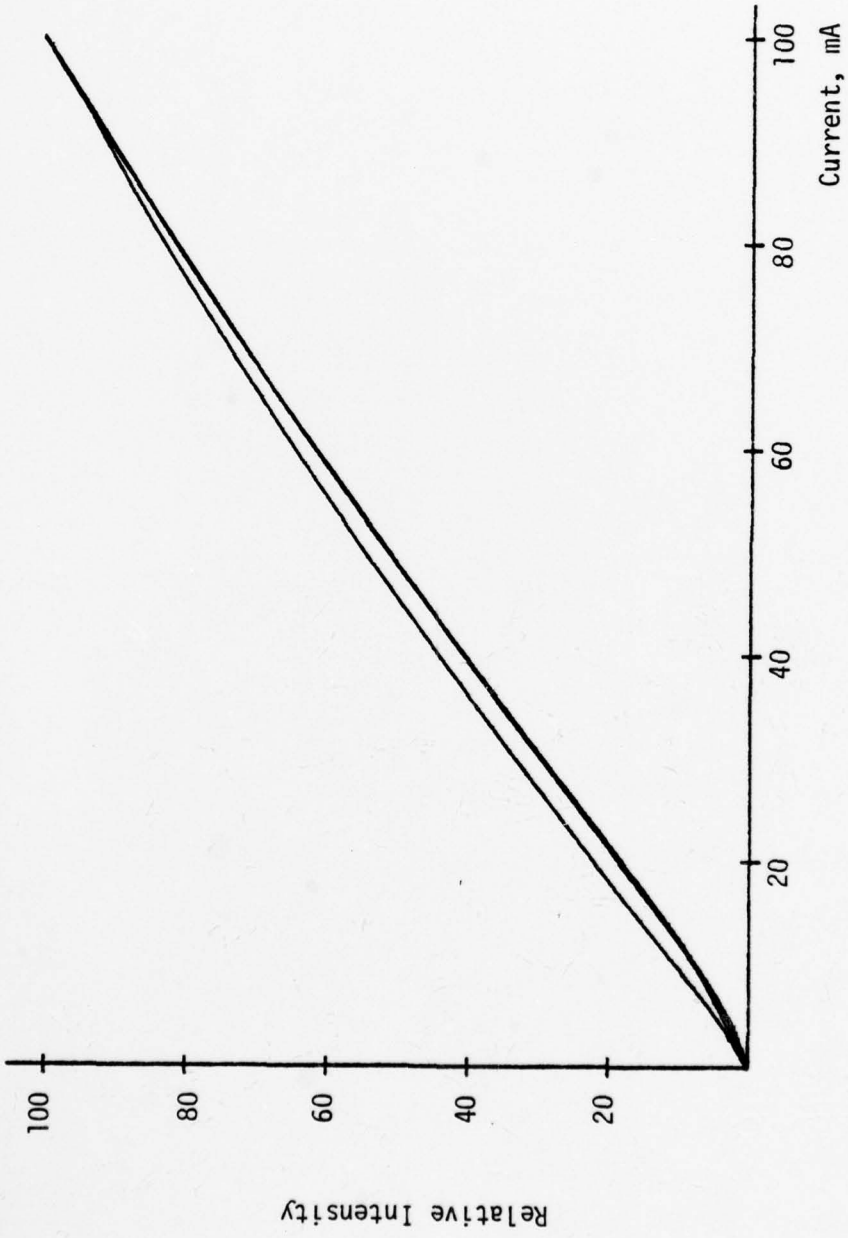

Figure 3-6. Static Characteristics of Four ME7124 LEDS.

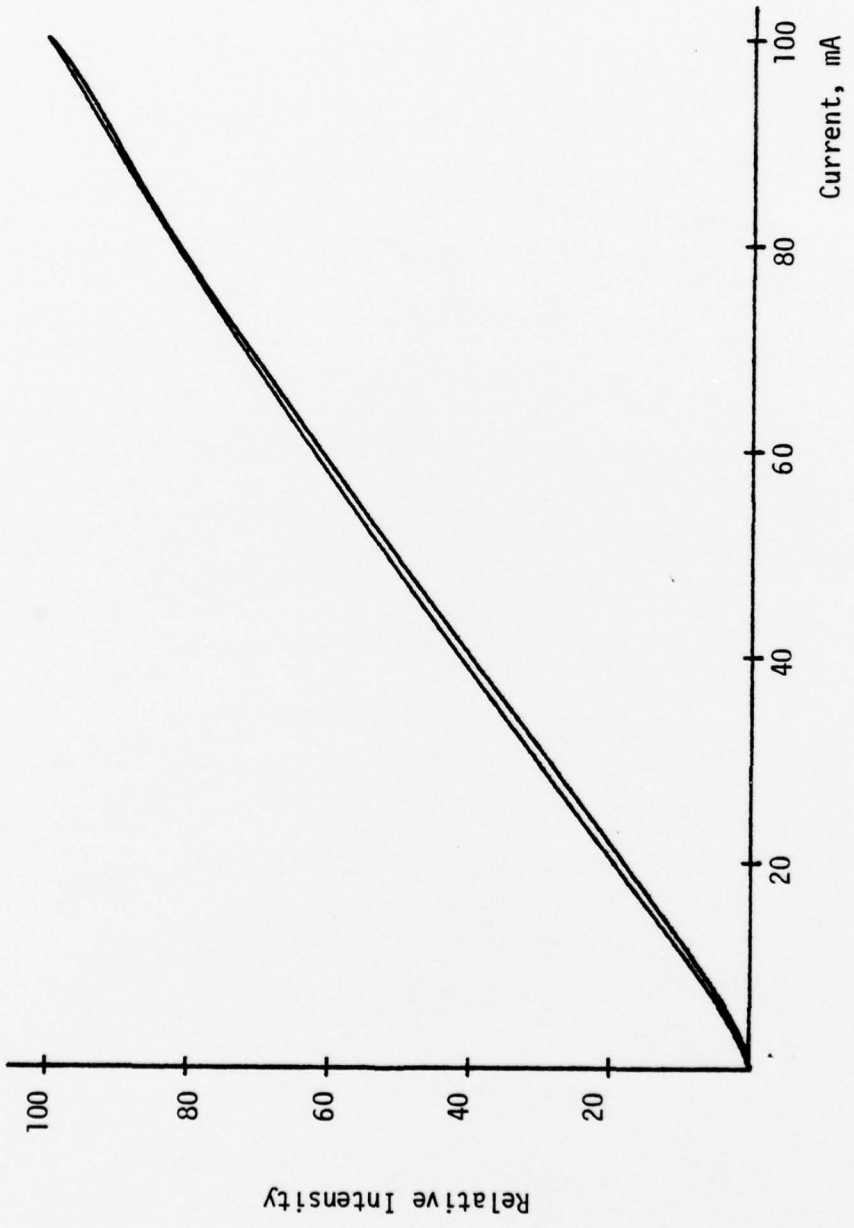

Figure 3-7. Static Characteristics of Two TIL31 LEDS.

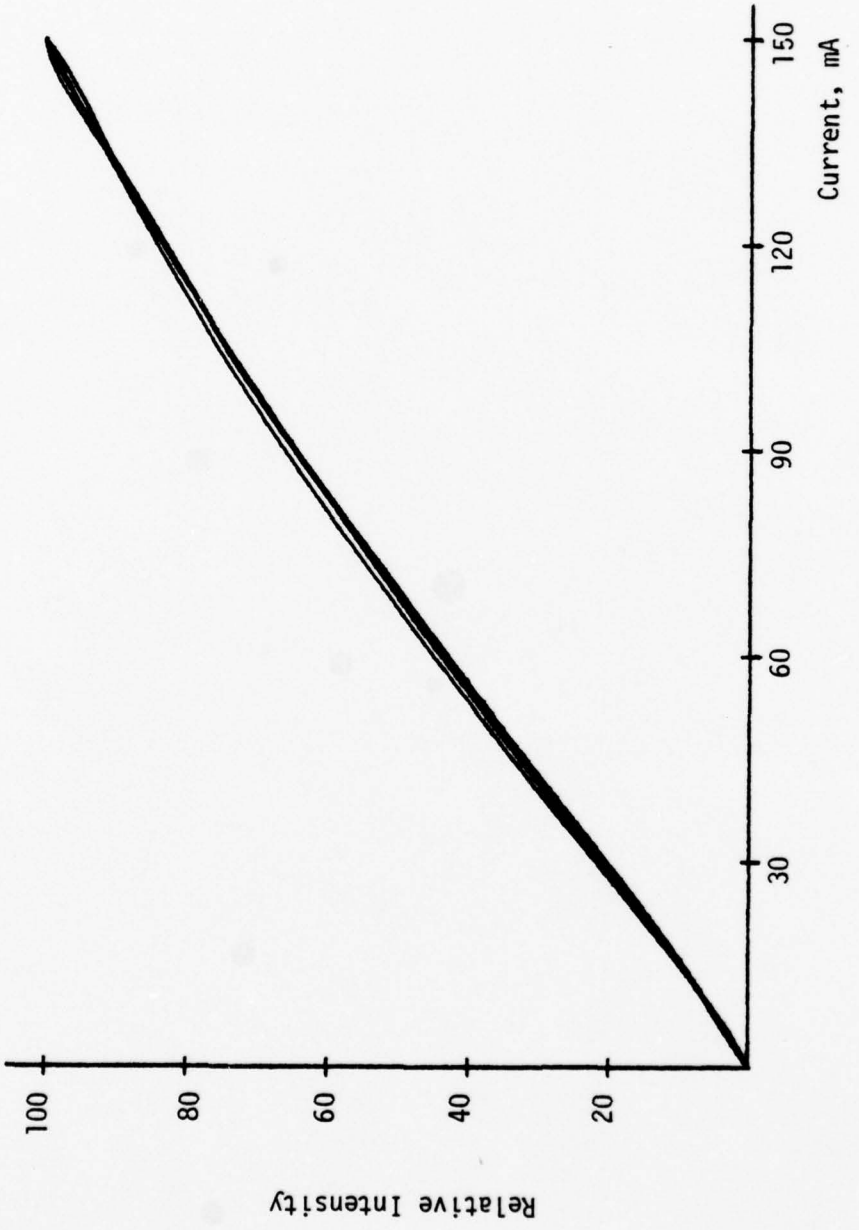

Figure 3-8. Static Characteristics of Four FPE500 LEDS.

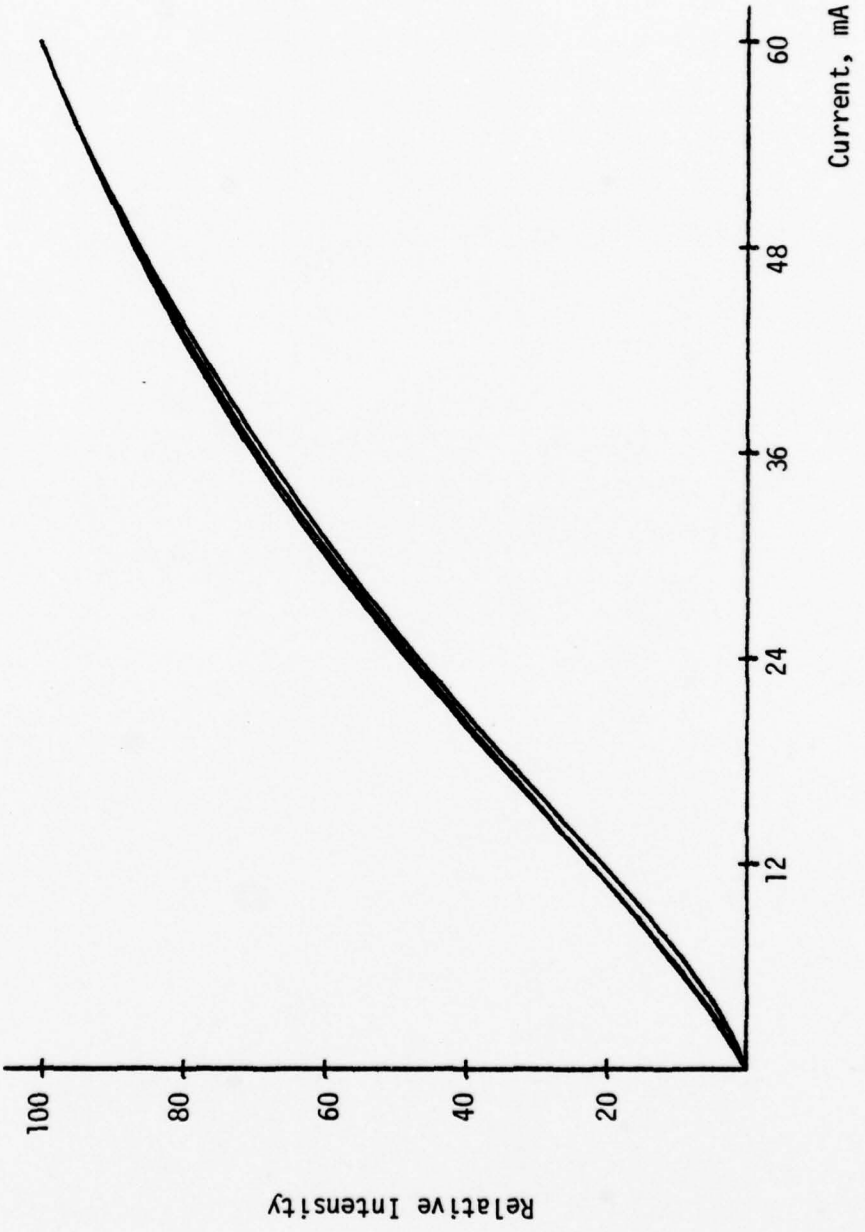

Figure 3-9. Static Characteristics of Four HEMT3300 LEDS.

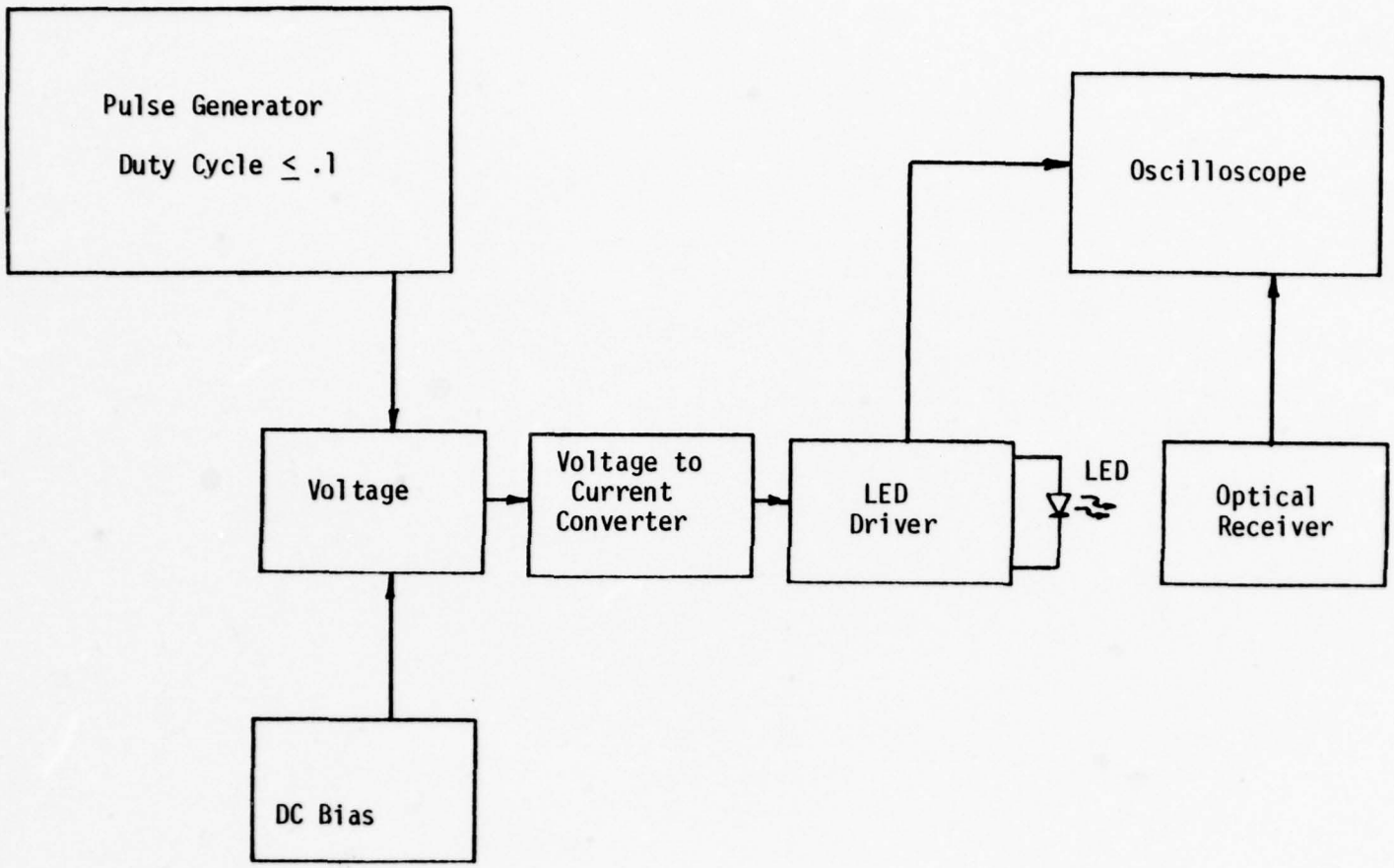

Figure 3-10. Block Diagram for Measuring LED Dynamic Characteristic.

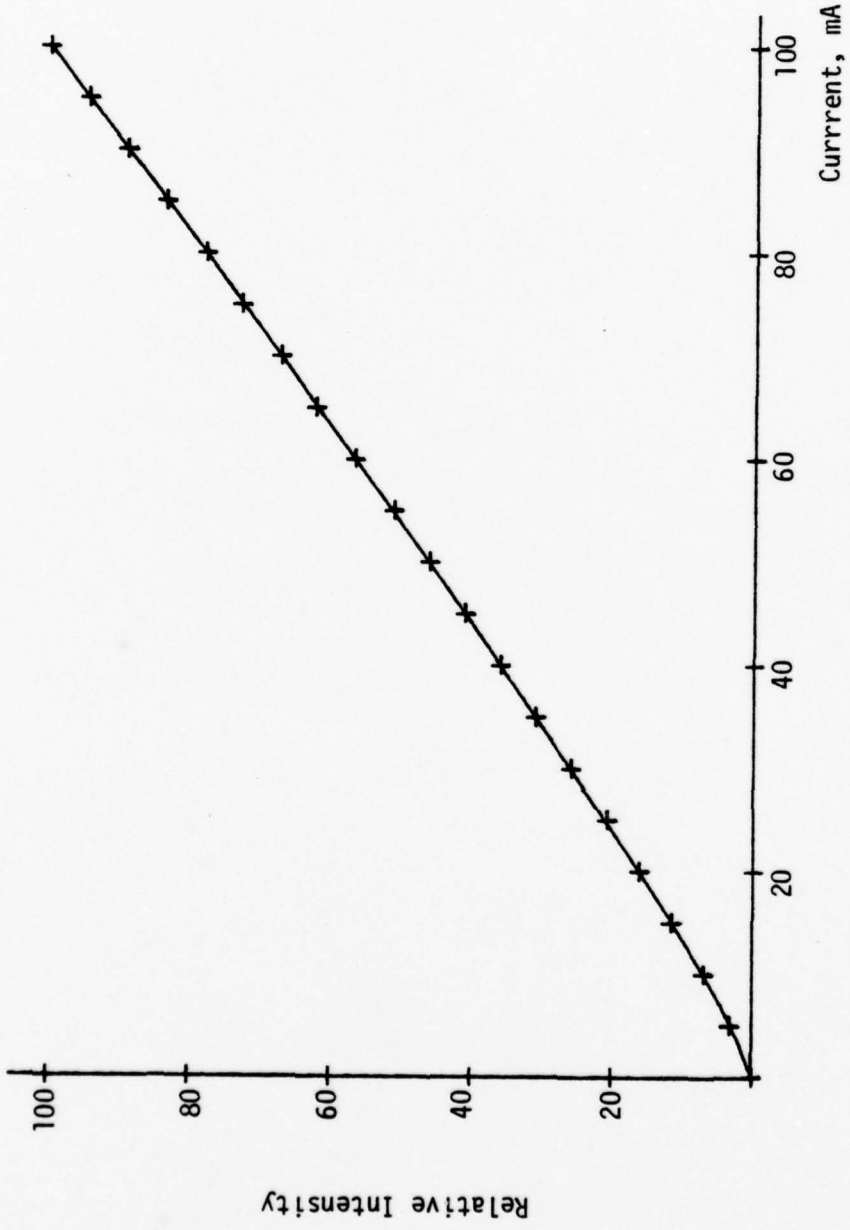

Figure 3-11. Best Fit Curve and Measured Data Points for the Dynamic Characteristic of One FLV104 LED.

TABLE 3-2

FOURTH ORDER COEFFICIENTS OF BEST FIT OF THE DYNAMIC CHARACTERISTICS OF 26 LEDS

LED	A_o	A_1	A_2	A_3	A_4
FLV104#1	46.2398	1.04832	4.18929E-04	-1.84400E-05	4.29682E-07
FLV104#2	45.5605	1.08294	7.09863E-04	-3.26690E-05	4.23832E-07
FLV104#3	44.7449	1.06709	1.21860E-03	-2.70223E-05	3.49650E-07
FLV104#4	45.6057	1.08086	7.81013E-04	-3.16653E-05	3.85833E-07
FPE104#1	46.8237	1.06878	3.55403E-04	-2.62328E-05	3.67612E-07
FPE104#2	47.4213	1.06419	-1.57045E-04	-2.50735E-05	4.68403E-07
FPE104#3	46.1700	1.06783	4.76175E-04	-2.58101E-05	4.18178E-07
FPE104#4	46.8727	1.05646	1.18436E.04	-2.16940E-05	4.49327E-07
ME7024#1	52.4451	1.08467	-3.04112E-03	-3.25958E-05	8.16148E-07
ME7024#2	49.9006	1.08897	-1.80011E-03	-3.58186E-05	7.26993E-07
ME7024#3	49.7484	1.07265	-9.17447E-04	-2.81757E-05	4.03905E-07
ME7024#4	48.4033	1.07616	-8.70418E-04	-2.98919E-05	6.02542E-07
ME7124#1	47.0512	1.09594	-2.47600E-04	-3.71171E-05	5.60862E-07
ME7124#2	46.8019	1.10956	-1.32048E-04	-4.29346E-05	5.58235E-07
ME7124#3	49.3116	1.05797	-1.21000E-03	-2.16260E-05	5.88490E-07
ME7124#4	47.1159	1.08897	-3.79358E-04	-3.40852E-05	6.04750E-07
TIL31#1	46.5423	1.09627	6.20595E-05	-3.77710E-05	5.12600E-07
TIL31#2	47.7888	1.06210	-3.75584E-04	-2.37520E-05	4.97121E-07
FPE500#1	46.7793	.680252	2.03082E-04	-8.47255E-06	4.60558E-08
FPE500#2	47.2649	.666316	1.34053E-04	-6.35053E-06	4.52573E-08
FPE500#3	47.6364	.666662	3.05660E-05	-6.35702E-06	5.25736E-08
FPE500#4	47.0417	.660663	3.06799E-04	-5.32284E-06	2.46388E-08
HEMT3300#1	46.0329	1.81995	-8.09578E-04	-1.69638E-04	5.78292E-06
HEMT3300#2	45.2755	1.87403	3.70282E-04	-2.29743E-04	5.41117E-06
HEMT3300#3	44.2039	1.81628	3.92816E-03	-1.64609E-04	2.80585E-06
HEMT3300#4	45.7850	1.87810	-2.60396E-04	-2.33249E-04	5.49399E-06

TABLE 3-3

SIXTH ORDER COEFFICIENTS OF BEST FIT OF THE DYNAMIC CHARACTERISTICS OF 26 LEDS

LED	A_o	A_1	A_2	A_3	A_4	A_5	A_6
FLV104#1	46.1625	1.03283	1.02445E-03	7.28480E-06	-2.37936E-07	-8.12363E-09	1.76959E-10
FLV104#2	45.5200	1.07322	1.02757E-03	-1.65226E-05	7.35495E-08	-5.09887E-09	9.28459E-11
FLV104#3	44.6466	1.06981	1.98894E-03	-3.15330E-05	-4.99685E-07	1.42442E-09	2.25125E-10
FLV104#4	45.5503	1.06411	1.21506E-03	-3.85744E-06	-9.27249E-08	-8.78143E-09	1.26847E-10
FPE104#1	46.8487	1.04166	1.59470E-04	1.88244E-05	5.83639E-07	-1.42286E-08	-5.72601E-11
FPE104#2	47.3058	1.05335	7.48372E-04	-7.07833E-06	-5.29865E-07	-5.68269E-09	2.64601E-10
FPE104#3	46.1057	1.04378	9.80920E-04	1.41305E-05	-1.38329E-07	-1.26128E-08	1.47508E-10
FPE104#4	46.8178	1.04075	5.49579E-04	4.39006E-06	-2.60295E-08	-8.23707E-09	1.25998E-10
ME7024#1	52.3033	1.05908	-1.92875E-03	9.91590E-06	-4.10300E-07	-1.34247E-08	3.25083E-10
ME7024#2	49.7464	1.09595	-5.91296E-04	-4.74211E-05	-6.05783E-07	3.66396E-09	3.53266E-10
ME7024#3	49.6831	1.05602	-4.05363E-04	-5.42536E-07	-1.60694E-07	-8.72625E-09	1.49653E-10
ME7024#4	48.3771	1.06429	-6.64204E-04	-1.01818E-05	3.75180E-07	-6.22424E-09	6.02645E-11
ME7124#1	46.8889	1.07156	1.02554E-03	3.38700E-06	-8.42834E-07	-1.27908E-08	3.72064E-10
ME7124#2	46.6953	1.08957	7.04035E-04	-9.73349E-06	-3.63589E-07	-1.04845E-08	2.44339E-10
ME7124#3	49.2185	1.02938	-4.80076E-04	2.58725E-05	-2.16284E-07	-1.49995E-08	2.13314E-10
ME7124#4	46.9864	1.05871	6.35974E-04	1.61841E-05	-5.14705E-07	-1.58745E-08	2.96723E-10
TIL31#1	46.2403	1.08354	2.43060E-03	-1.66258E-05	-2.09884E-06	-6.67744E-09	6.92188E-10
TIL31#2	47.6554	1.04037	6.71119E-04	1.23263E-05	-6.56923E-07	-1.13931E-08	3.05891E-10
FPE500#1	46.6001	.669504	7.68049E-04	-1.52975E-06	-2.01164E-07	-8.44394E-10	2.56549E-11
FPE500#2	47.1603	.658394	4.63969E-04	-1.23384E-06	-9.91082E-08	-6.22300E-10	1.49813E-11
FPE500#3	47.5672	.654900	2.48655E-04	1.24070E-06	-4.28585E-08	-9.24047E-10	9.90333E-12
FPE500#4	47.1100	.640789	9.12669E-05	7.51462E-06	1.18952E-07	-1.56131E-09	-9.78719E-12
HEMT3300#1	45.8015	1.80407	5.04670E-03	-9.54186E-05	-1.37830E-05	-6.36165E-08	1.48431E-08
HEMT3300#2	45.1128	1.85840	4.49036E-03	-1.56645E-04	-8.35406E-06	-6.26559E-08	1.04426E-08
HEMT3300#3	44.4444	1.77778	-2.16050E-03	1.54265E-05	2.31482E-05	-1.54316E-08	-1.54321E-08
HEMT3300#4	45.8015	1.83842	-6.78487E-04	-4.77250E-05	6.89083E-06	-1.59020E-07	-1.05968E-09

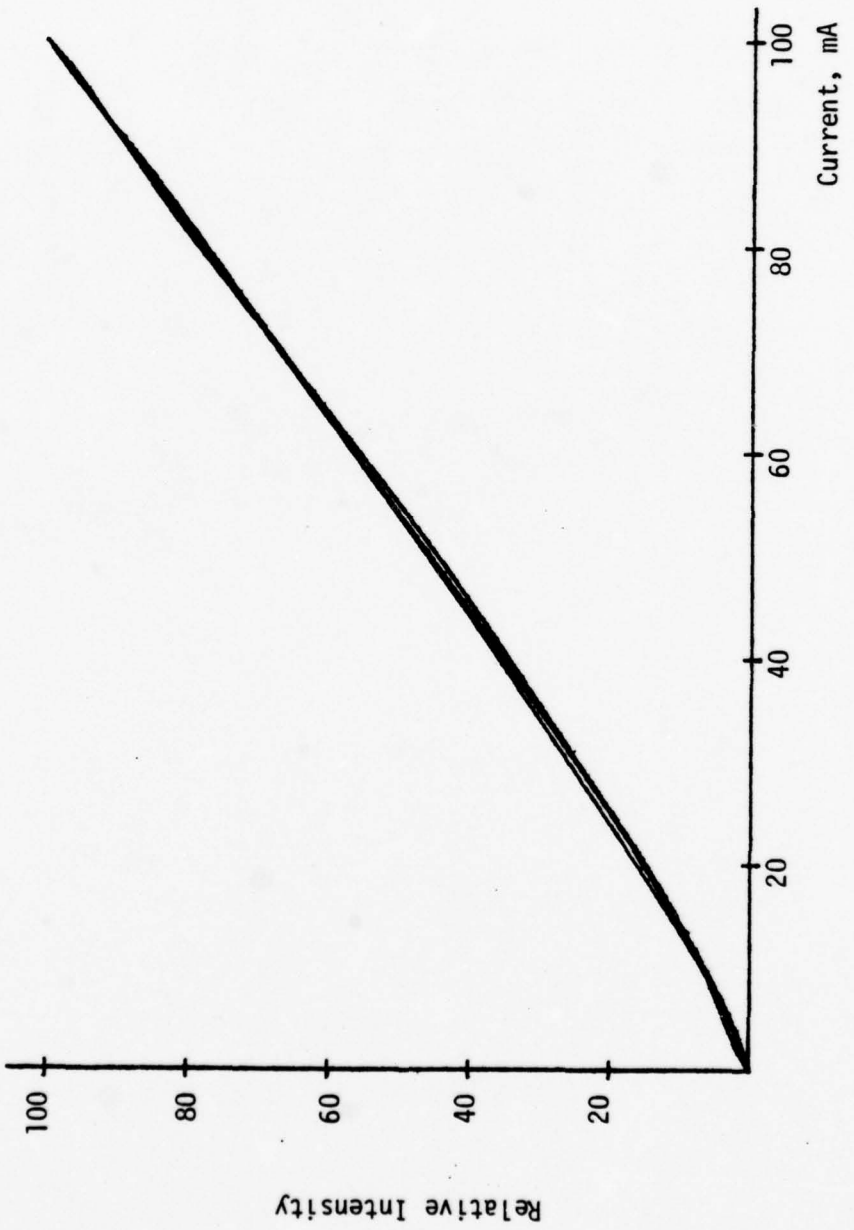

Figure 3-12. Dynamic Characteristic of Four FLV104 LEDS.

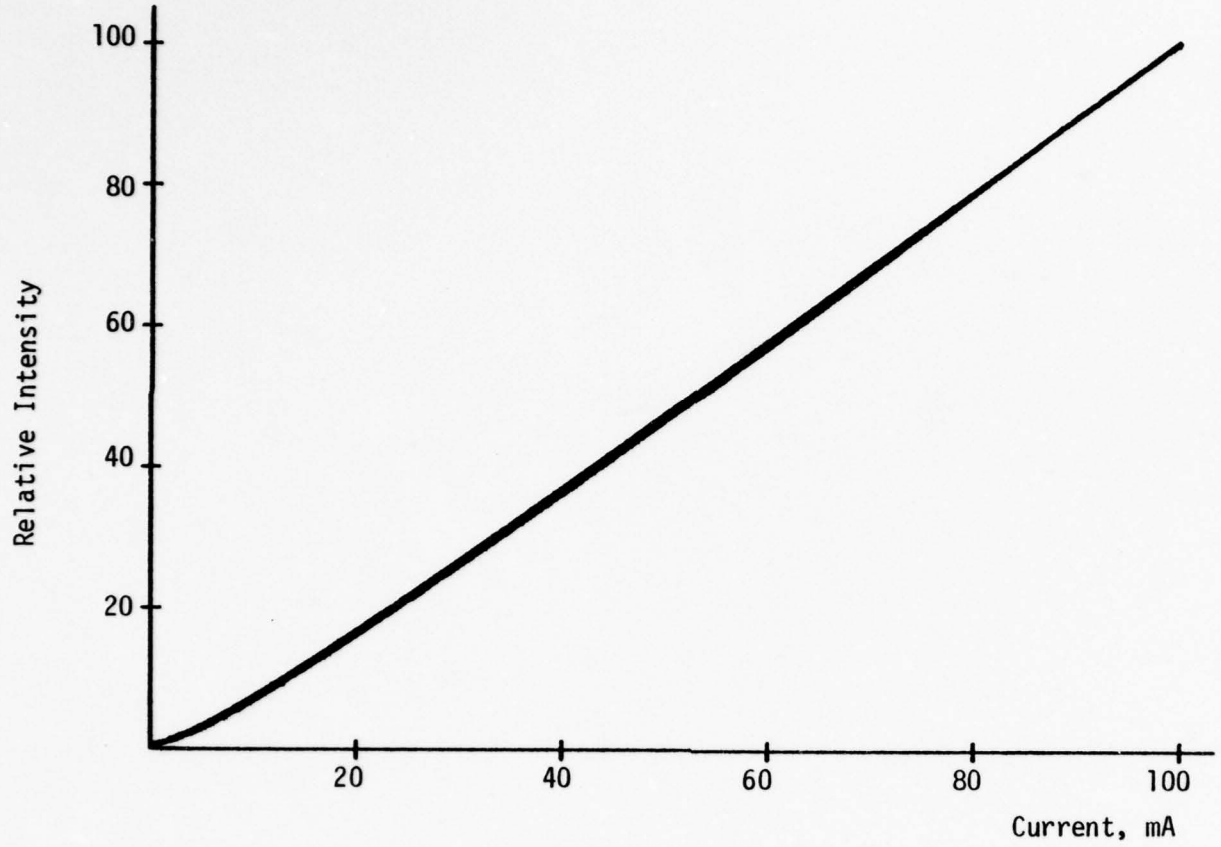

Figure 3-13. Dynamic Characteristics of Four FPE104 LEDS.

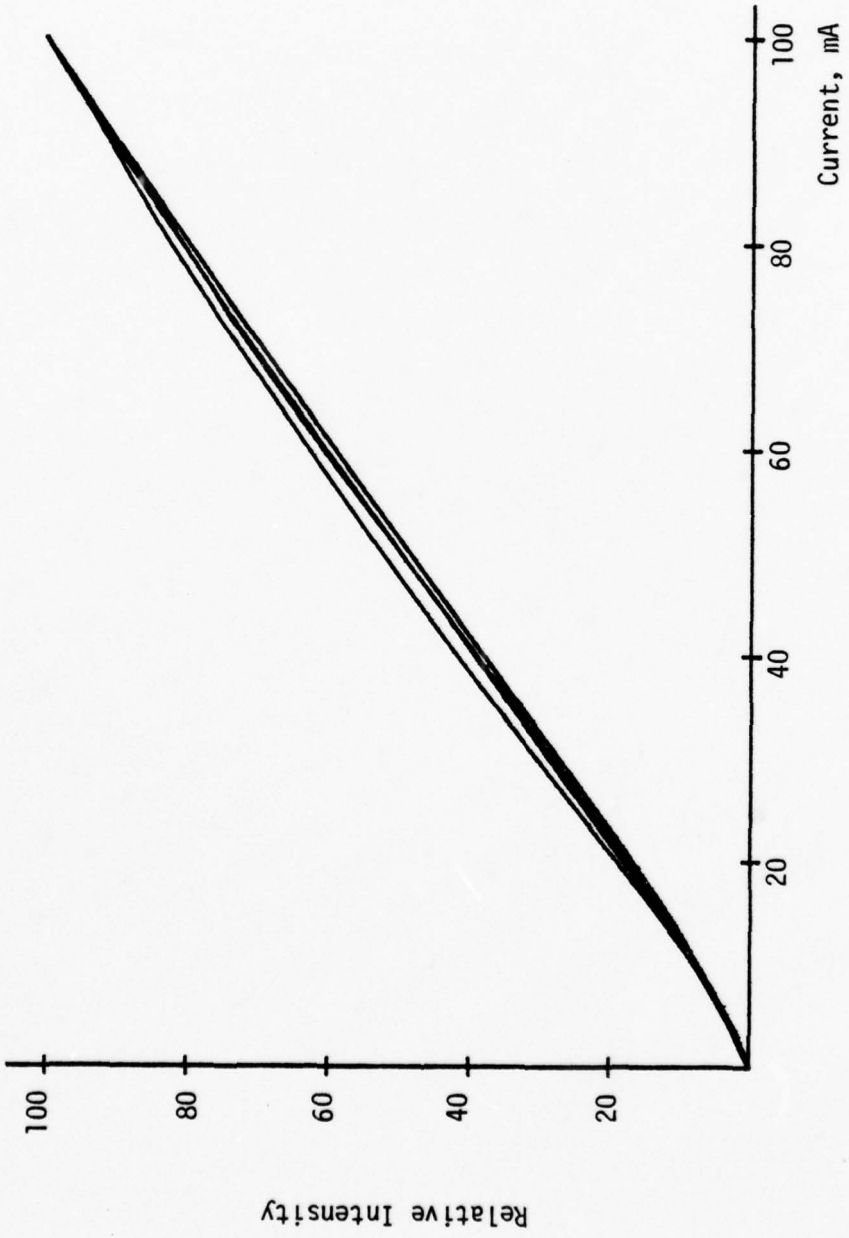

Figure 3-14. Dynamic Characteristics of Four ME7024 LEDS.

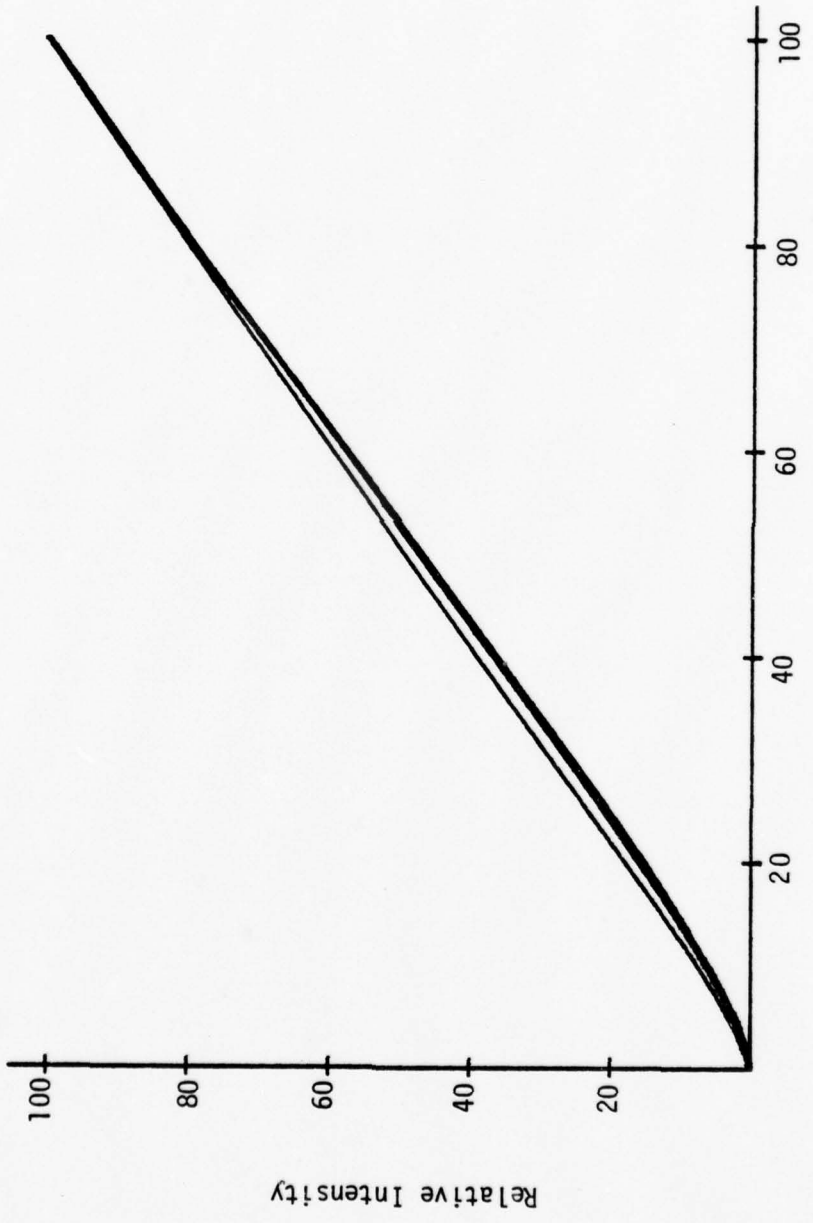

Figure 3-15. Dynamic Characteristics of Four ME7124 LEDS.

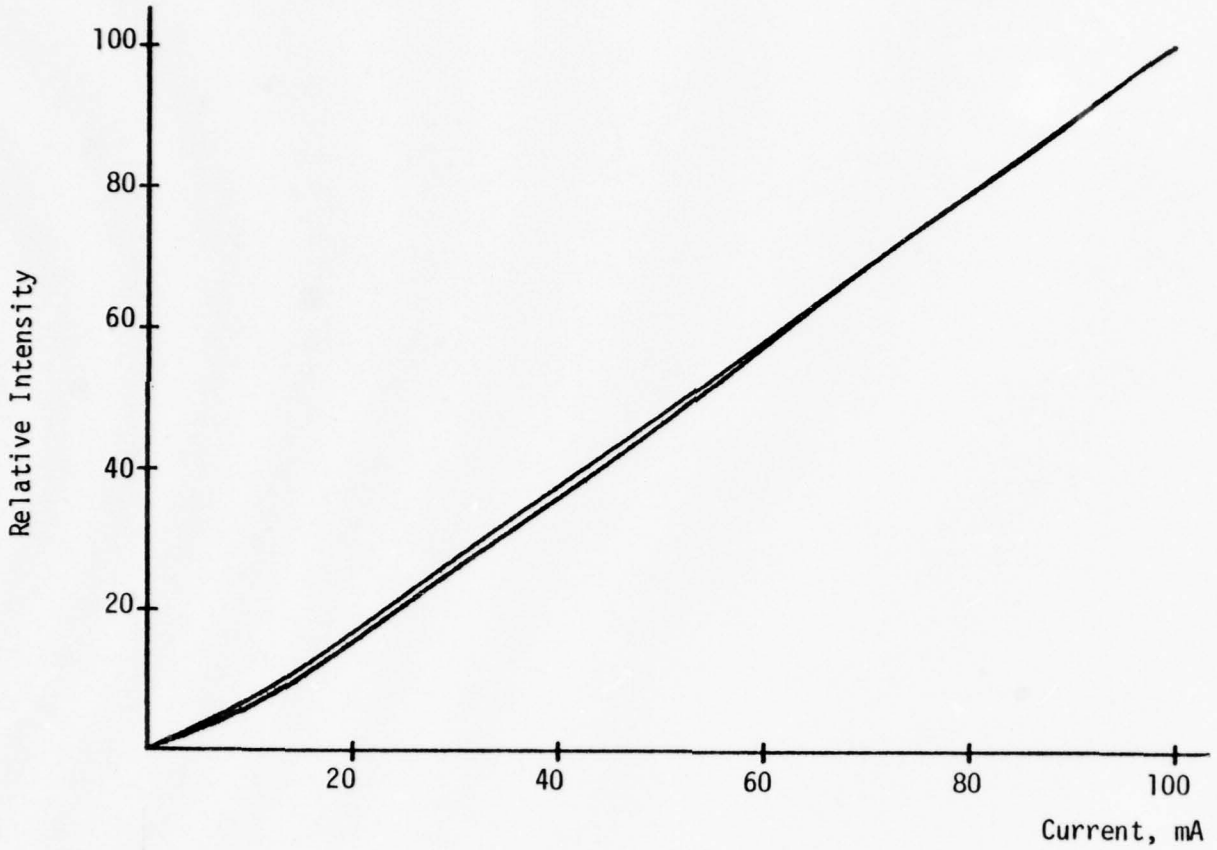

Figure 3-16. Dynamic Characteristics of Two TIL31 LEDS.

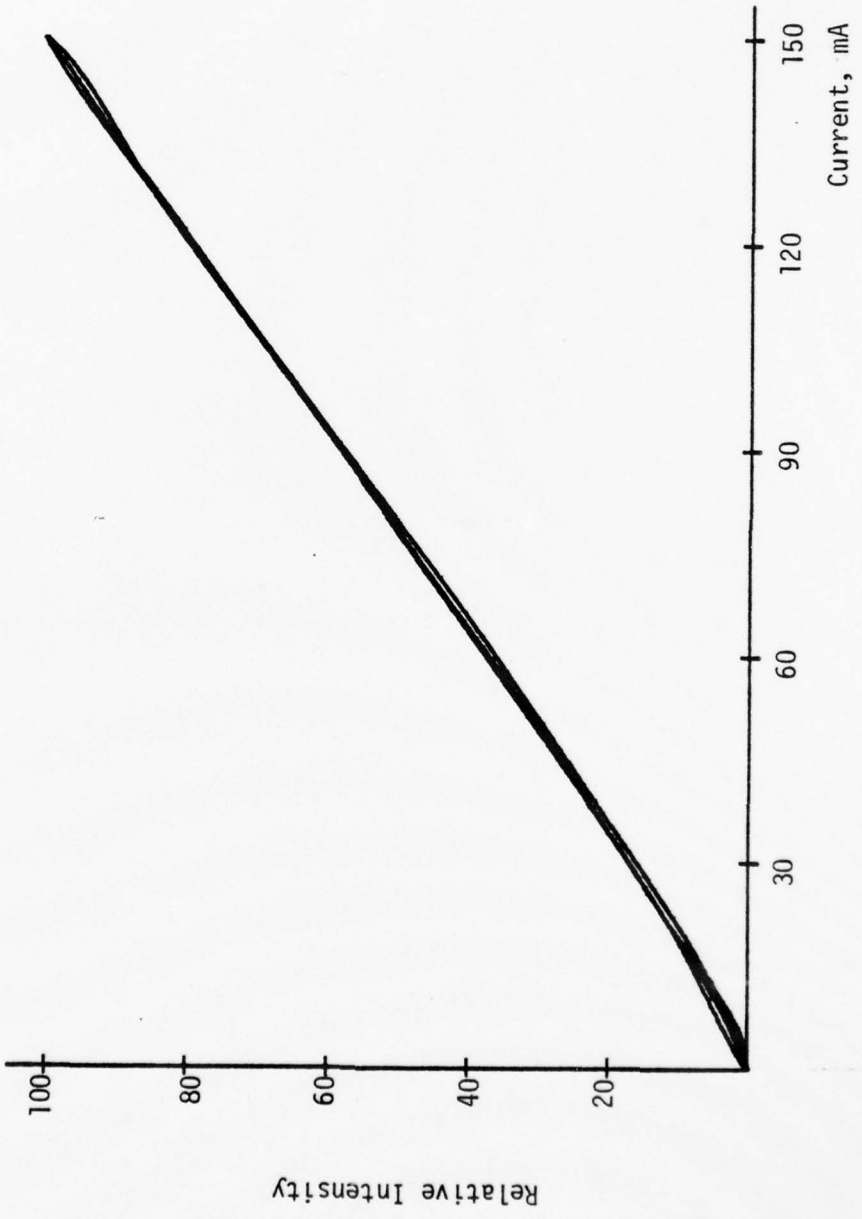

Figure 3-17. Dynamic Characteristics of Four FPE500 LEDS.

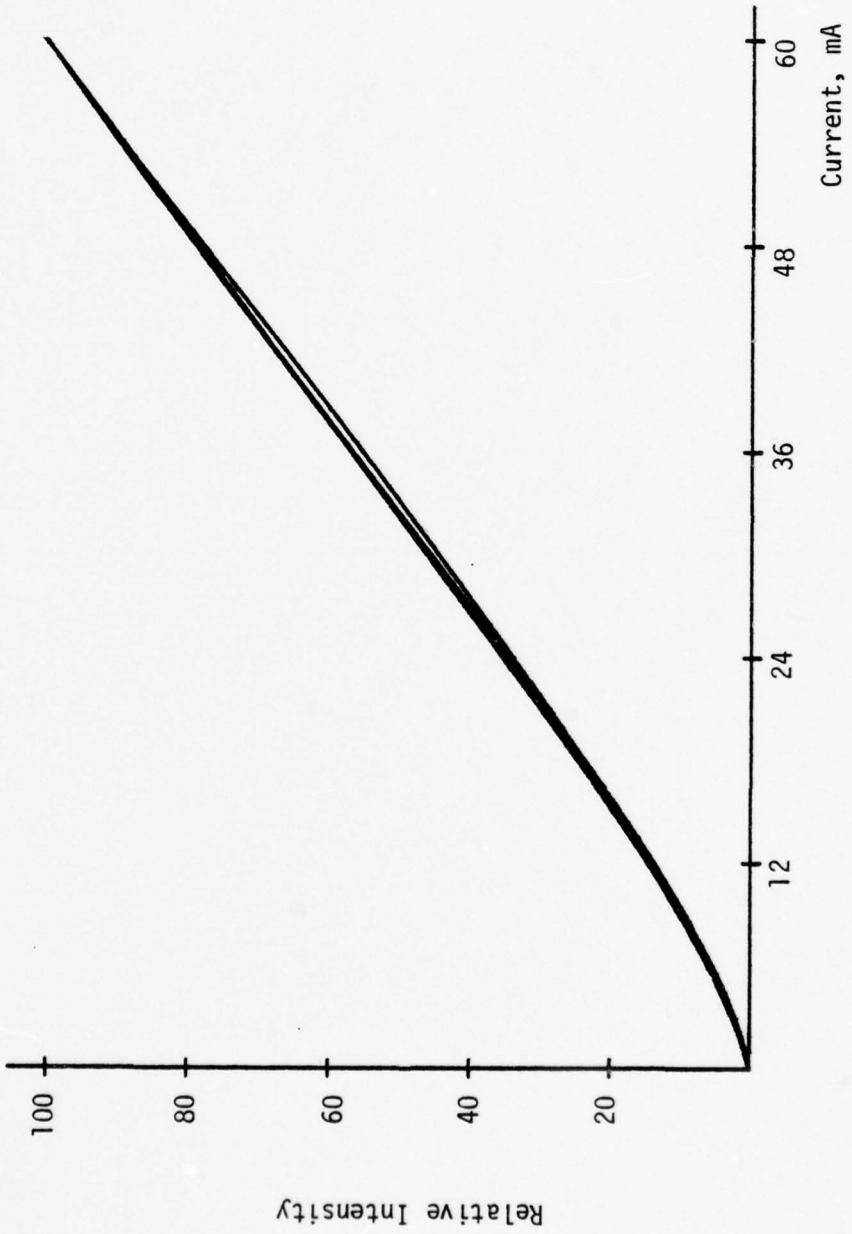

Figure 3-18. Dynamic Characteristics of Four HEMT3300 LEDS.

Figure 3-19 is an example of an LED showing both its static and dynamic characteristics. For the most part, the two curves are not the same. The curves describing the static and dynamic characteristics for all the LEDS considered in this study were found to be different. Attention is therefore concentrated on the dynamic characteristic, since it is this curve which represents the transfer function for the LED when modulated by some time varying source.

The optical output of a LED may be modulated by the current from a signal source. This current is summed with the bias current flowing through the LED. The ratio of the amplitude of the optical variation produced by the modulating current to the constant optical output produced by the bias current is a measure of the depth of modulation and may be expressed as a percent modulation. For a linear characteristic, or to a good approximation for a near linear characteristic, this percent modulation is the ratio of the amplitude of the modulating current to the bias current. At 100 percent modulation the total current through the LED varies from zero to twice the bias current.

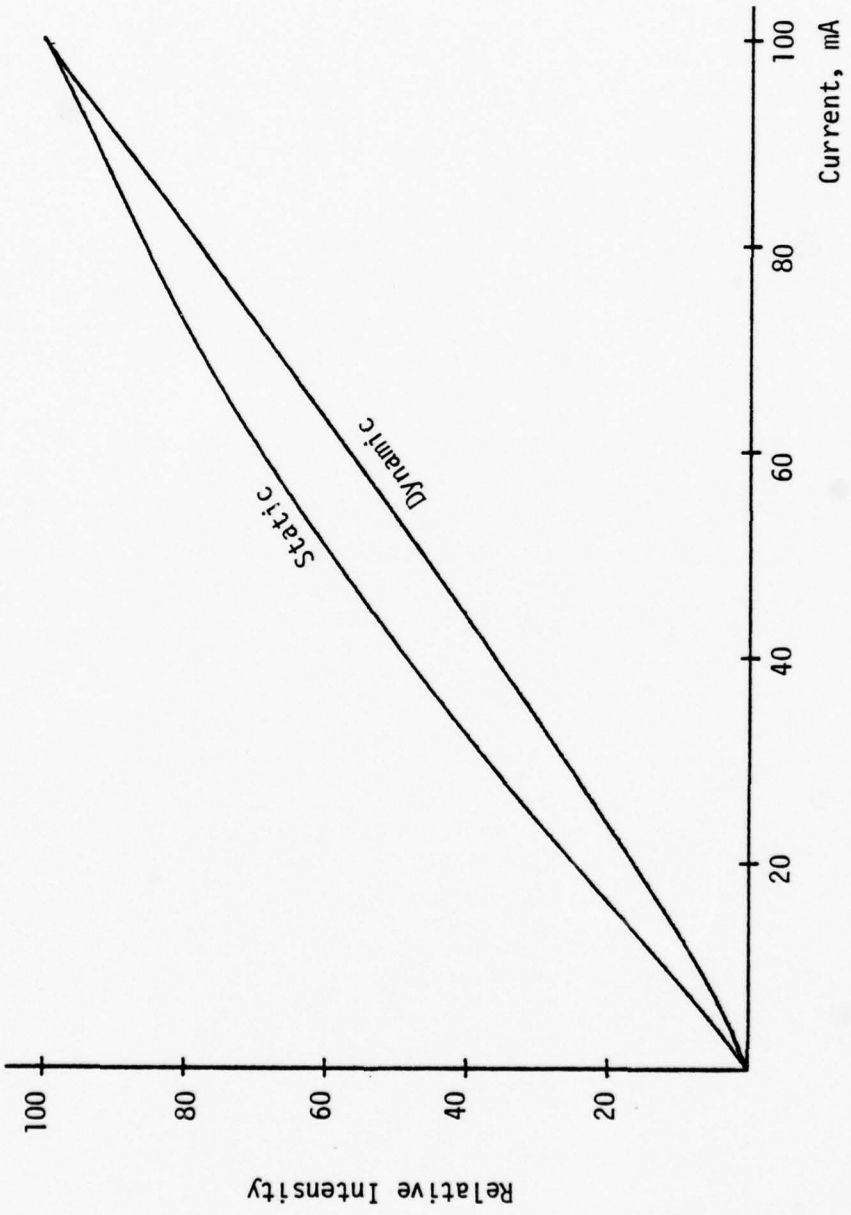

Figure 3-19. Static and Dynamic Characteristic of One FLV104 LED.

CHAPTER 4

INTERMODULATION DISTORTION

The light-emitting diode may be biased with a dc current in the vicinity of the middle of the characteristic. A modulating current may then be applied yielding an intensity modulation in the optical output. The modulating current "i" may be expressed as:

$$i = I - I_{DC} \tag{2}$$

where I is the total current and I_{DC} is the bias current. A polynomial expressing the relative optical intensity, p, in terms of the modulating current is:

$$p(i) = A_0 + A_1 i + A_2 i^2 + A_3 i^3 + \ldots \tag{3}$$

where "i" is in mA. This transfer function between modulating current and the varying intensity of light is described by the dynamic characteristic of the LEDS. The coefficients of Eq. (3) have been determined for specific LEDS in Chapter 3 and are outlined in Table 3-3 where the bias current

$$I_{bias} = I_{max/2} \tag{4}$$

for the particular LEDS. A sixth order polynomial is adequate in describing the LED characteristic so that:

$$p(i) = A_0 + A_1 i + A_2 i^2 + A_3 i^3 + A_4 i^4 + A_5 i^5 + A_6 i^6 \tag{5}$$

For a sinusoidal modulating current with two frequency components, "i" may be expressed as:

$$i = I_1 \cos\omega_1 t + I_2 \cos\omega_2 t \tag{6}$$

substituting Eq. (6) into Eq. (5) yields:

$$p(i) = \sum_{n=o}^{6} A_n \left(I_1 \cos \omega_1 t + I_2 \cos \omega_2 t\right)^n \tag{7}$$

Applying the binomial theorem to Eq. (7) yields:

$$p(i) = \sum_{n=o}^{6} A_n \sum_{m=o}^{n} \binom{n}{m} I_1^{n-m} I_2^{m} \cos^{n-m} \omega_1 t \cos^{m} \omega_2 t \tag{7a}$$

where $\binom{n}{m} = \dfrac{n!}{m!(n-m)!}$

Writing the cosine terms in their exponential form and again applying the binomial theorem yields:

$$p(i) = \sum_{n=o}^{6} \frac{A_n}{2^n} \sum_{m=o}^{n} \binom{n}{m} I_1^{n-m} I_2^{m} \sum_{\ell=o}^{n-m} \sum_{k=o}^{m} \binom{n-m}{\ell} \binom{m}{k} \cdot$$

$$e^{j[(n-m-2\ell)\omega_1 t + (m-2k)\omega_2 t]} \tag{8}$$

which reduces to

$$p(i) = \sum_{n=o}^{6} \frac{A_n}{2^n} \sum_{m=o}^{n} I_1^{n-m} I_2^{m} \sum_{\ell=o}^{n-m} \sum_{k=o}^{m} \frac{n!}{\ell!k!(m-k)!(n-m-\ell)!}$$

$$\cdot \cos\left[(n-m-2\ell)\omega_1 t + (m-2k)\omega_2 t\right] \tag{8a}$$

Letting $I_2 = I_1 = I$ yields:

$$p(i) = \sum_{n=o}^{6} \frac{A_n I^n}{2^n} \sum_{m=o}^{n} \sum_{\ell=o}^{n-m} \sum_{k=o}^{m} \frac{n!}{\ell!k!(m-k)!(n-m-\ell)!} \tag{9}$$

$$\cdot \cos[(n-m-2\ell)\omega_1 t + (m-2k)\omega_2 t]$$

The amplitude of the ω_1 term may be found by letting $n-m-2\ell=\pm 1$ and $m-2k=o$. This results in an amplitude of

$$A_1 + \frac{9}{4} A_3 I^2 + \frac{25}{4} I^4.$$

The amplitude of the ω_2 term may be found by letting n-m-2ℓ=o and m-2k=$\pm$1. This also results in an amplitude of

$$A_1 + \frac{9}{4} A_3 I^2 + \frac{25}{4} I^4.$$

The amplitude of the $\omega_1+\omega_2$ term may be found by letting n-m-2ℓ=1 with m-2k=1 and n-m-2ℓ=-1 with m-2k=-1. This results in an amplitude of

$$A_2 I + 3A_4 I^3 + \frac{75}{8} A_6 I^5.$$

Amplitudes of higher order terms may be found in a similar manner.

The value of the first order intermodulation distortion is then

$$\frac{\text{Amplitude of } \omega_1+\omega_2 \text{ terms}}{\text{Amplitude of } \omega_1 \text{ and } \omega_2 \text{ terms}} = \frac{A_2 I + 3A_4 I^3 + \frac{75}{8} A_6 I^5}{A_1 + \frac{9}{4} A_3 I^2 + \frac{25}{4} A_5 I^4} \qquad (10)$$

Higher order intermodulation terms are listed in Table 4-1. Since the intermodulation distortion and percent modulation are both functions of I, the intermodulation distortion may be plotted as a function of percent modulation using current modulation. Figure 4-1 illustrates typical intermodulation distortion curves of an LED. The crosses represent the measured values of the first order intermodulation distortion levels. While not necessarily typical, Figure 4-2 represents the intermodulation characteristics together with the measured values of the first order intermodulation components of another LED. Note that at higher depths of modulation, the first order IM term begins to decrease. The higher order

TABLE 4-1

INTERMODULATION DISTORTION AMPLITUDES

Frequency	Distortion
$\omega_1 \pm \omega_2$	$\dfrac{A_2 I + 3A_4 I^3 + \frac{75}{8} A_6 I^5}{A_1 + \frac{9}{4} A_3 I^2 + \frac{25}{4} A_5 I^4}$
$2\omega_1 \pm \omega_2, \omega_1 \pm 2\omega_2$	$\dfrac{\frac{3}{4} A_3 I^2 + \frac{25}{8} A_5 I^4}{A_1 + \frac{9}{4} A_3 I^2 + \frac{25}{4} A_5 I^4}$
$3\omega_1 \pm \omega_2, \omega_1 \pm 3\omega_2$	$\dfrac{\frac{1}{2} A_4 I^3 + \frac{25}{8} A_6 I^5}{A_1 + \frac{9}{4} A_3 I^2 + \frac{25}{4} A_5 I^4}$
$2\omega_1 \pm 2\omega_2$	$\dfrac{\frac{3}{4} A_4 I^3 + \frac{15}{4} A_6 I^5}{A_1 + \frac{9}{4} A_3 I^2 + \frac{25}{4} A_5 I^4}$
$4\omega_1 \pm \omega_2, \omega_1 \pm 4\omega_2$	$\dfrac{\frac{5}{16} A_5 I^4}{A_1 + \frac{9}{4} A_3 I^2 + \frac{25}{4} A_5 I^4}$
$3\omega_1 \pm 2\omega_2, 2\omega_1 \pm 3\omega_2$	$\dfrac{\frac{5}{8} A_5 I^4}{A_1 + \frac{9}{4} A_2 I^2 + \frac{25}{4} A_5 I^4}$
$5\omega_1 \pm \omega_2, \omega_1 \pm 5\omega_2$	$\dfrac{\frac{1}{2} A_6 I^5}{A_1 + \frac{9}{4} A_3 I^2 + \frac{25}{4} A_5 I^4}$
$4\omega_1 \pm 2\omega_2, 2\omega_1 \pm 4\omega_2$	$\dfrac{\frac{25}{32} A_6 I^5}{A_1 + \frac{9}{4} A_3 I^2 + \frac{25}{4} A_5 I^4}$
$3\omega_1 \pm 3\omega_2$	$\dfrac{\frac{5}{8} A_6 I^5}{A_1 + \frac{9}{4} A_3 I^2 + \frac{25}{4} A_5 I^4}$

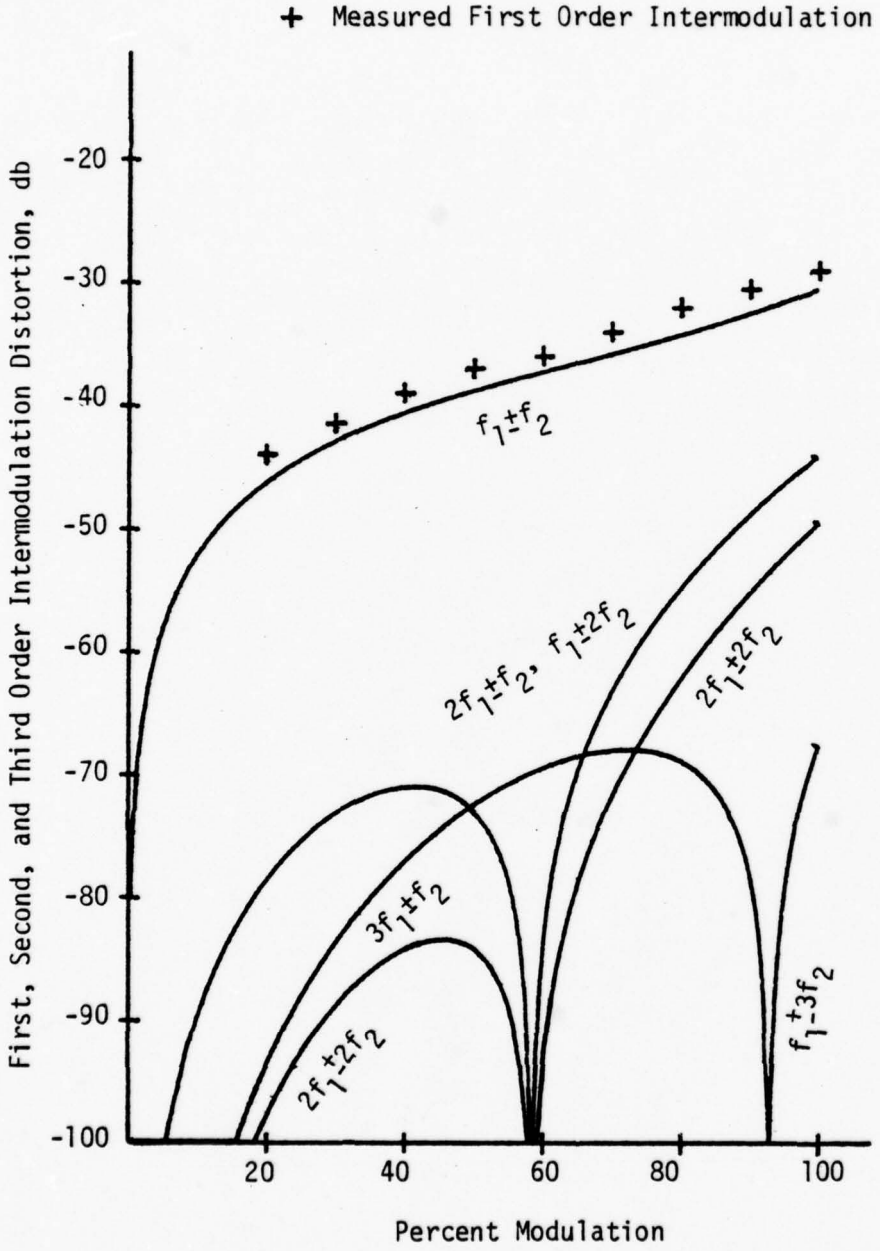

Figure 4-1. Intermodulation Distortion vs Percent Modulation for FLV104 Diode #1.

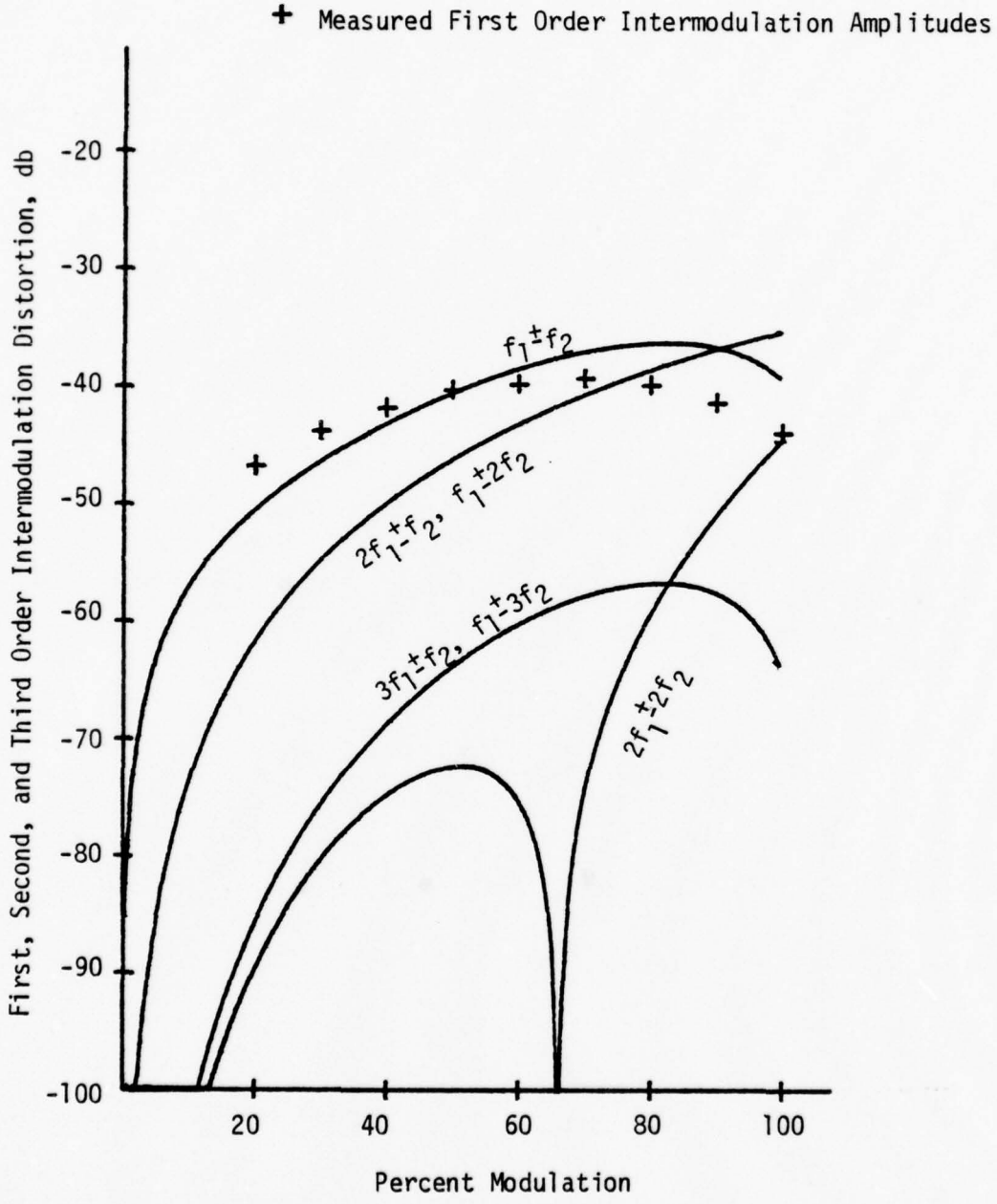

Figure 4-2. Intermodulation Distortion vs Percent Modulation for ME7024 Diode #2.

terms make dramatic increases at that point as can be seen from the graph. In good quality multichannel television, it is desired to keep intermodulation distortion at -45 db or lower. Of the diodes considered, this would limit modulation depths to around twenty percent.

CHAPTER 5

PREDISTORTION NETWORK

To compensate for the nonlinearity of the LED using the predistortion approach, a network which is complementary to the LEDS nonlinearity is used in series with the input. To get an exact complement of the LED characteristic would be difficult and may be very complex to realize. To simplify the analysis and the compensating network, a piecewise linear circuit is used. Figure 5-1 shows the general form for an "n" breakpoint piece-wise linear network.

For the network containing diodes with cutin voltage V_γ the breakpoints are set by adjusting the R_{N1} and R_{N2} so that the breakpoint voltage is

$$V_{BN} = E \frac{(R_{N2} - R_{N1})}{(R_{N1} + R_{N2})} \pm V_\gamma \tag{11}$$

The + sign is used when the cathode of the diode is toward the op amp. The - sign is used when the anode is toward the op amp. The capacitances make each of the breakpoints noninteractive. The change in slope is a function of the resistances R_N. The gain at any point is

$$A = \frac{V_o}{V_{in}} = - \frac{R_f}{R_{in}} . \tag{12}$$

The gain of the circuit will change when the input passes through a breakpoint. The change in gain is

$$\Delta A = \frac{-R_f}{R_{in}} \pm \frac{R_f}{(R_{in} \| R_N)} . \tag{13}$$

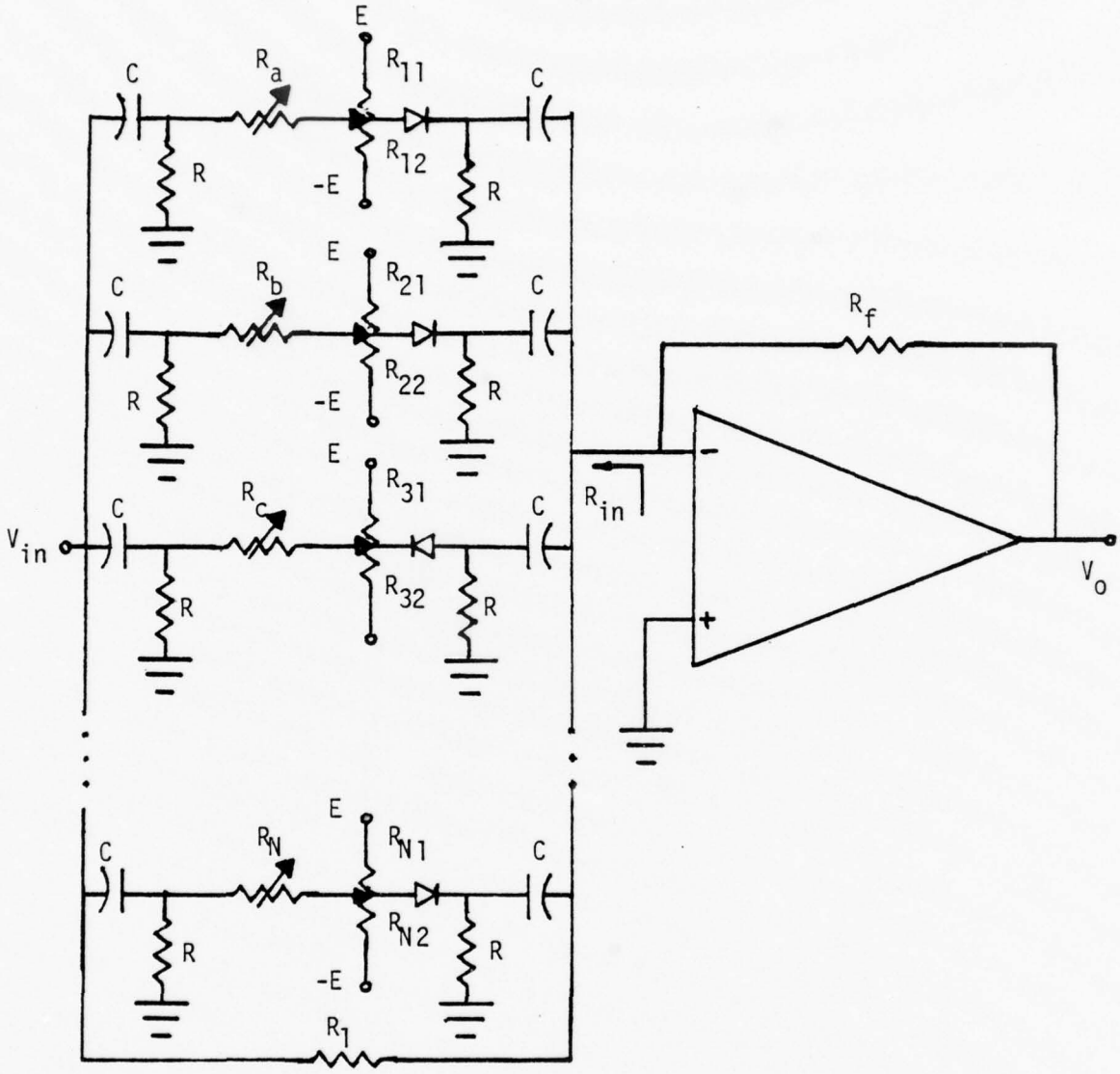

Figure 5-1. General n-Breakpoint Compensating Network.

The polarity of the second term depends on the direction of the diode and the direction that the input is passing through the breakpoint.

An nth order network is not an easy network with which to work. A one breakpoint network would simplify the compensating procedure if it does, in fact, satisfy the criteria. Figure 5-2 shows the configuration used as the simplified single breakpoint compensating network.

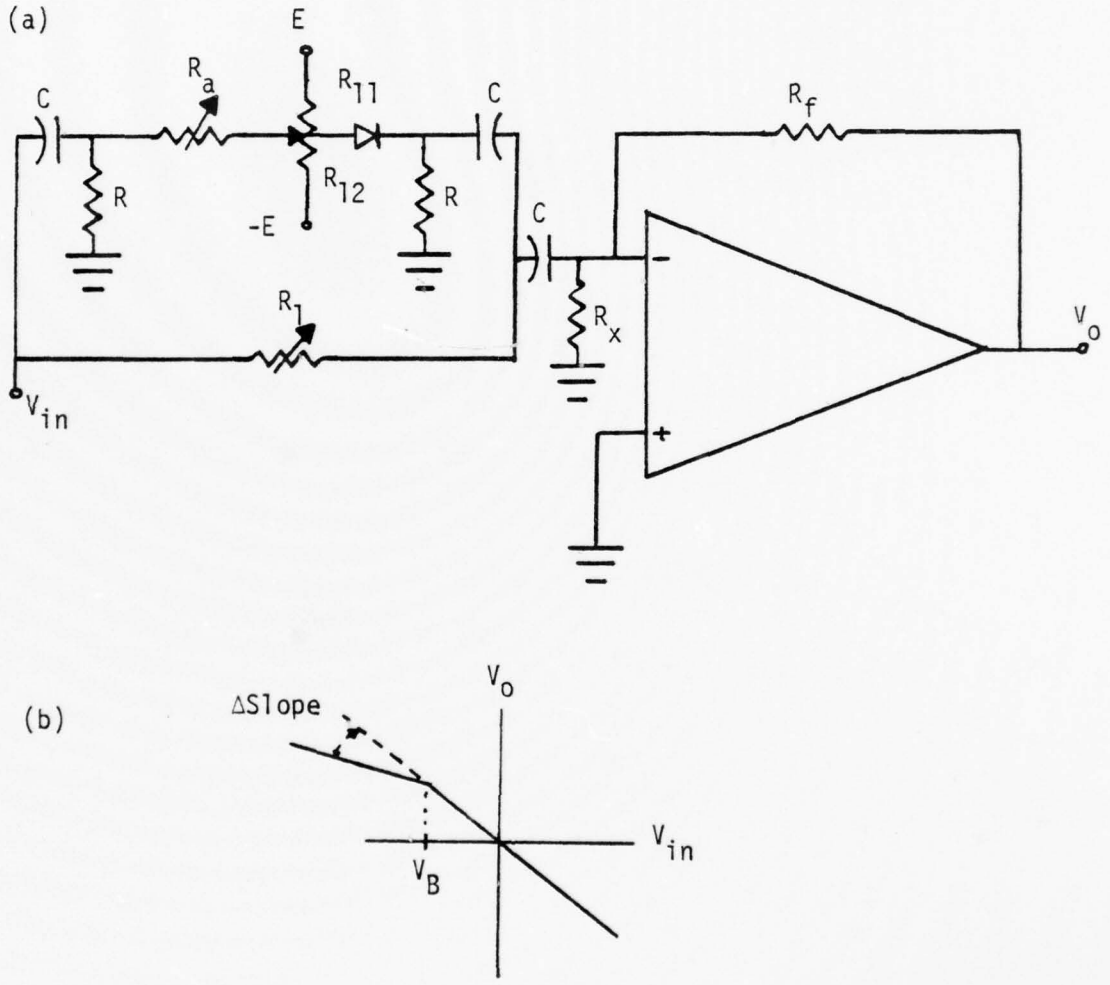

Figure 5-2. Simplified Single Breakpoint Compensating Network
a) Circuit Diagram, b) Transfer Function.

R_x represents a dc path to ground for the input of the op amp. The gain on one side of the breakpoint is

$$\text{Gain} = \frac{V_o}{V_{in}} = -\frac{R_f}{R_1} \tag{14}$$

The change in gain can be written as

$$\Delta \text{ Gain} = -\frac{R_f}{R_1} + \frac{R_f}{(R_1 \parallel R_A)} = \frac{R_f}{R_A} \tag{15}$$

The location of the breakpoint is described by

$$V_B = E\,\frac{(R_{12} - R_{11})}{(R_{11} + R_{12})} \pm V\gamma \tag{16}$$

The polarity of $V\gamma$ in Eq. (16) is determined by the direction of the diode as was the case in Eq. (11).

For a single breakpoint compensating network, the location of the breakpoint is best predicted to be at the same location as the dominant breakpoint of the diode characteristic. This is where the change in slope of the characteristic is greatest in magnitude. This is represented by maximums of the second derivative or zeroes of the third derivative of the LED characteristic. If a fourth order best fit curve is used to describe the characteristic, only one breakpoint is predicted. The fourth order best fit curve is used to locate the breakpoint by finding the zero of each of the third derivatives for all 26 LEDS. Since the breakpoints are given as currents from the bias point, the appropriate breakpoint voltage for the compensating network can be determined by

$$V_B = E\,\frac{(I_{Breakpoint})}{(I_{Max})} \pm V\gamma \tag{17}$$

where I_{Max} is the maximum allowable diode current and the polarity of $V\gamma$ is determined by the direction of the diode in the compensating network. The change in slope is adjusted by R_a so as to maximize the

performance of the compensating network by minimizing the intermodulation distortion of the received signal.

The location of breakpoints and the change in gain for each LED are given in Table 5-1. Using these values in the compensating network, yielded an average of an overall 8 db reduction in the first order intermodulation terms as compared to the distortion introduced without the predistortion network. The results for each of the LEDS are graphed in Figures 5-3 through 5-28. In most cases, the predistortion network reduces the intermodulation distortion through 100% modulation. For some LEDS, the predistortion networks help within certain modulation depths. Figure 5-13 shows that the useful region for the compensating network is when the diode is modulated no more than 90%. LEDS ME7024 Diode #1, ME7024 Diode #4, and ME7124 Diode #1, represented by Figures 5-11, 5-14, and 5-15, are LEDS where compensation could not aid in their linearity. Those three LEDS did, however, have adequate linearity to satisfy the criteria of -45 db IMD for 50% modulation depth. All other diodes achieved this standard with the one breakpoint compensating network. The graphs of Figures 5-15, 5-25, and 5-28 show that at certain modulation levels the first order intermodulation distortion decreases significantly. This is due to the change in polarity of the numerator of the distortion amplitude given in Table 4-1 describing the intermodulation level.

TABLE 5-1

LOCATION OF BREAKPOINT AND CHANGE IN GAIN

OF THE COMPENSATING NETWORK

LED	I_B (mA)	V_B (Volts)	ΔGain
FLV104#1	10.72886	1.09	.89
FLV104#2	17.23659	.67	.94
FLV104#3	19.32096	.18	.80
FLV104#4	20.51749	.23	.83
FPE104#1	17.84001	1.44	.85
FPE104#2	13.38244	1.22	.91
FPE104#3	15.43009	1.32	.90
FPE104#4	12.07027	1.15	.90
ME7024#1	-9.984647	-1.05	-.93
ME7024#2	12.31738	-.55	-.94
ME7024#3	17.43956	*	*
ME7024#4	12.40241	*	*
ME7124#1	16.54467	.55	.94
ME7124#2	19.22783	1.51	.91
ME7124#3	9.187072	*	*
ME7124#4	14.09062	1.25	.93
TIL31#1	18.42128	1.47	.89
TIL31#2	11.94478	1.15	.92
FPE500#1	45.99068	2.85	.94
FPE500#2	35.08014	2.30	.78
FPE500#3	30.22915	2.06	.84
FPE500#4	54.00872	3.25	.90
HEMT3300#1	7.333579	.92	.90
HEMT3300#2	10.61429	1.08	.87
HEMT3300#3	14.66659	1.28	.65
HEMT3300#4	10.61383	1.08	.88

*Diode has sufficient linearity before predistortion network.

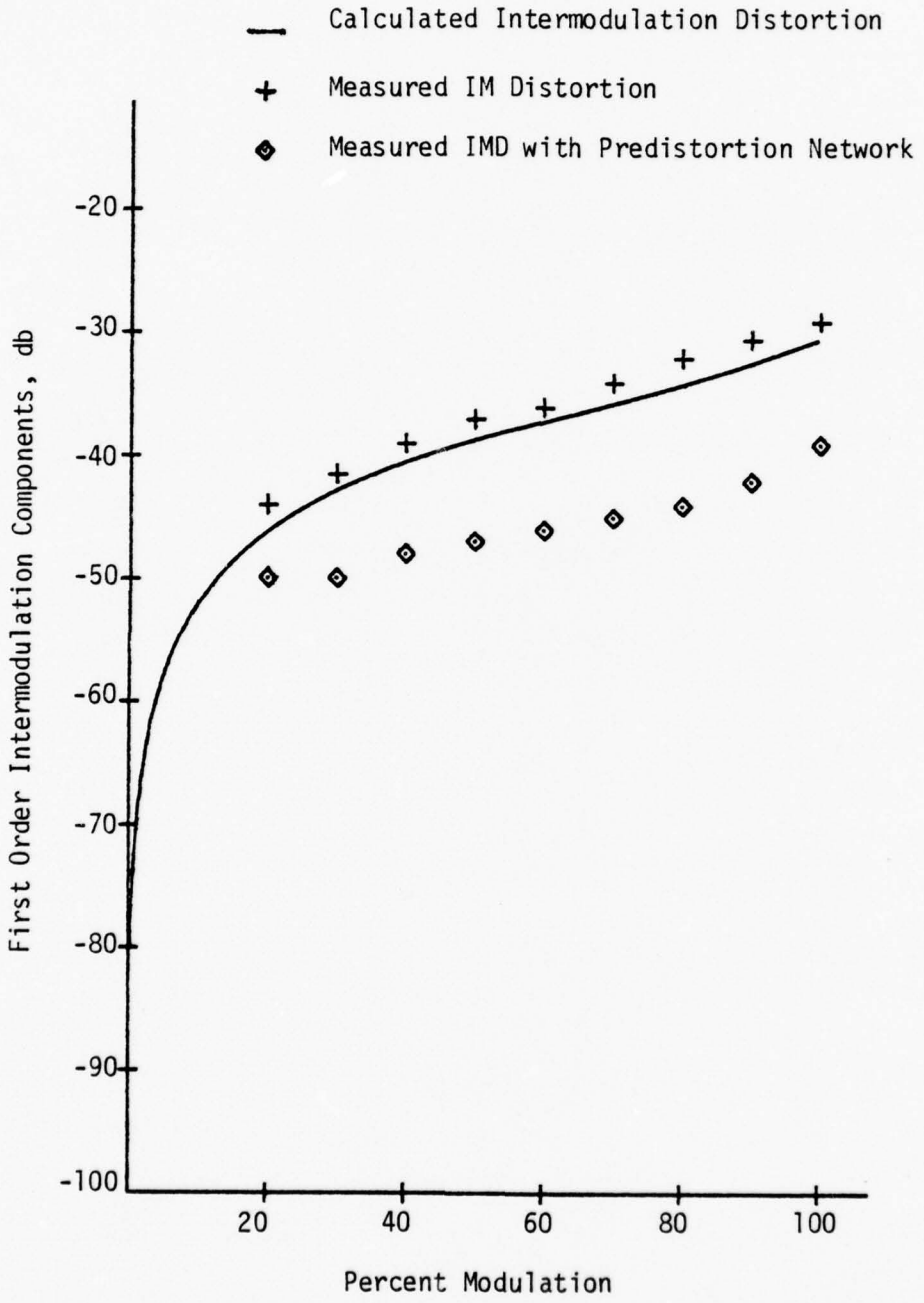

Figure 5-3. Intermodulation Distortion vs Percent Modulation for FLV104 Diode #1.

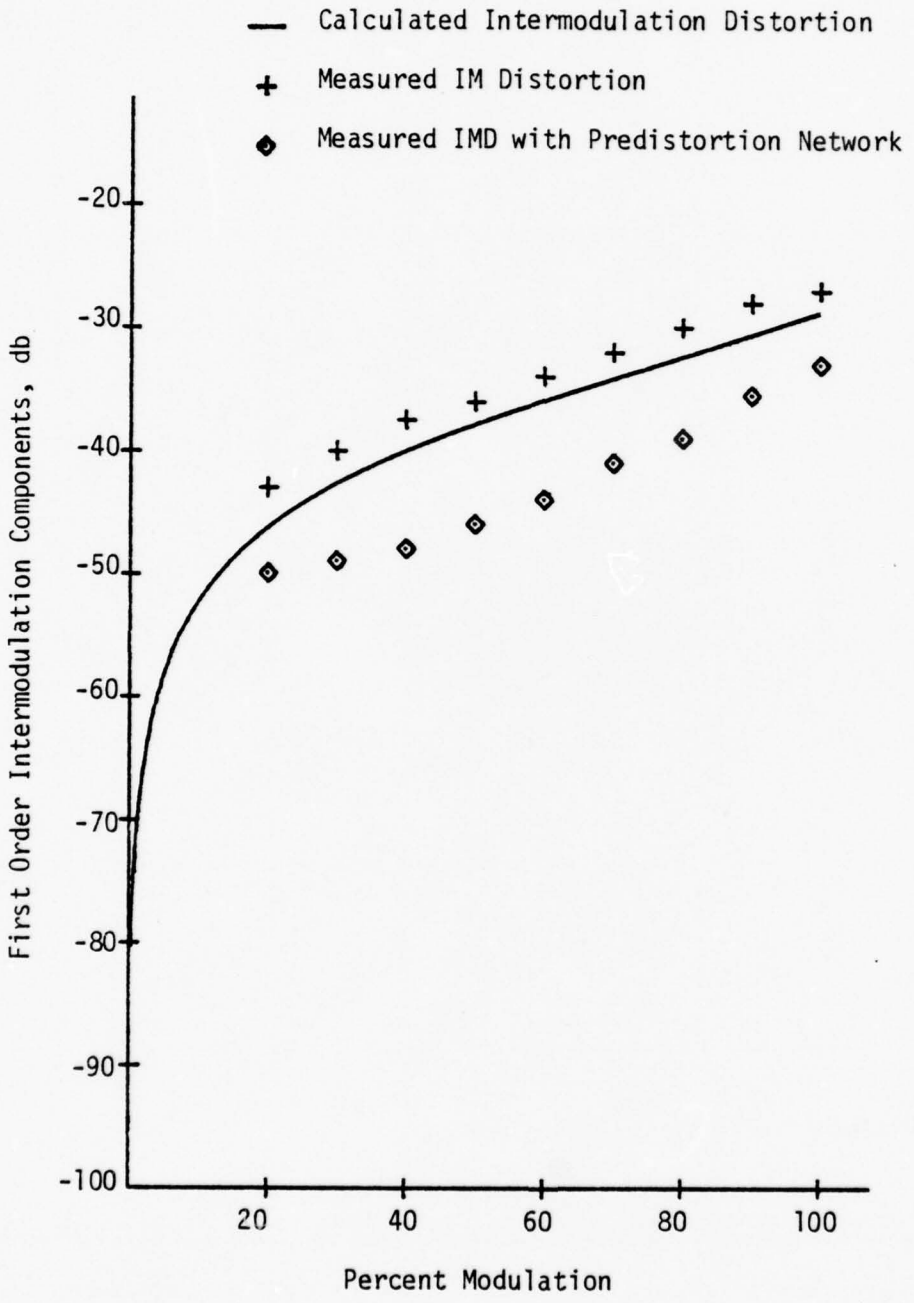

Figure 5-4. Intermodulation Distortion vs Percent Modulation for FLV104 Diode #2.

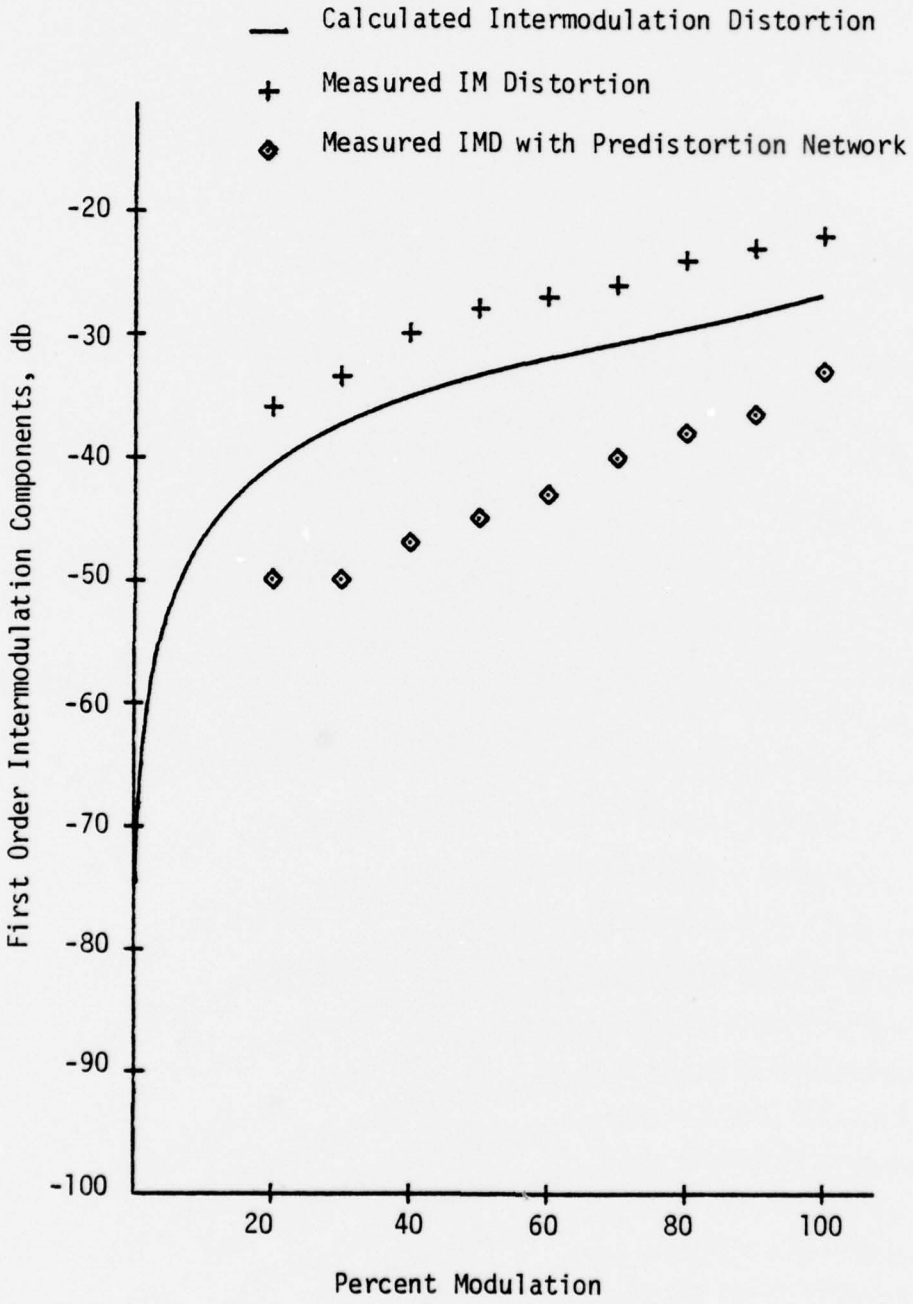

Figure 5-5. Intermodulation Distortion vs Percent Modulation for FLV104 Diode #3.

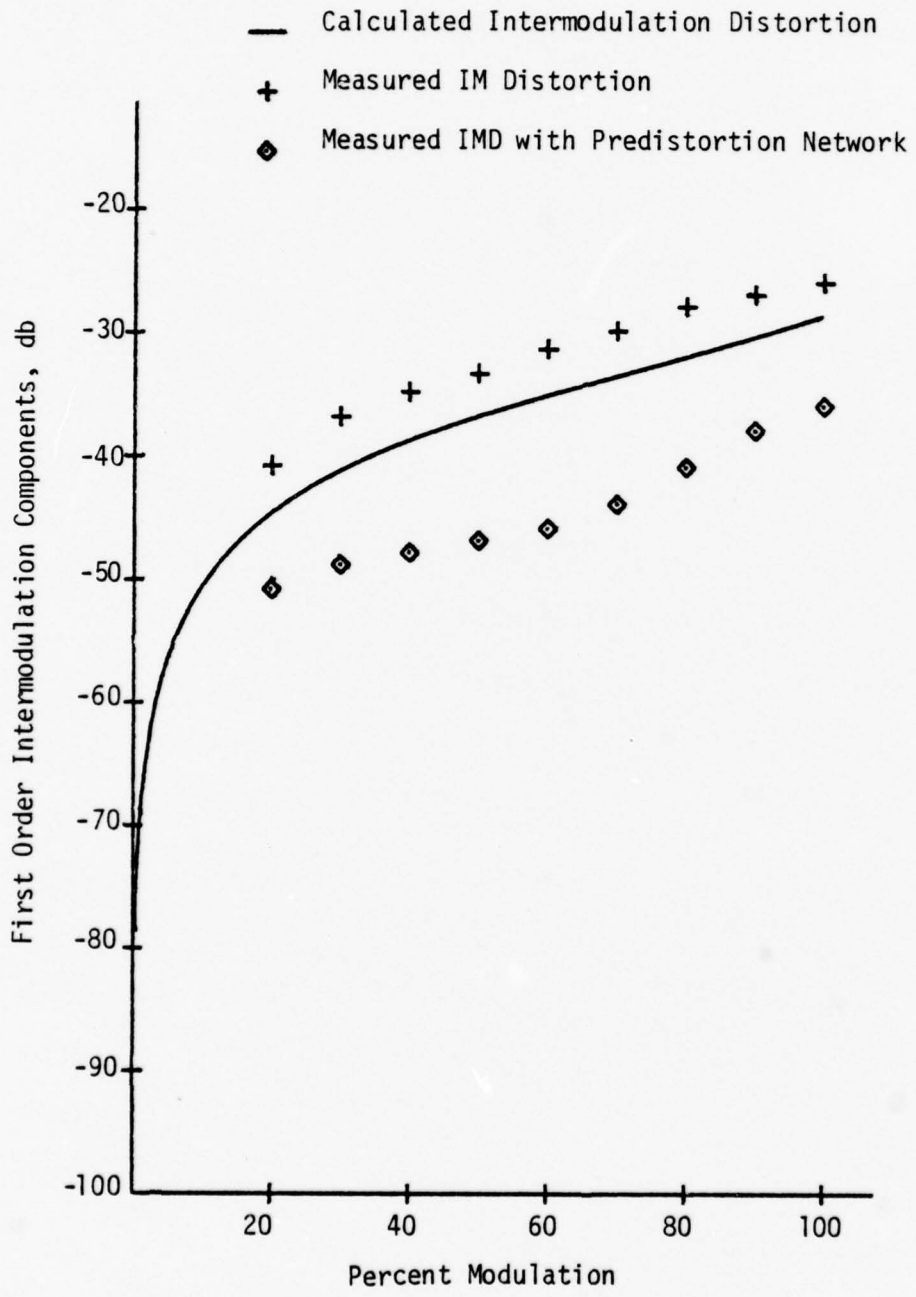

Figure 5-6. Intermodulation Distortion vs Percent Modulation for FLV104 Diode #4.

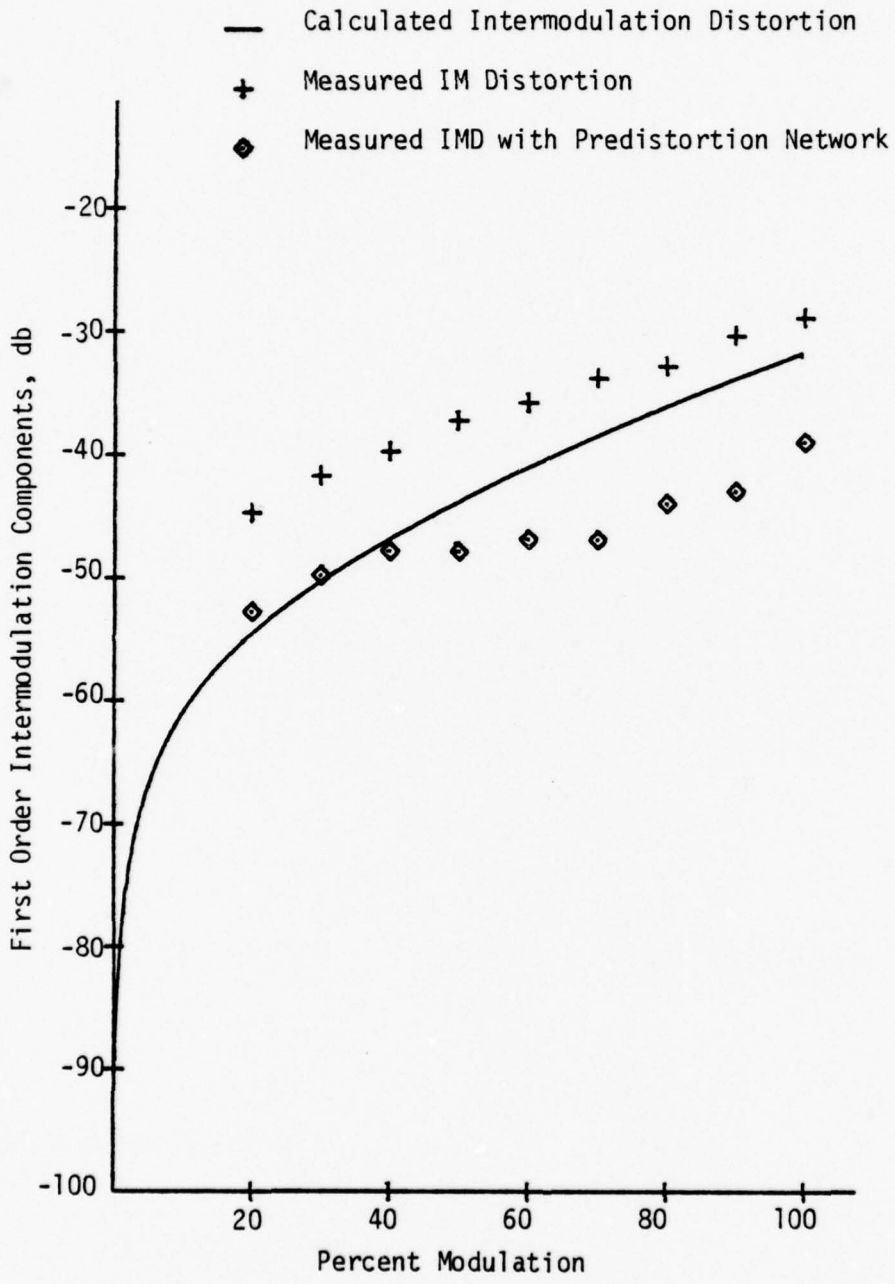

Figure 5-7. Intermodulation Distortion vs Percent Modulation for FPE104 Diode #1.

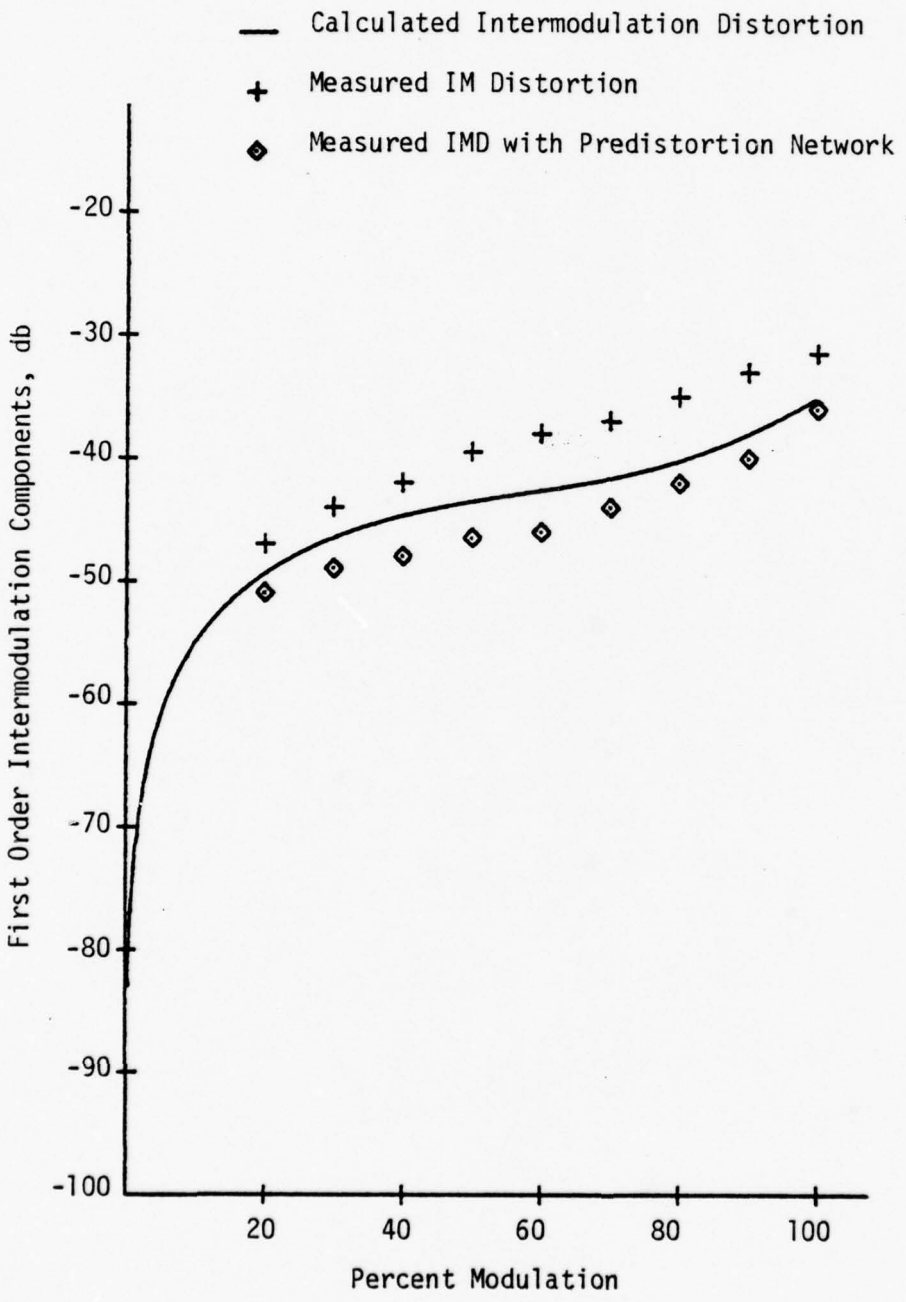

Figure 5-8. Intermodulation Distortion vs Percent Modulation for FPE104 Diode #2.

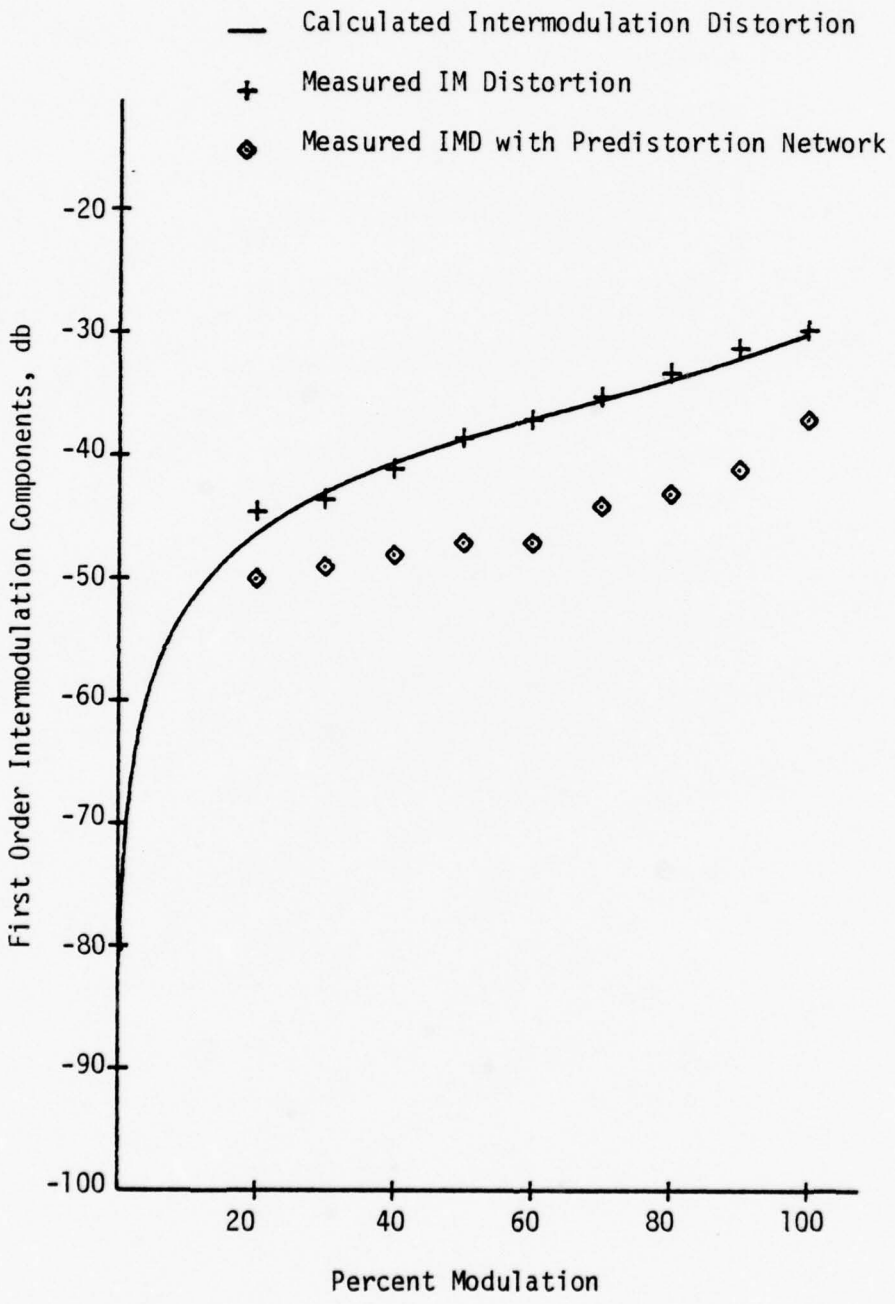

Figure 5-9. Intermodulation Distortion vs Percent Modulation for FPE104 Diode #3.

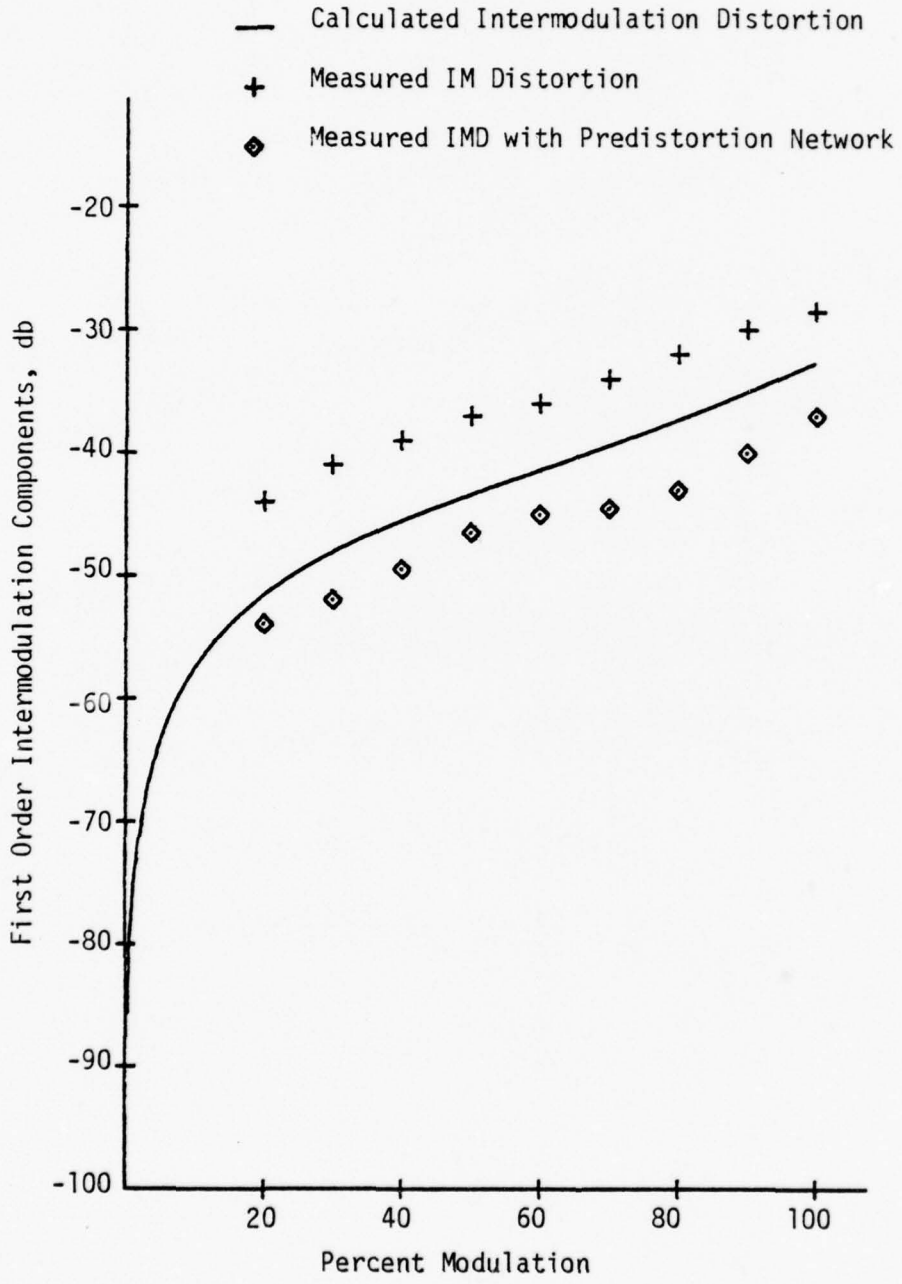

Figure 5-10. Intermodulation Distortion vs Percent Modulation for FPE104 Diode #4.

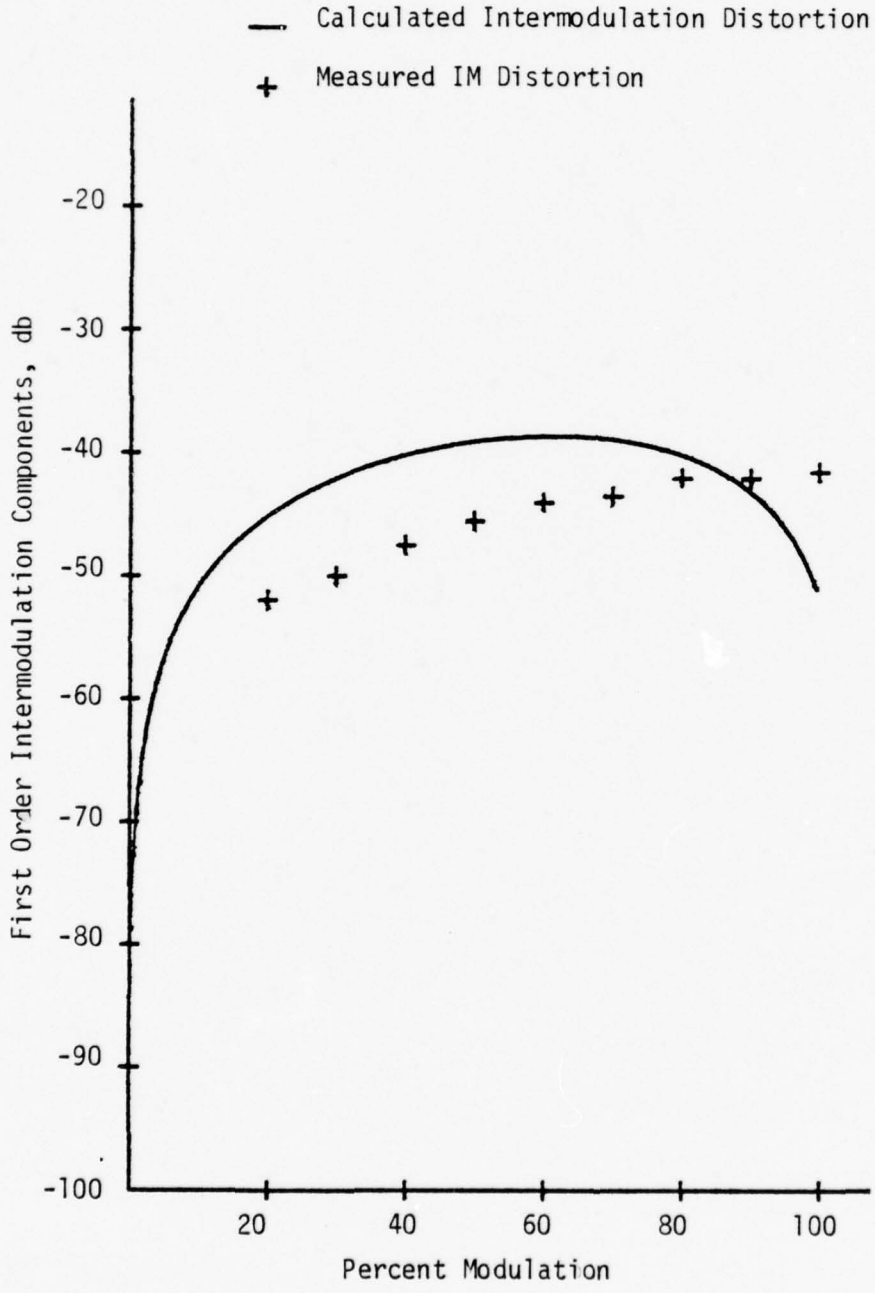

Figure 5-11. Intermodulation Distortion vs Percent Modulation for ME7024 Diode #1.

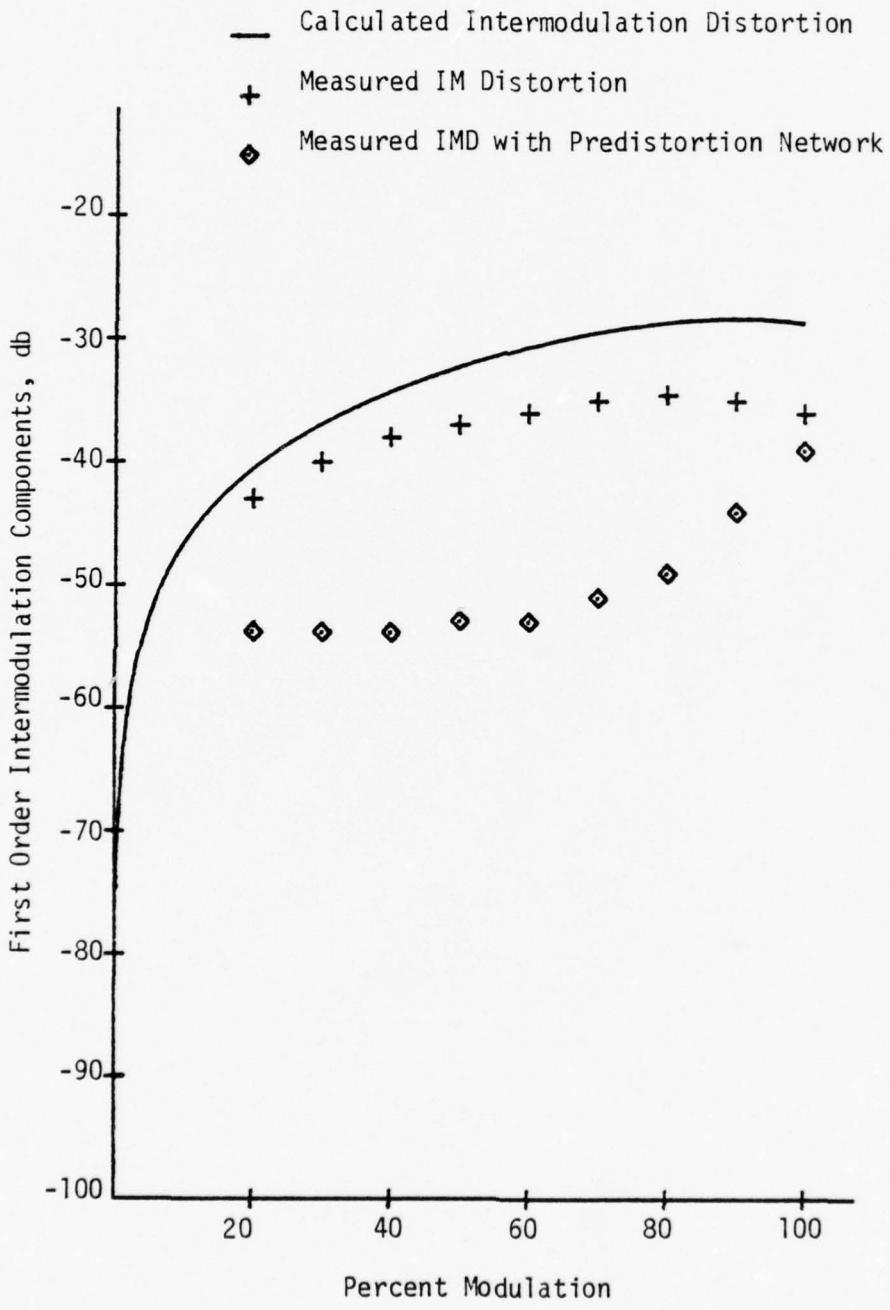

Figure 5-12. Intermodulation Distortion vs Percent Modulation for ME7024 Diode #2.

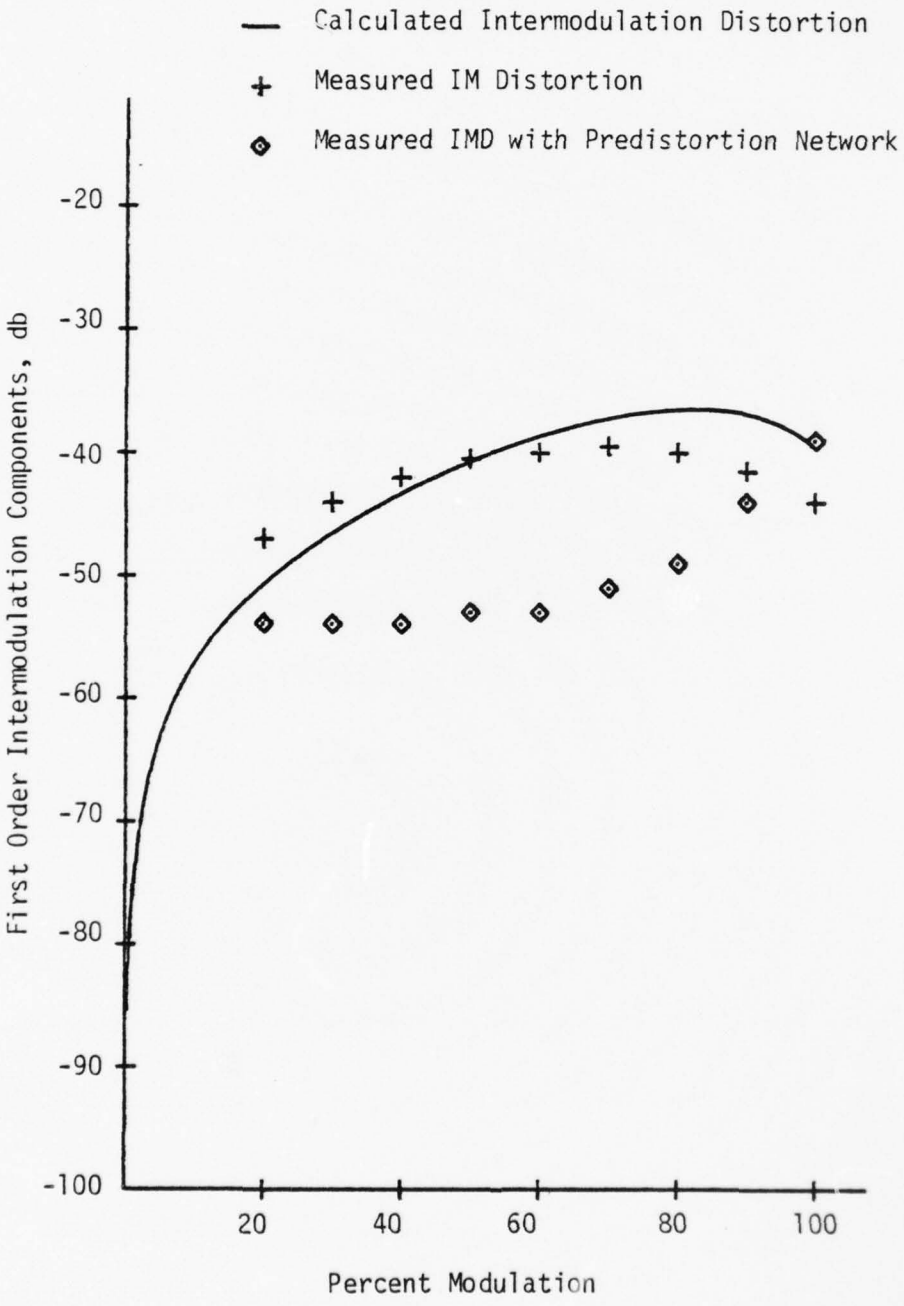

Figure 5-13. Intermodulation Distortion vs Percent Modulation for ME7024 Diode #3.

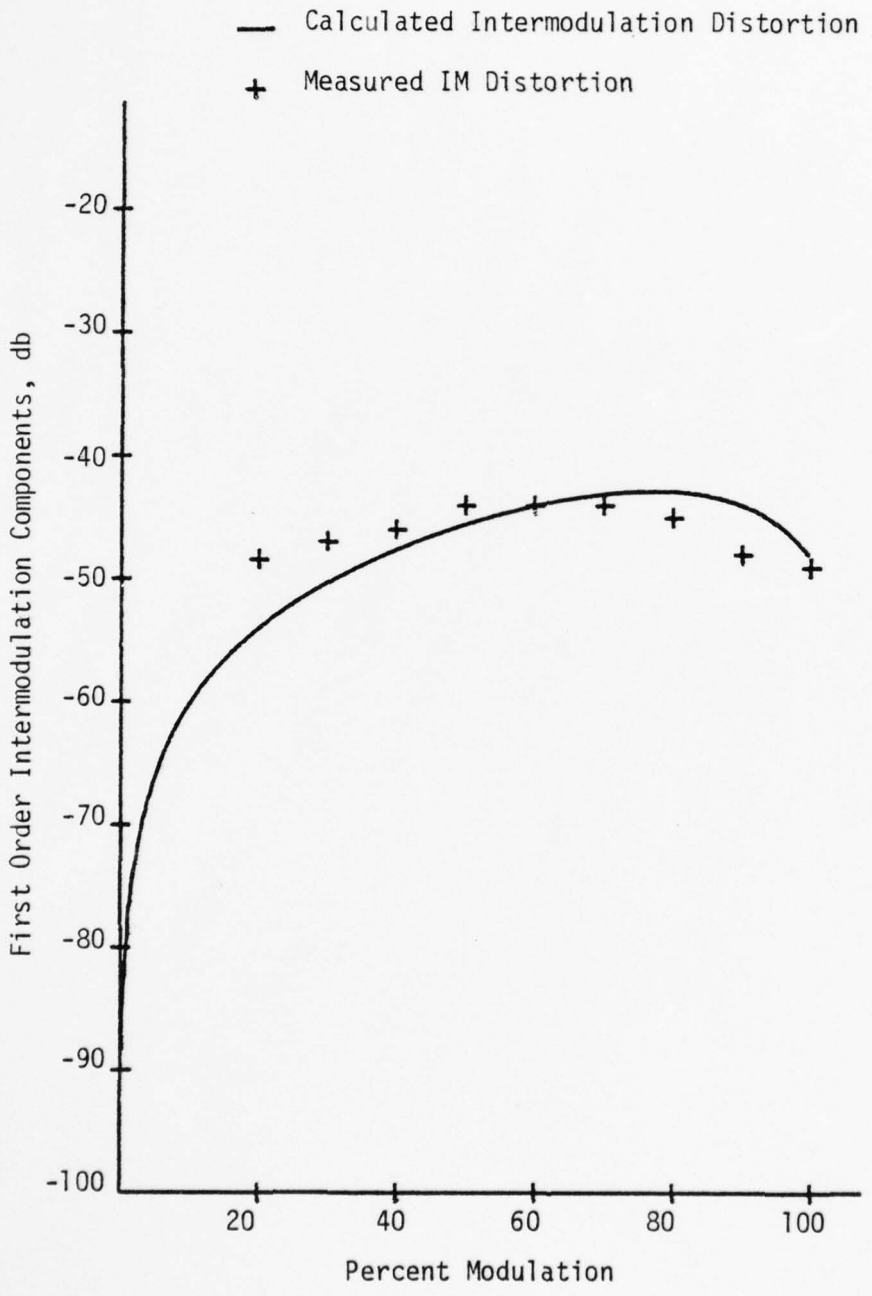

Figure 5-14. Intermodulation Distortion vs Percent Modulation for ME7024 Diode #4.

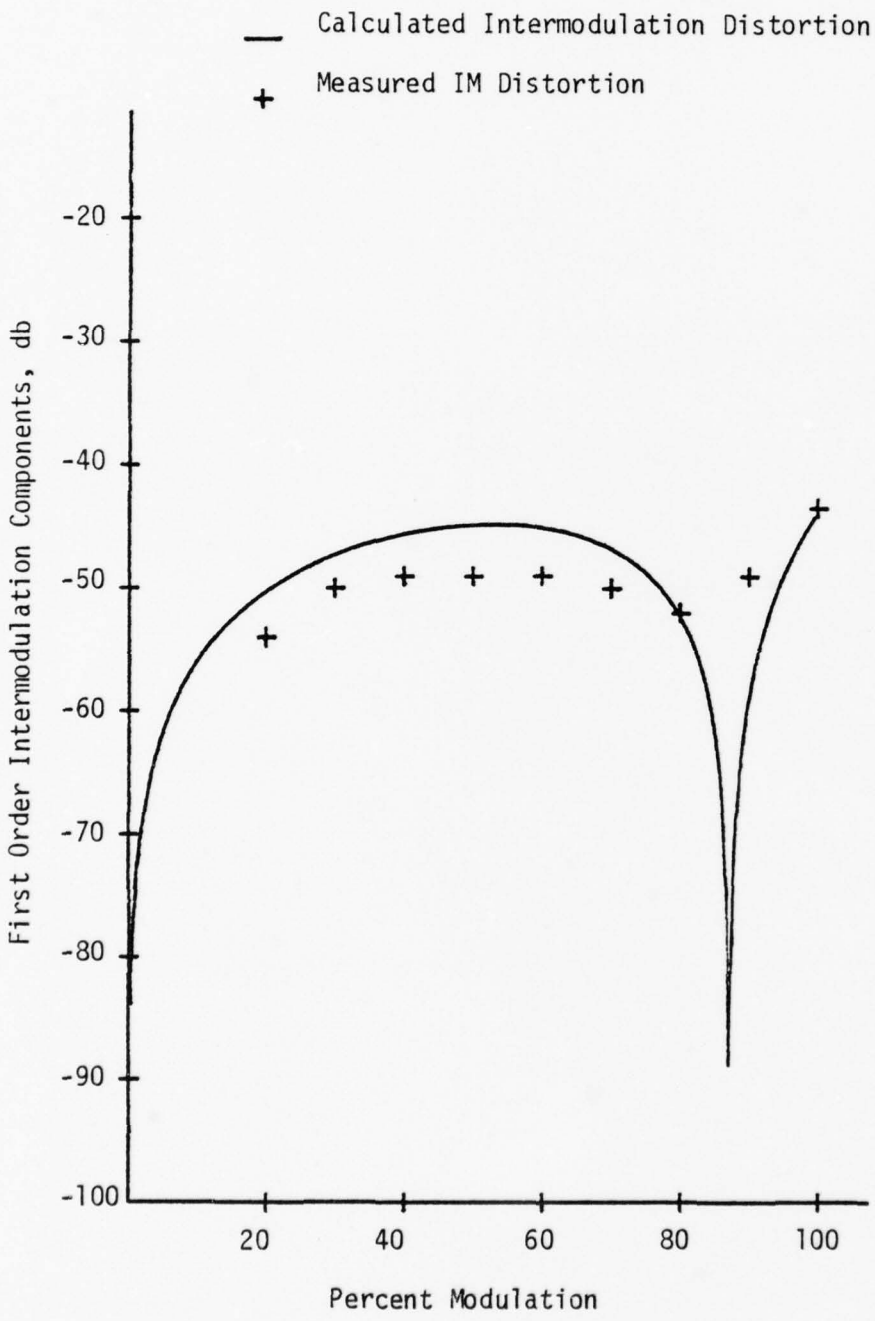

Figure 5-15. Intermodulation Distortion vs Percent Modulation for ME7124 Diode #1.

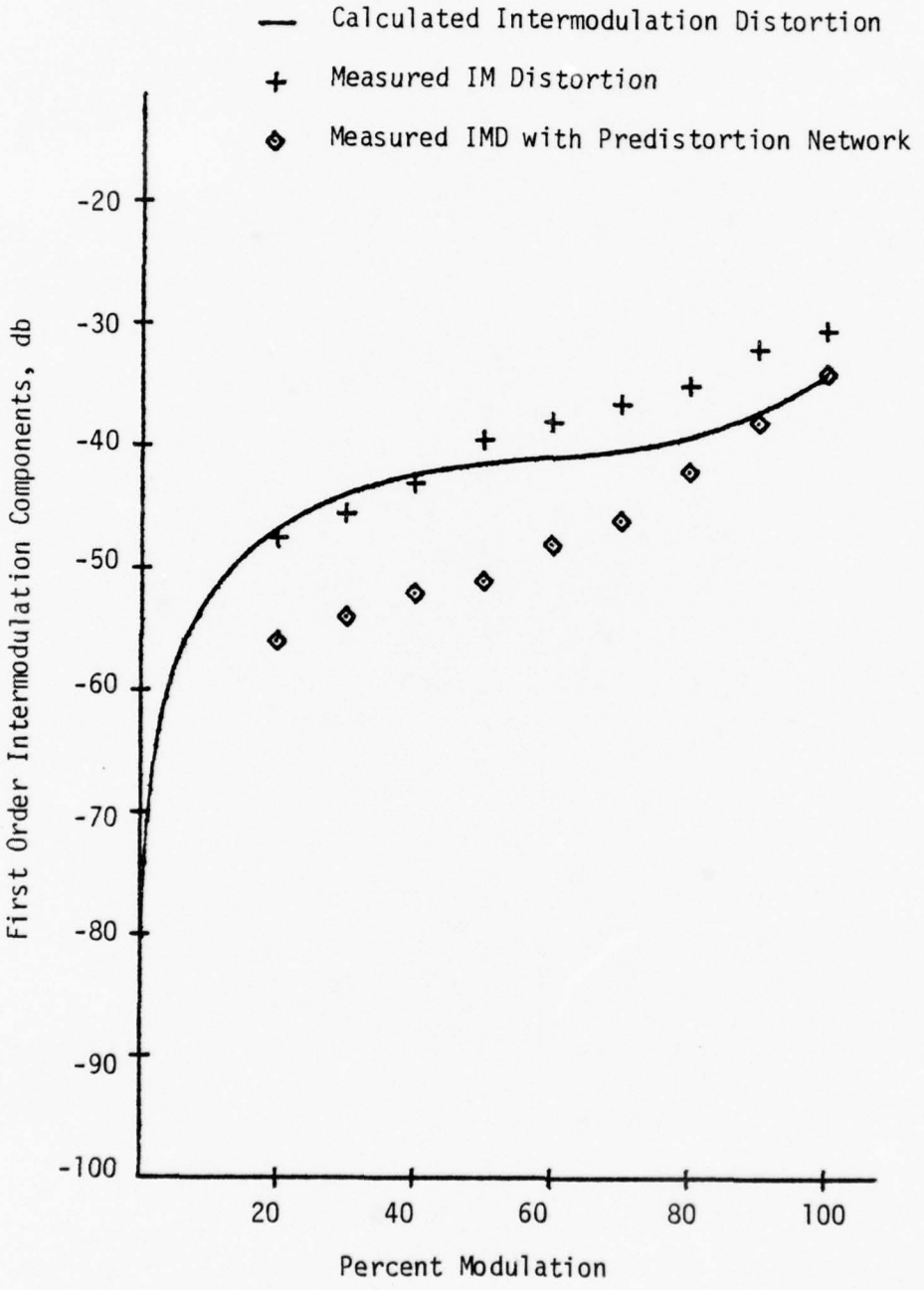

Figure 5-16. Intermodulation Distortion vs Percent Modulation for ME7124 Diode #2.

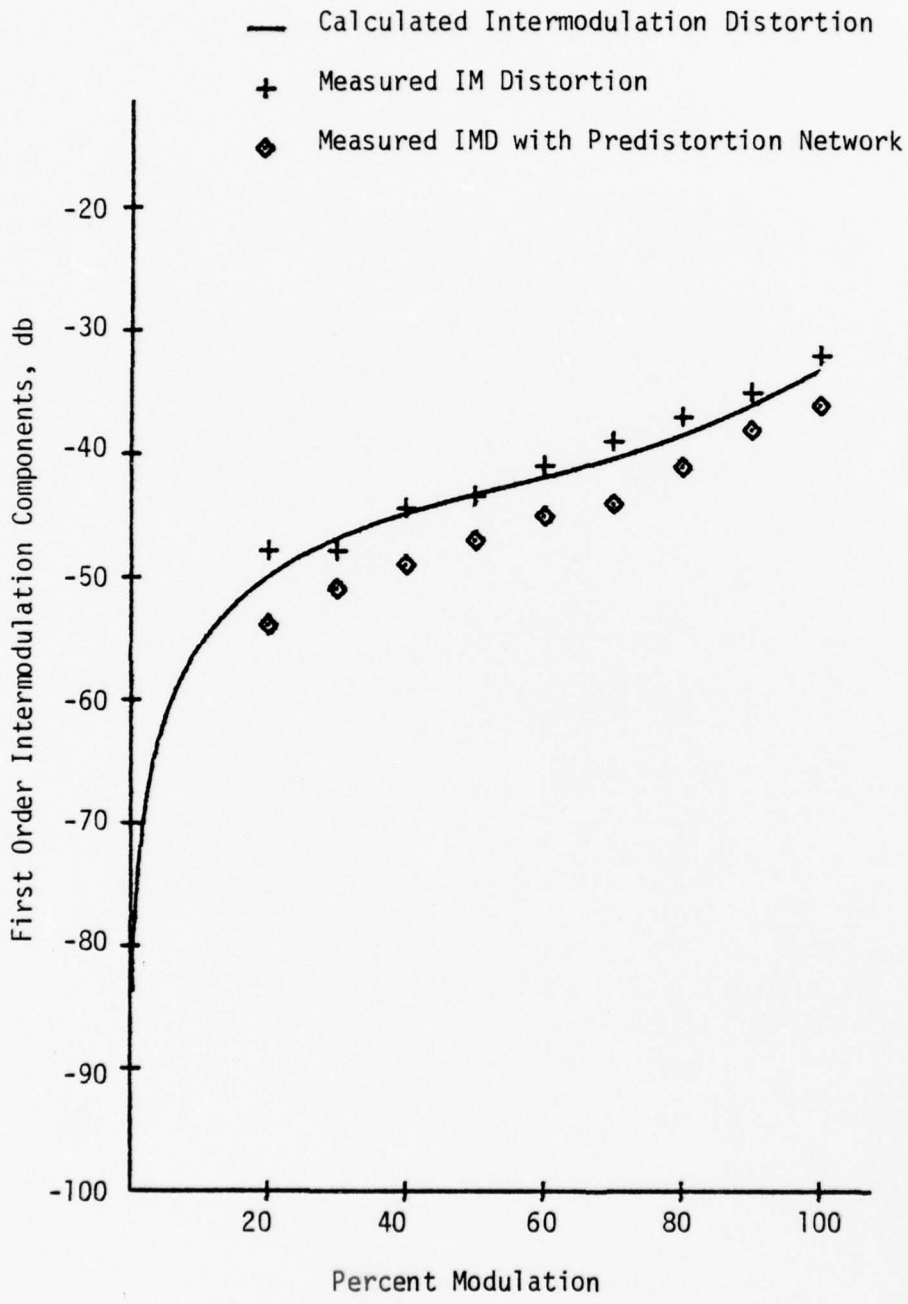

Figure 5-17. Intermodulation Distortion vs Percent Modulation for ME7124 Diode #3.

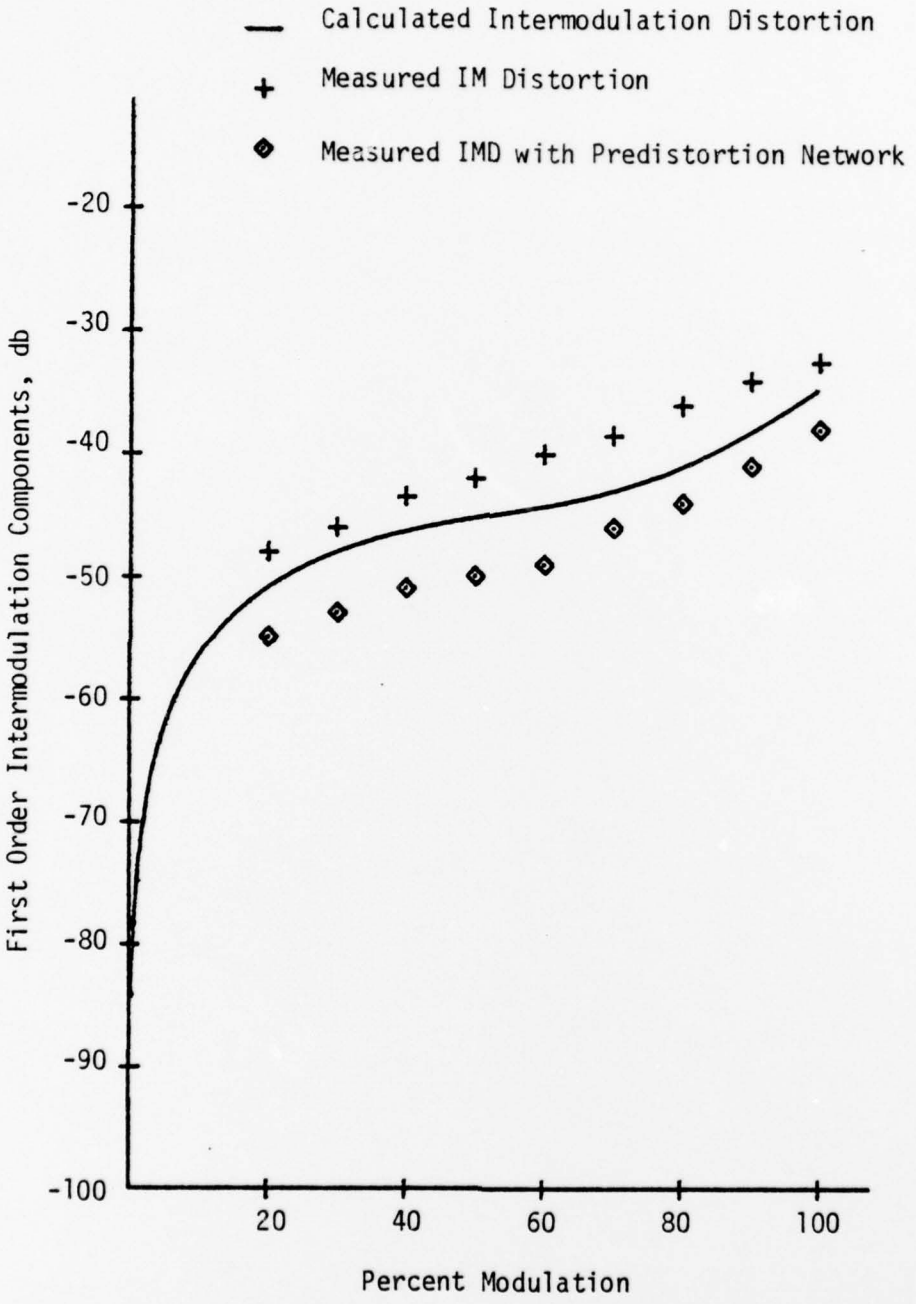

Figure 5-18. Intermodulation Distortion vs Percent Modulation for ME7124 Diode #4.

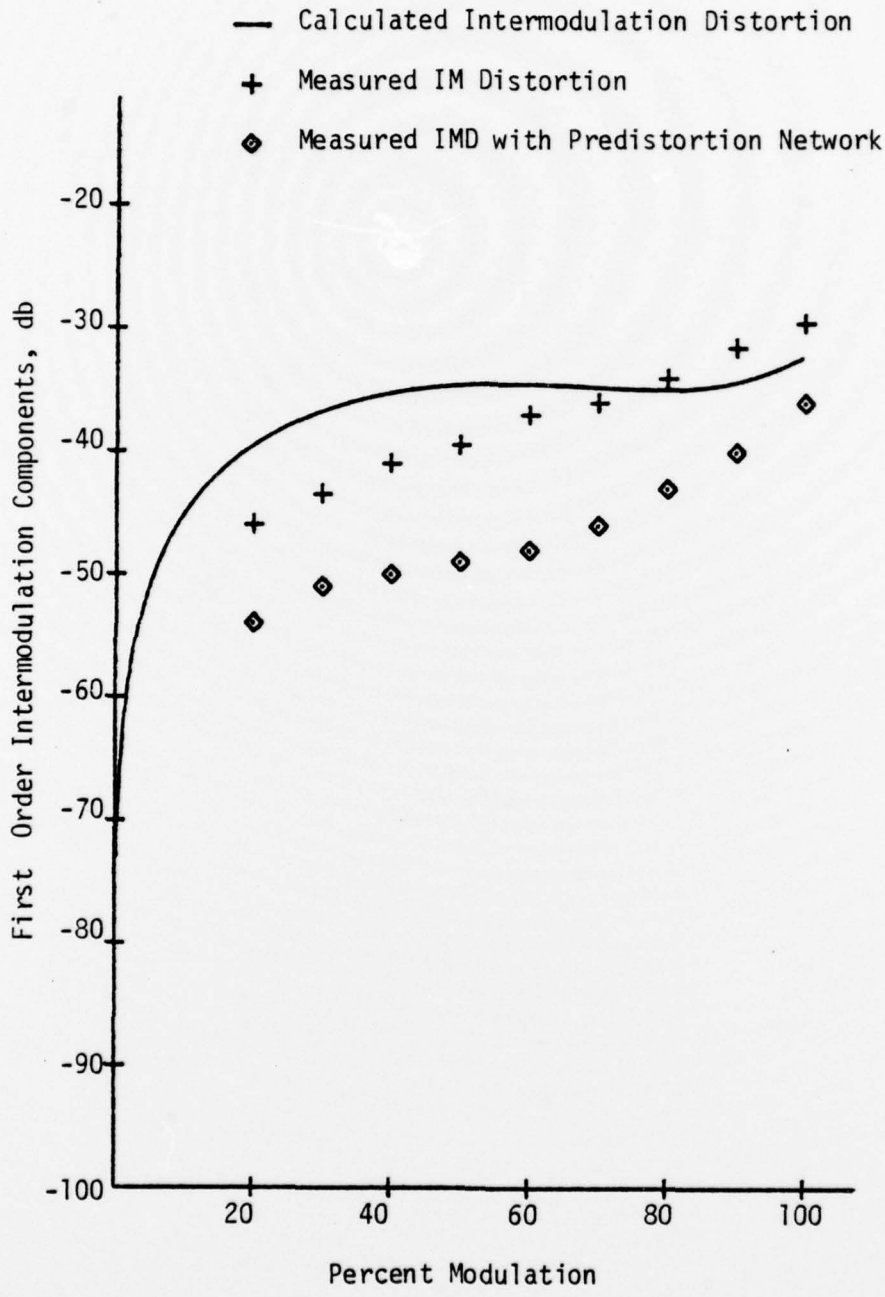

Figure 5-19. Intermodulation Distortion vs Percent Modulation for TIL31 Diode #1.

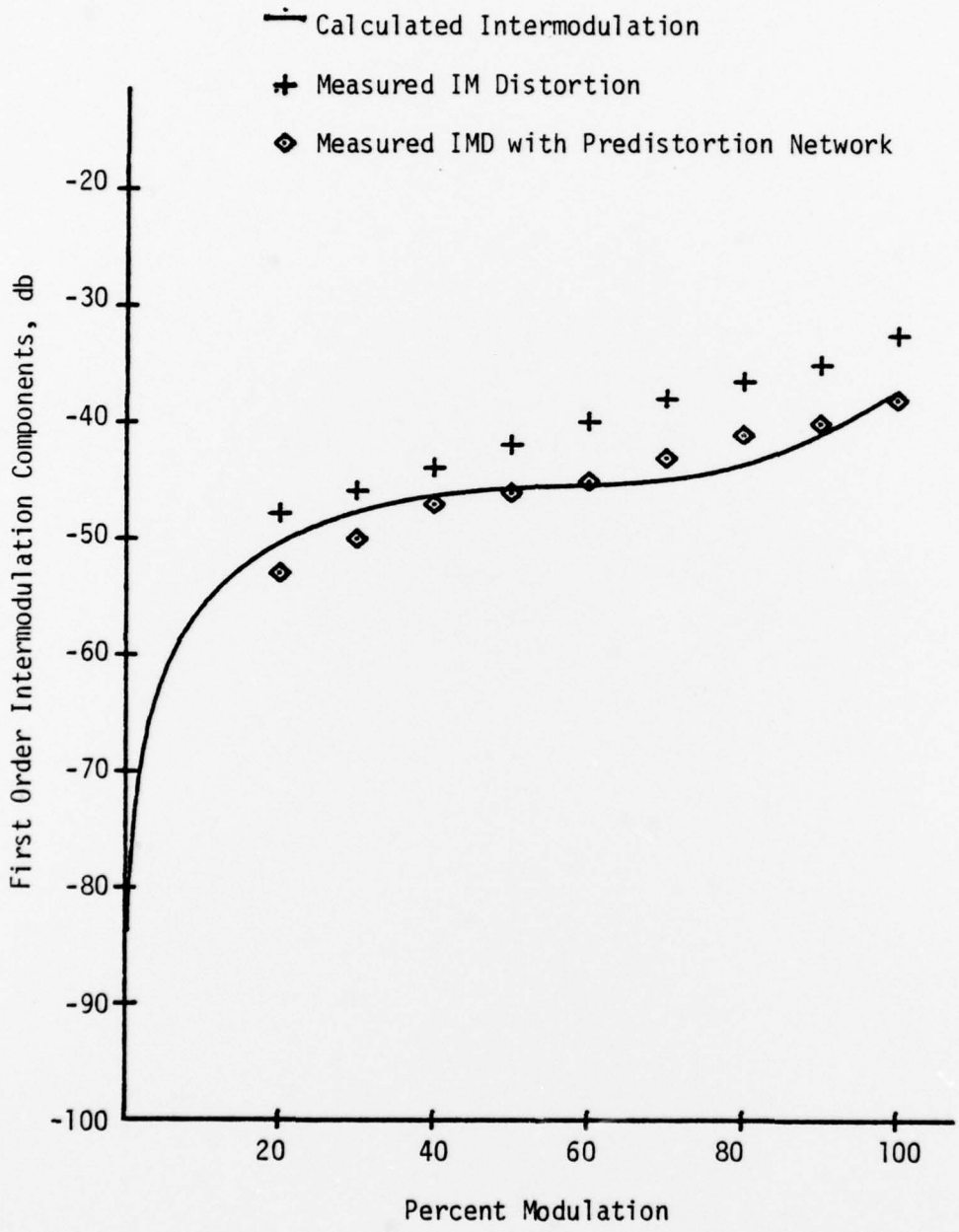

Figure 5-20. Intermodulation Distortion vs Percent Modulation for TIL31 Diode #2.

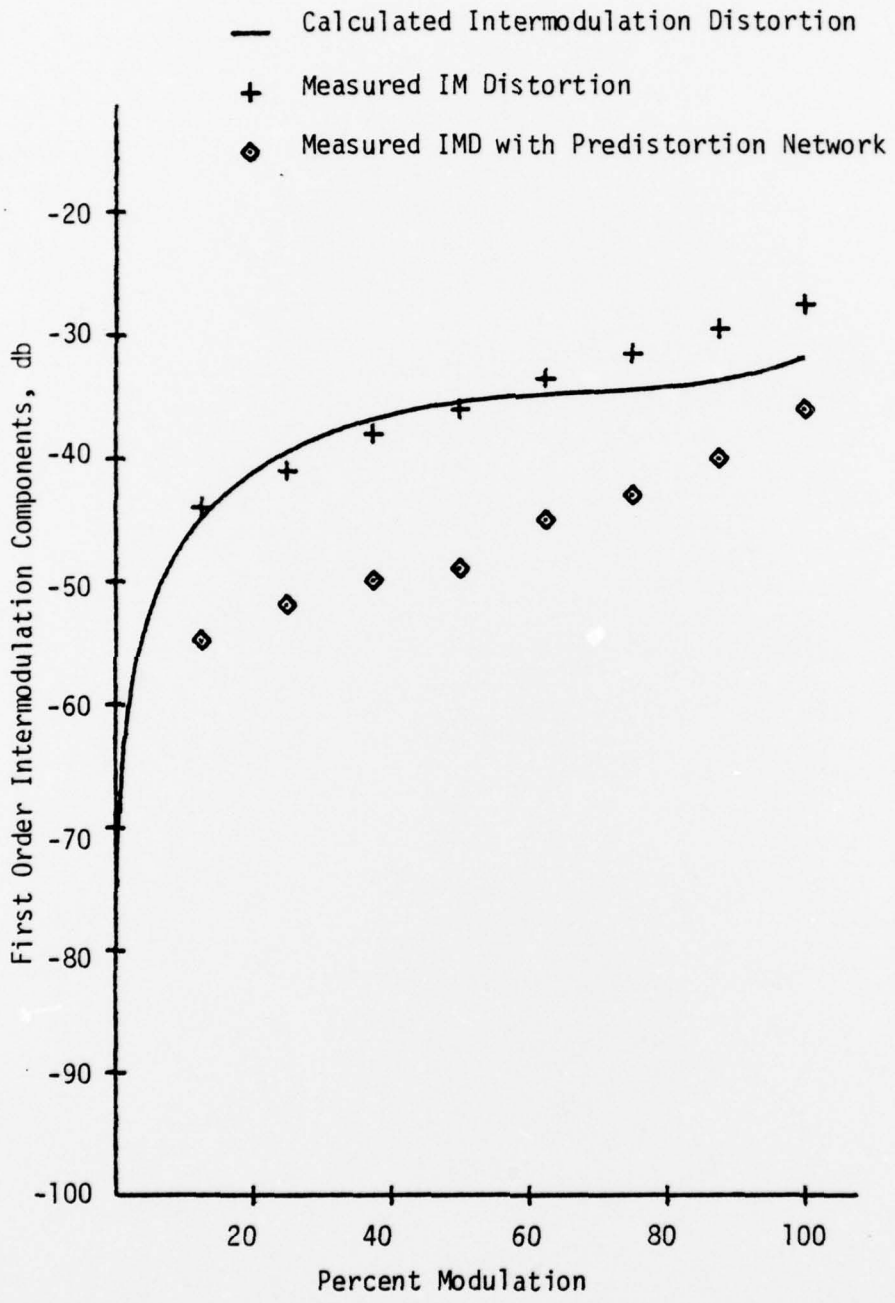

Figure 5-21. Intermodulation Distortion vs Percent Modulation for FPE500 Diode #1.

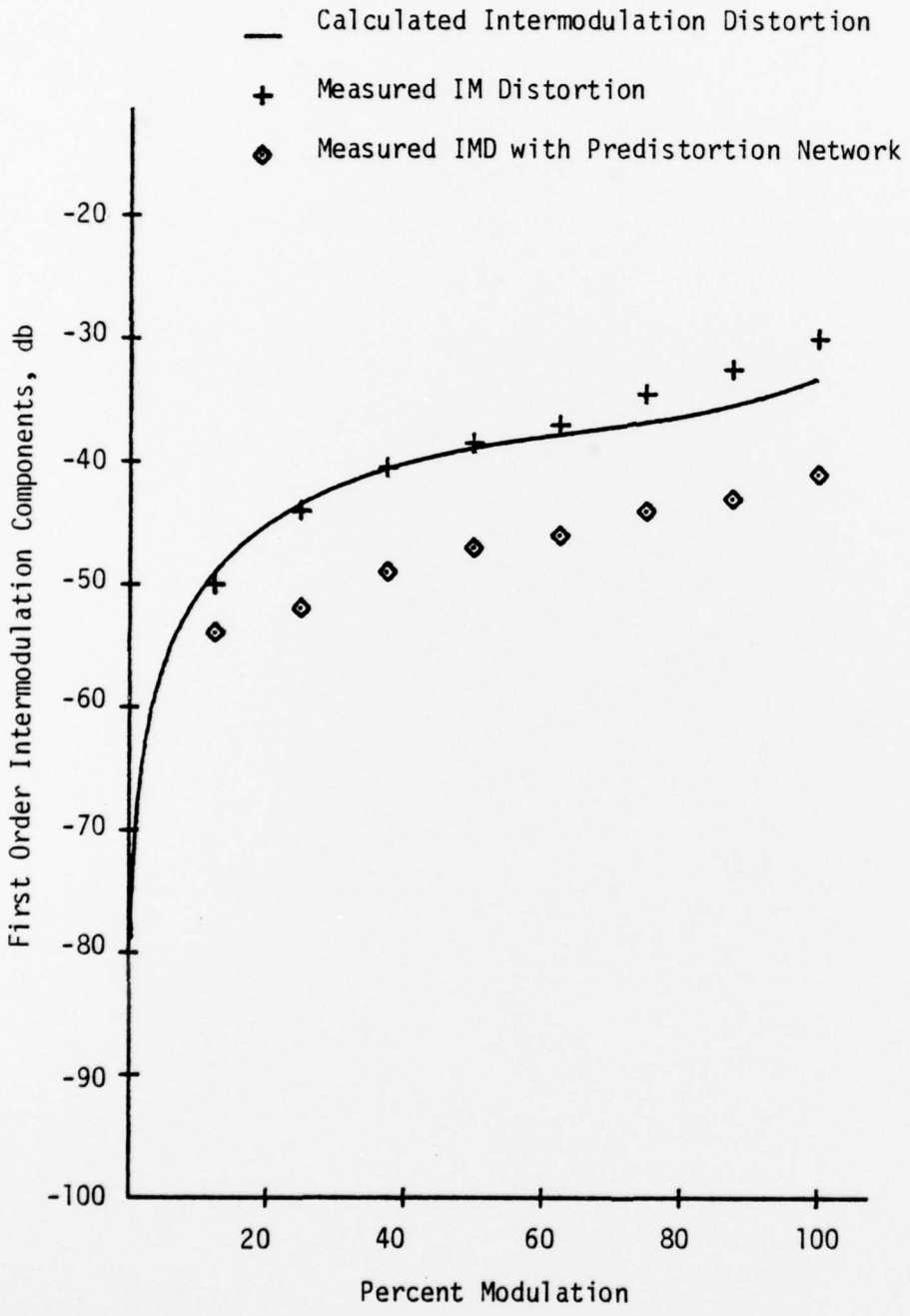

Figure 5-22. Intermodulation Distortion vs Percent Modulation for FPE500 Diode #2.

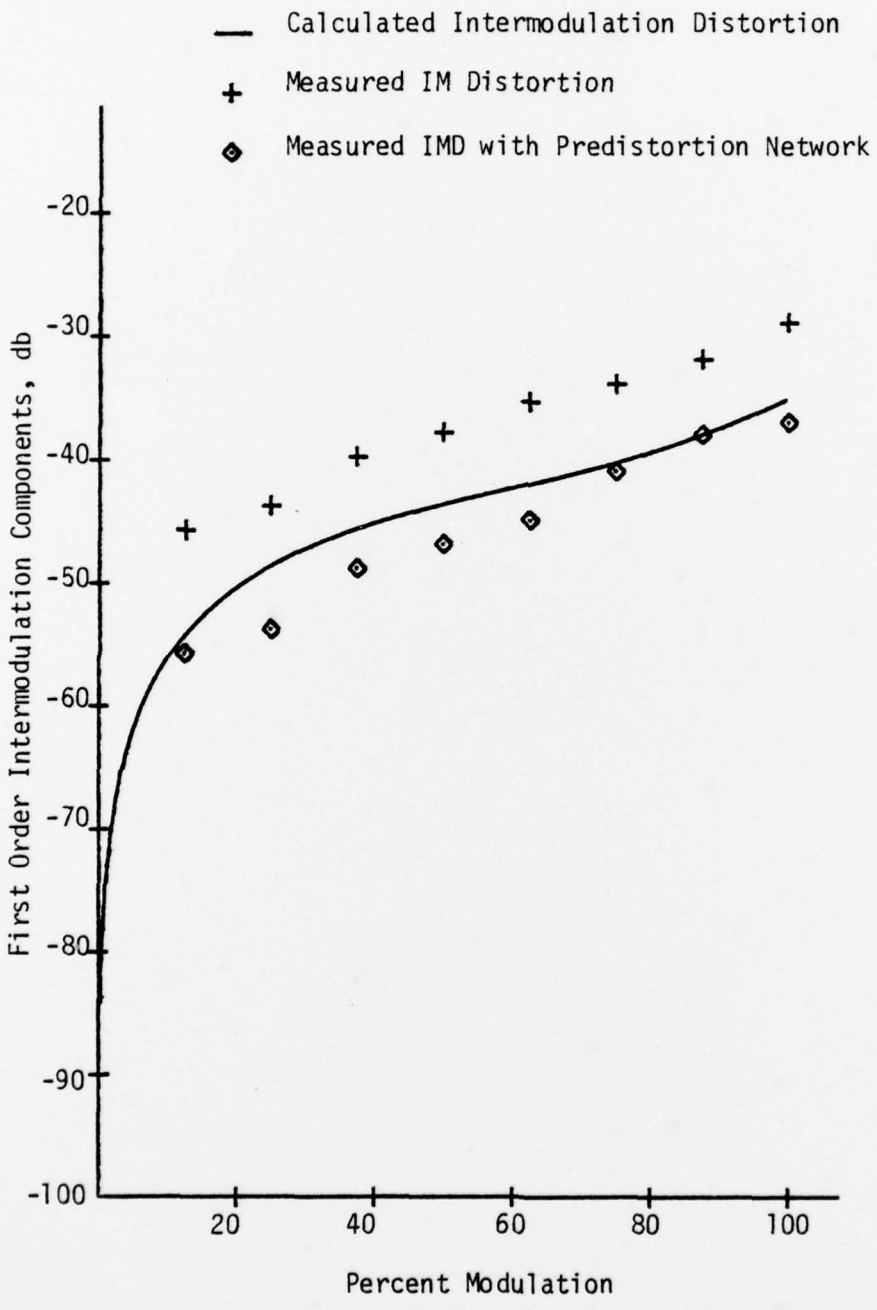

Figure 5-23. Intermodulation Distortion vs Percent Modulation for FPE500 Diode #3.

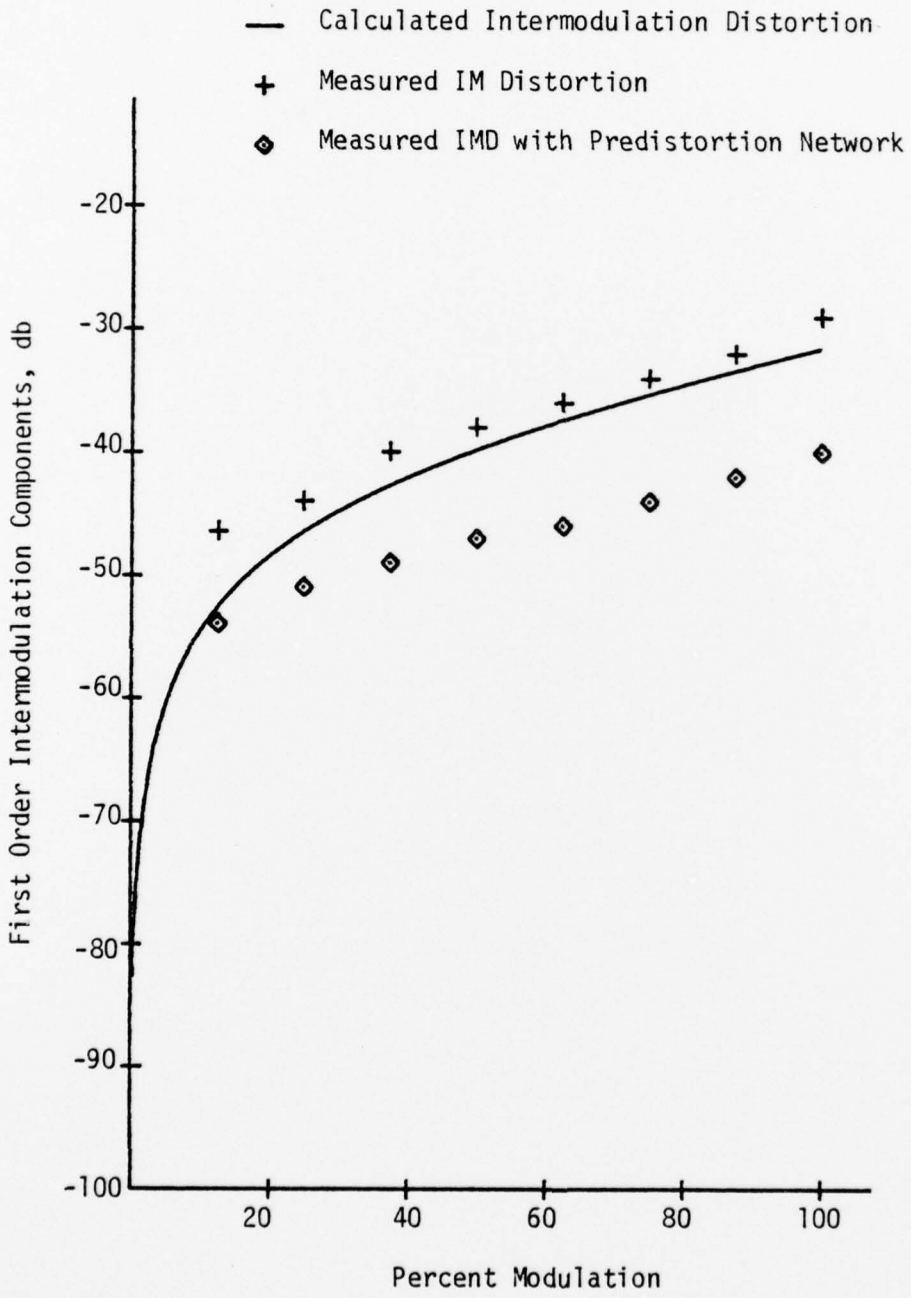

Figure 5-24. Intermodulation Distortion vs Percent Modulation for FPE500 Diode #4.

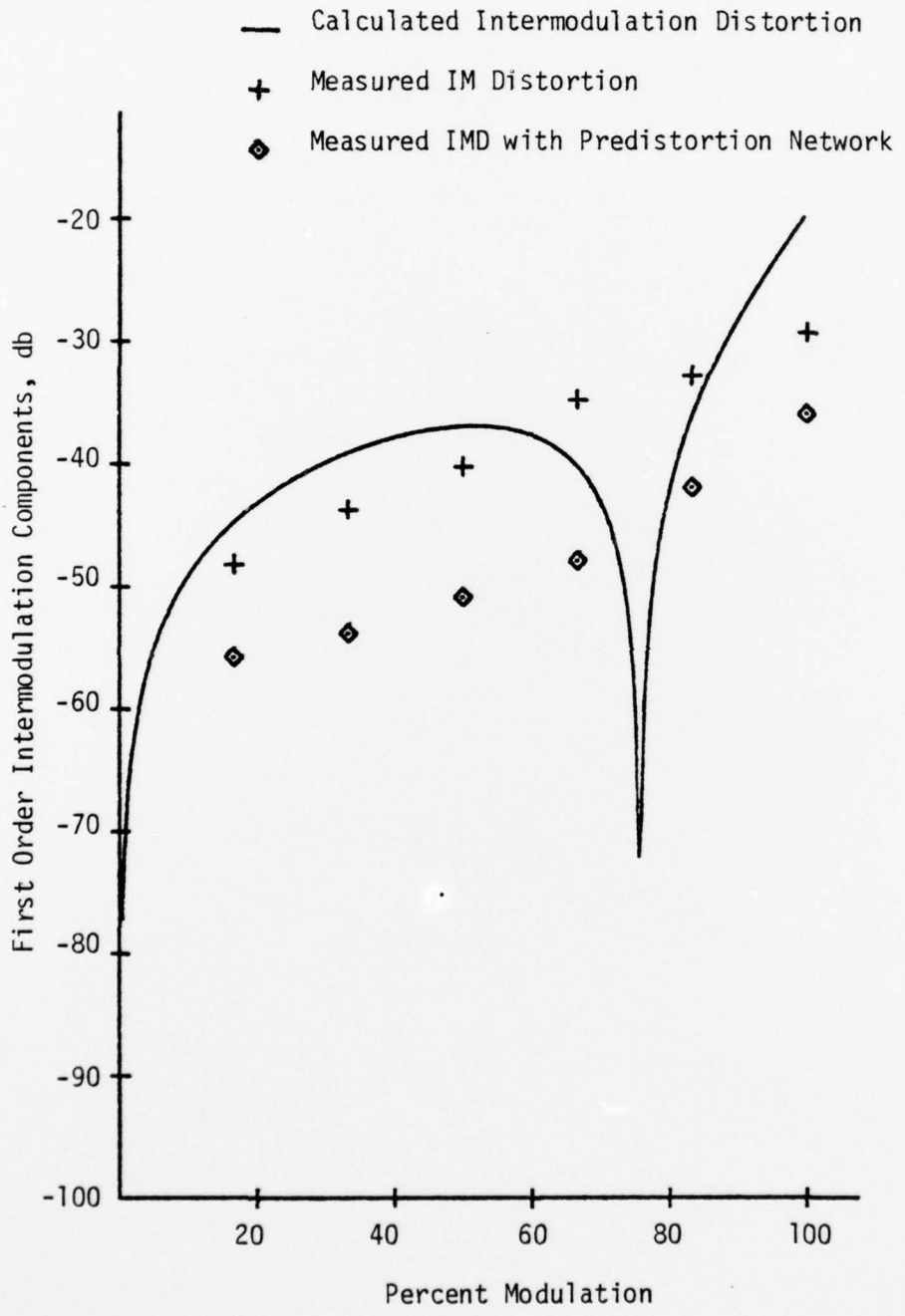

Figure 5-25. Intermodulation Distortion vs Percent Modulation for HEMT3300 Diode #1.

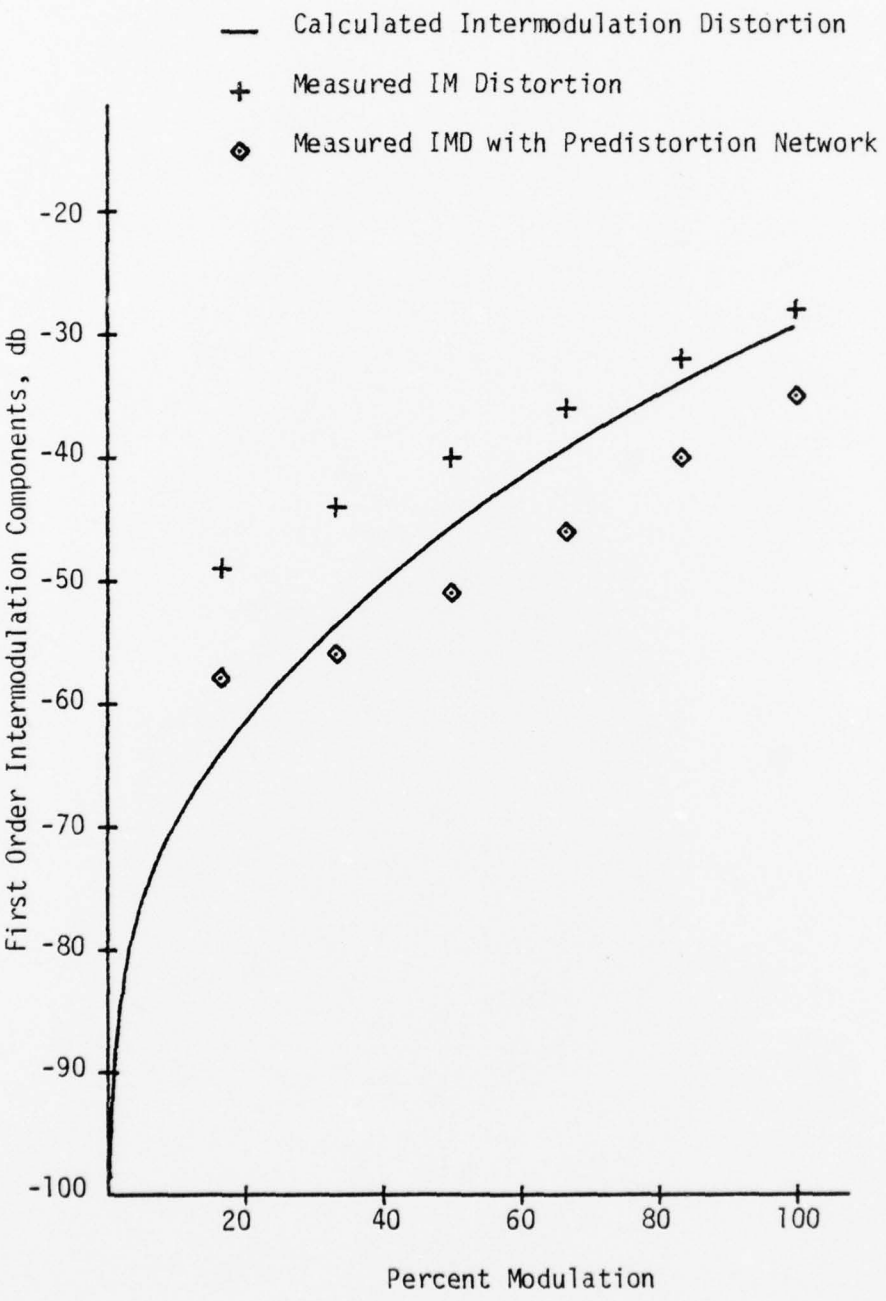

Figure 5-26. Intermodulation Distortion vs Percent Modulation for HEMT3300 Diode #2.

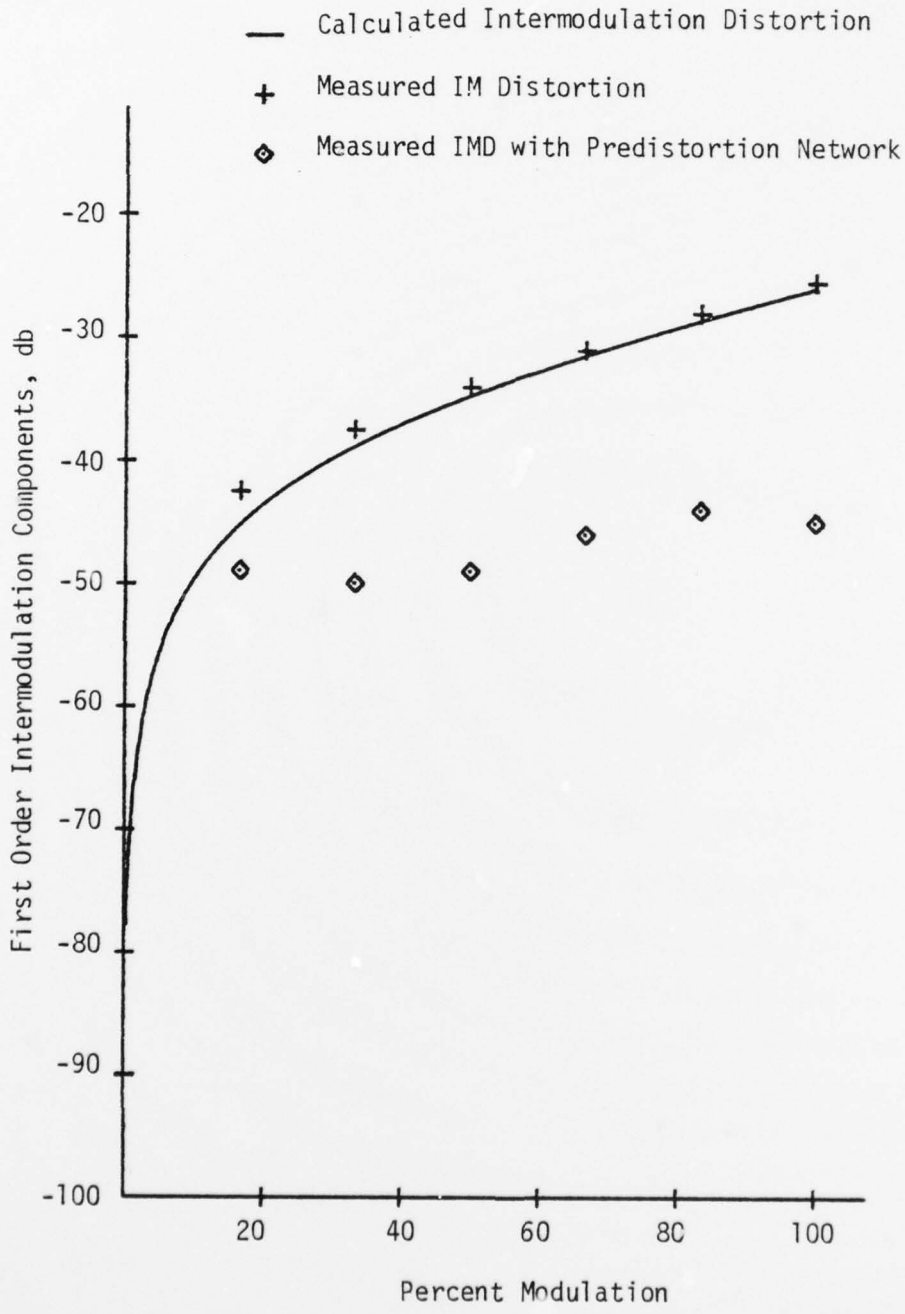

Figure 5-27. Intermodulation Distortion vs Percent Modulation for HEMT3300 Diode #3.

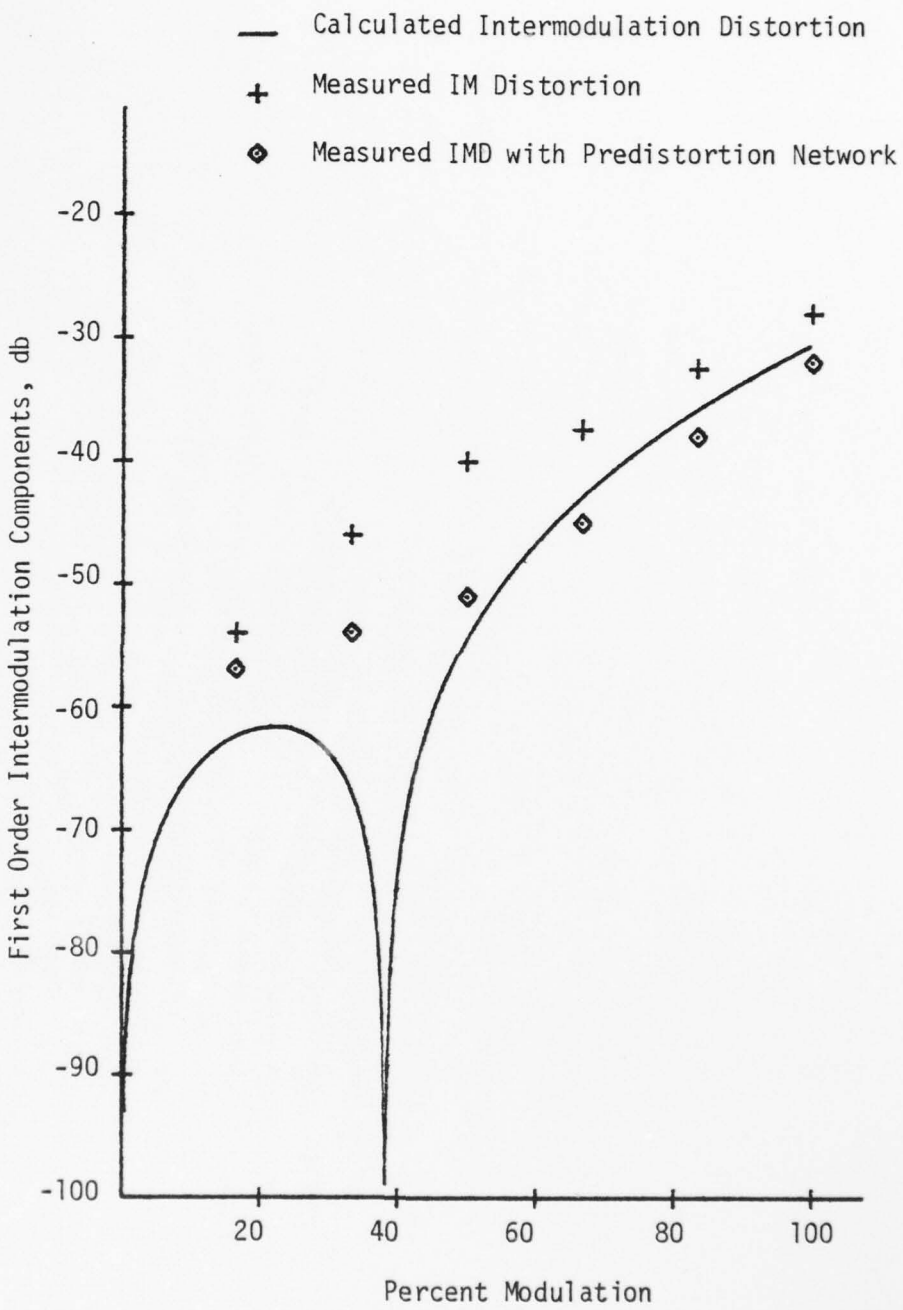

Figure 5-28. Intermodulation Distortion vs Percent Modulation for HEMT3300 Diode #4.

CHAPTER 6

CONCLUSION

The predistortion approach of correcting for nonlinearities of a system is very useful when the transfer characteristic of the system is known. By differentiating the transfer function to find the breakpoints of the nonlinear system, knowledge of the breakpoints of the compensating network is also determined. By using the predistortion network described, much control is given to the location of the breakpoints as well as the change in the slope of its transfer function.

If a higher order compensating network is needed, another parallel branch to the input is all that is required. Capacitances couple both sides of each leg of the input network to keep the breakpoints noninteractive. With one breakpoint, the network provided approximately 8 db reduction of intermodulation distortion. This was enough compensation to keep the intermodulation levels to -45 db at 50% modulation. If the one breakpoint approach does not adequately increase the linearity of the system, a two breakpoint network can be implemented. The actual data points would then be fit to a fifth order polynomial. The zeroes of the third derivative would then give the location of both breakpoints. The order of polynomial to use is then

$$\text{Order of Polynomial} = \text{Number of Breakpoints} + 3 \qquad (18)$$

Thoughts of expanding this approach may include using an automatic control over the location and magnitude of the breakpoints. An approach would be to detect the output light at the transmitter and feed that

signal back to the predistortion network in such a way as to control the location and magnitude of the breakpoints.

It was noticed that by increasing bias current level a reduction of IMD would occur. When looking at the dynamic characteristics of the LEDS, it is noted that the portion of the curve at higher current levels is more linear. By increasing the bias level by 10% - 15% a substantial increase in linearity may be realized.

REFERENCES

1. Ettenberg, M., Lockwood, H.F., Wittke, J.P, and Kressel, H, "High Radiance, High Speed $A\ell_xGa_{1-x}As$ Heterojunction Diodes for Optical Communications," International Devices Meeting Technical Digest, p. 317 (1973).

2. Liu, Y.S. and Smith, D.A., "The Frequency Response of an Amplitude Modulated GaAs Luminescense Diode," Proc. of IEEE 63:542-544 (March 1975).

3. Straus, Josef, "Linearized Transmitters for Analog Fiber Links," Laser Focus, p. 54-61 (October 1978).

4. Straus J., and Szentesi, O.I., "Linearized Transmitters for Optical Communications," Proc. of IEEE International Symposium on Circuits and Systems, Phoenix, AZ, pp. 288-292 (April 1977).

5. Asatani, K., and Kimura, T., "Linearization of LED Nonlinearity by Predistortions," IEEE J. Solid-State Circuits SC-13:133-138 (February 1978).

6. EG&G, "Silicon Diffused PIN Photodiodes," Data Sheet D3003B-2 (1974).